Thermodynamic and Raman Spectroscopic Studies on Mixed Gas Hydrates and Their Application for Hydrogen Storage

A thesis submitted to

the Graduate School of Engineering Science, Osaka University

in partial fulfillment of the requirements for the degree of

Doctor of Philosophy

Written by

Shunsuke HASHIMOTO

***March* 2008**

Preface

This dissertation is composed of ten author's studies that were carried out under the guidance of Professor Kazunari Ohgaki at Division of Chemical Engineering, Department of Materials Engineering Science, Graduate school of Engineering Science, Osaka University from 2002 to 2008.

The objective is to investigate the thermodynamic stability, cage occupancy, and structural property of mixed gas hydrates. In addition, I propose that the properties of mixed gas hydrate containing hydrogen should be maximized for the application to gas storage. The purification, storage, and transportation of hydrogen are the significant techniques for realizing a new society sustained by hydrogen energies. Much attention has been directed toward gas hydrates because of its huge potential applicability as a promising medium for hydrogen storage and transportation. These technologies can contribute to both the energy resource and global environmental problems. The authors believe that the present studies would establish the sustainable society for creating "Integrated EcoChemistry" in order to live in coexistence with nature.

Shunsuke HASHIMOTO

Division of Chemical Engineering, Department of Materials Engineering Science,
Graduate School of Engineering Science, Osaka University,
1-3, Machikaneyama, Toyonaka, Osaka 560-8531, Japan.

Table of Contents

Part A Thermodynamic Properties of Mixed Gas Hydrates

Chapter II: Isothermal Phase Equilibria for Hydrogen + Carbon Dioxide + Water Mixtures Containing Gas Hydrate

Chapter III: Thermodynamic and Raman Spectroscopic Studies on Hydrocarbon Hydrates Coexisting with Hydrogen and Aqueous Solutions

Part B Thermodynamic Stability of Hydrogen-containing Mixed Gas Hydrates for Hydrogen Storage

Chapter VI: Stability Boundary and Cage Occupancy on Hydrogen + Tetrahydrofuran Mixed Gas Hydrate

Chapter VII: Stability Boundary and Cage Occupancy on Hydrogen + Tetra-*n*-butyl Ammonium Bromide Mixed Gas Hydrate

Chapter VIII: General Conclusion

General Abstract

Gas hydrate is one kind of inclusion compounds. It consists of cages constructed by hydrogen-bonded water molecules and guest species enclathrated in these cages. Recently, gas hydrates have attracts much attention as a medium for the gas separation, storage, and transportation. In this thesis, the author proposes the applied techniques using gas hydrates, such as gas storage and transportation. The objectives are (1) to reveal the thermodynamic properties of various mixed systems containing gas hydrate, (2) to investigate the thermodynamic stability of hydrogen-containing hydrate systems and cage occupancy of hydrogen by use of thermodynamic and Raman spectroscopic methods.

The gas hydrate systems generated from various mixtures containing from the smallest (hydrogen molecule) to the largest guest (dimethylcyclohexane stereo isomers) were studied. In the systems of dimethylcyclohexane stereo isomers, the *cis*-1,4-dimethylcyclohexane does not generate the structure-H hydrate in the presence of xenon, while the mixture of *cis*-1,4-dimethylcyclohexane and methane generates the structure-H hydrate. That is, the U-cage occupancy limit of large guest species depends on the function of help gas. In the ternary or quaternary systems containing hydrogen, hydrogen molecule cannot be encaged in the carbon dioxide, ethane, and cyclopropane hydrates, while it can occupy the vacant hydrate cages which exist in the propane, tetrahydrofuran, and tetra-*n*-butyl ammonium bromide hydrates under the present experimental conditions.

For the application to hydrogen storage, mixed gas hydrates containing hydrogen were investigated in detail. Especially in the case of hydrogen + water-soluble guest species such as tetrahydrofuran and tetra-*n*-butyl ammonium bromide mixed gas hydrates, mixed gas hydrates are much more stable than the pure hydrogen hydrate. The equilibrium temperature of hydrogen + tetra-*n*-butyl ammonium bromide mixed gas hydrate is about 8 K higher than that of hydrogen + tetrahydrofuran mixed gas hydrate at same pressure condition (~10 MPa). The Raman spectra reveal that the large cages are occupied by the additive guest molecules while one hydrogen molecule occupies the small cages selectively. The cage occupancy of hydrogen is independent of the concentration in the aqueous solution. Interestingly, the results also reveal the characteristic property that hydrogen occupation may depend on the structure of unit-cell.

The structure of the hydrogen + tetrahydrofuran mixed gas hydrate and the cage selectivity of hydrogen do not change with the pressure increases up to 200 MPa. The storage capacity of hydrogen in the tetrahydrofuran hydrate was also investigated by the data obtained from Raman spectroscopic measurements. The storage amount would reach about 1.0 mass% at about 80 MPa, which is almost equal to the maximum amount of hydrogen storage in the structure-II tetrahydrofuran hydrate on the assumption that the only one hydrogen molecule can occupy the small cage of tetrahydrofuran hydrate.

Chapter I

General Introduction

Needless to say, energy supports our convenient life today. Almost of us consume huge amount of energy every day without being conscious of quantities of energy resource and supply. Now, there is little doubt but that the stable supply of energy is due to oil, power, gas companies and so on. If this stable supply of energy came to stop, our daily lives would go under quickly. Energy resource problems are very important, serious, and universal in the world, especially for nation poor in natural energy resources, Japan.

I-1 Background

I-1.1 Energy Resource and Geoenvironmental Problems

Since the Industrial Revolution, scientific technologies have developed at a rapid rate, and consequently our lifestyle has become affluent. Our lifestyle depends on fossil fuels of coal, oil, and natural gas for the most part of industrial productive energy. In particular, Our lifestyle rely heavily on oil today. In populous developing countries, mechanization of agriculture and increase in the use of chemical fertilizer are essential for the solution of population and food issues. In these countries, the consumption of fossil fuels is also getting larger and larger. For using fossil fuels, it is important to find a fresh energy resource equal to the current energy consumption. On the other hand, it is likely that conventional subterranean energy resources such as crude oil run dry decades later, and consequently soaring crude oil prices are now beginning to affect the global as well as Japanese economy. That is, humankind has a

global-scale energy resource problem. In future, novel energy resources instead of oil will be required.

As mentioned above, in about 200 years after the Industrial Revolution, the consumption of fossil fuels has dramatically increased. Now the increase of carbon dioxide (CO_2) concentration in atmosphere becomes serious environmental problem. Eventually since the 1980's, the "global warming" has attracted much attention, which is caused by the extreme increasing of atmospheric CO_2 concentration. The heat ray radiating from the earth is absorbed by greenhouse effect gas such as CO_2 and the heat is stored. The global warming is worldwide problem and would cause some more crises.

Figure I-1 shows the trend of atmospheric CO_2 and methane (CH_4) concentration and temperature in Vostok station, Antarctica in the past 220 thousand years [1]. Raynaud et al. [2] have obtained this trend by the direct measurement of the atmosphere entrapped with the past ice

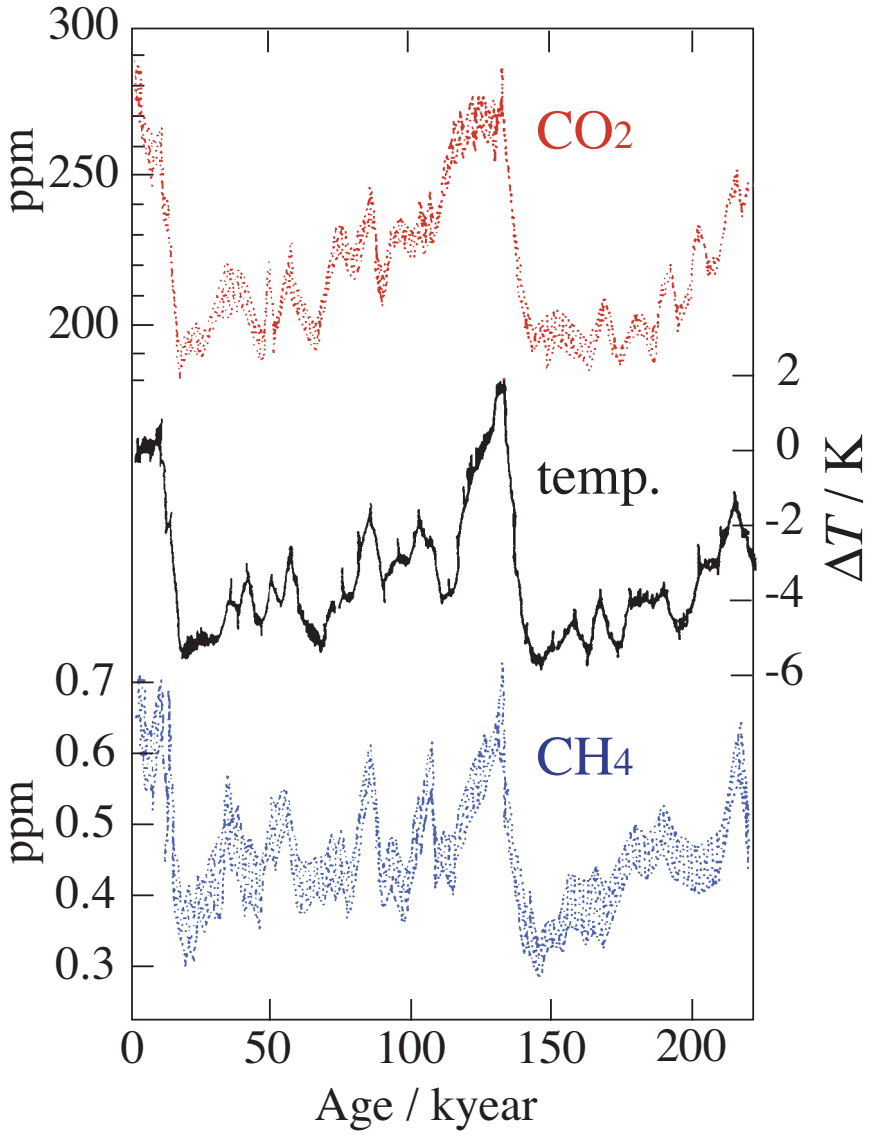

Figure I-1 Trend of atmospheric CO_2 and CH_4 concentration and temperature in Vostok station, Antarctica.

sheet core. Global environment has alternated between glacial and interglacial stages every 100 thousand years. This cycle is linked to the eccentricity of the earth's orbit or precession cycle of the earth, and well known as "Milankovich Cycle". As shown in **Fig. I-1**, the concentration of CO_2 fluctuates between 200 ppm in the glacial stage and 280 ppm in the interglacial one. This can be regarded as "Natural Cycle". In addition, the concentration of CO_2 or CH_4 correlates closely with the past temperature trend. Recently, the concentration of CO_2 indicates much higher value than that of the past. To make matters worse, the concentration of CO_2 increases by an average of 1.5 ppm per year. This speed is about 1500 times as rapid as Natural Cycle. That is, it is obvious that the increase of greenhouse effect gas such as CO_2 promotes the global warming.

A few methods to solve the global warming have been proposed before now. **Figure I-2** shows the relation between the density and the depth, and favorable storage method at each depth. In the region upper than 3000 m, the density of CO_2 is smaller than that of sea water and the dissolution of CO_2 is usually used. In this method, the absorption amount of CO_2 is small and this method would cause marine pollution and insoluble CO_2 is re-emitted into the atmosphere. In addition, it is likely that the dissolved CO_2 returns to the atmosphere as a result of seawater circulation after 100 years. Therefore, the storage of CO_2 as the liquid state is required. It is possible to store CO_2 utilizing CO_2 hydrate at the bottom of the ocean under a depth of 3000 m [3, 4]. Under the conditions of the low-temperature and high-pressure in the

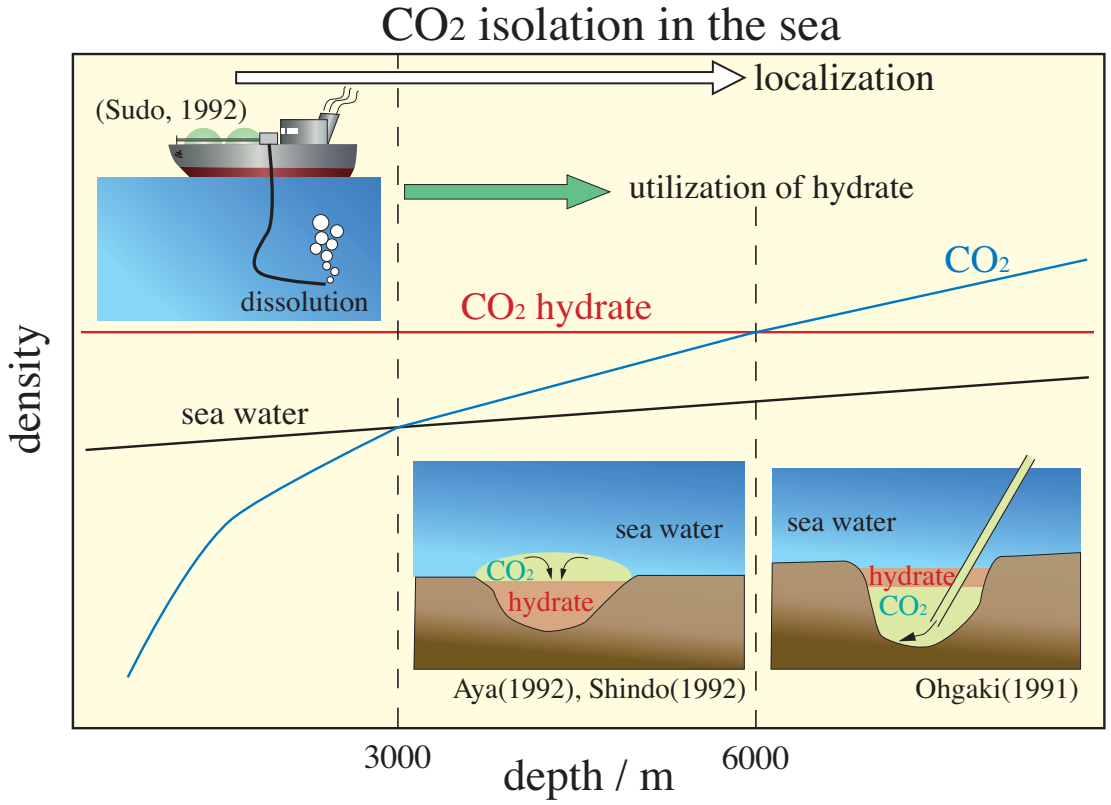

Figure I-2 Density profile of the sea water, liquefied CO_2, and CO_2 hydrate. And the insets are schematic illustration of CO_2 isolation process in each depth.

deep ocean, the sea water and the condensed CO_2 fluid generate CO_2 hydrates [5]. In the region from 3000 to 6000 m, the liquefied CO_2 reacts with the seawater and consequently generated CO_2 hydrates are stored at a crater place. On the other hand, Ohgaki and Inoue [6] have proposed the innovative CO_2 storage method on deep ocean floor above 6000 m in depth using gas hydrates. In this method, the retrieved CO_2 is transported to the sensibly deep depression though the pipelines. As shown in **Fig. I-2**, it is at 6000 m in depth that the density becomes larger in the order of sea water, CO_2 hydrate, and liquefied CO_2 [5]. Therefore, above 6000 m in depth, the hydrate generated from poured CO_2 and sea water exists as the cap and plays an important role in preventing the stored liquefied CO_2 from diffusing into the sea water. That is, this method enables CO_2 to be stored more stably and in larger amounts (because of liquefied state) than any other method applying the ocean.

In order to stop the global warming, the emission limitation of CO_2 is also essential. That is, the usage of low-carbon fuel is the desirable method in the near term. Natural gas is relatively clean and promising energy resource because the main component of natural gas is CH_4 and consequently the amount of CO_2 emission is fewer than any other fossil fuel. The usage of natural gas is increasing in the decade ahead. In addition, we can use alternate energies such as hydraulic power, force of wind, atomic energy, solar energy, and so on. However, the energy density of non-fossil energy such as solar power is so small that much time and cost are required. Atomic energy has the problems of safety and waste disposal. Therefore, we have to find novel energies instead of normal fossil fuels pretty soon.

I-1.2 Utility of Hydrogen Energy & Fuel Cell [7]

As mentioned above, not only the emission limitation of CO_2 but also novel energies instead of normal fossil fuels are essential to stop the global warming. Hydrogen (H_2) energy has attracted much attention as a clean and potential energy resource because its combustion product is only water. The elemental substances of H_2 do not exist naturally for the primary energy resource. However, there are a lot of the elemental hydrogen in hydrocarbons or water on the earth. In addition, the chemical energy of H_2 per unit mass is 142 MJ / kg, which is at least three times as much as that of other chemical fuels. Therefore, H_2 energy has bright prospects of large advantage for the future energy resource. In the early 19^{th} century, it was revealed that the reverse reaction of water electrolysis is capable of electric generation. This is the first discovery of fuel cell. Fuel cells combine H_2 with O_2 in an efficient electrochemical process that is clean and flameless. Available fuels include not only H_2 but also methanol, natural gas, and so on. In the case of H_2 fuel, nothing is produced but electric power and pure distilled water, along with heat that can be recovered and used. Unlike batteries, fuel cells need no recharging and they will operate as long as fuels are supplied. Decades of research have resulted in the evolution of

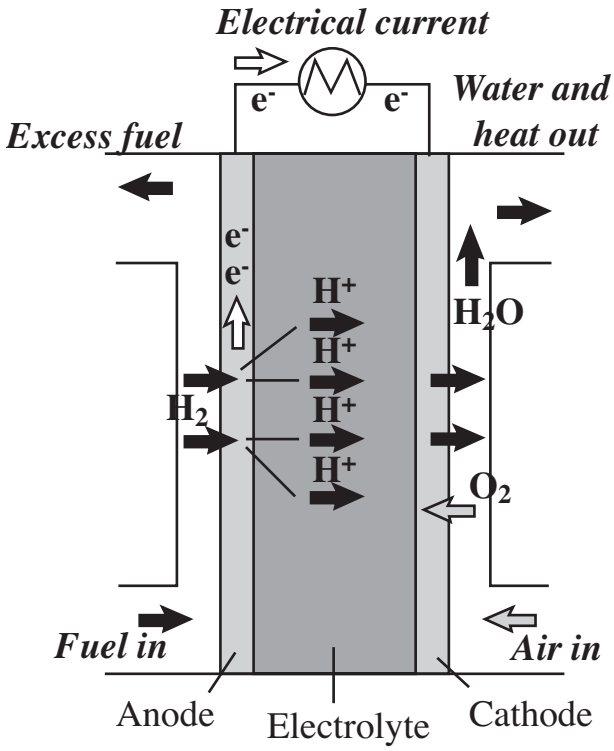

Figure I-3 Schematic illustration of PEM fuel cell.

different fuel cell technologies, which fall into a handful of categories based on their type of electrolyte.

The types of electrolyte for the fuel cell are summarized as follows: molten carbonate, solid oxide, phosphoric acid, and solid polymer membrane (this type is called as PEM). Each fuel cell type is used for the different purpose in particular application. For example, PEM fuel cell (hereafter, PEM-FC) is often used at relatively low-temperatures. **Figure I-3** shows summary of PEM-FC. PEM-FC delivers high power density and offers the advantages of low weight and volume, compared to other types. It operates at around 350-370 K. Low-temperature operation allows it to start quickly (less warm-up time) and results in less wear on system components, which makes the PEM-FC durable. PEM-FC also responds rapidly to changes in demand for the power, and it does not require corrosive fluids as some types do. All of these factors make PEM-FC good candidates for the vehicles and micropower applications. On the other hand, PEM technology uses a solid polymer membrane (thin plastic film) and porous carbon electrodes containing a platinum catalyst or other noble metal. The catalyst is very expensive and also makes the cell extremely sensitive to poisoning by carbon monoxide (CO), which must be eliminated in the fuel gas along with sulfur and other impurities. There are many problems on the PEM-FC and developers are searching catalysts instead of platinum that are more resistant to CO.

All along, Japanese industry has been a global leader in developing fuel cell technology. In addition, some of the major automakers in Japan such as Toyota and Honda have also led implementation of H_2 fuel cells in vehicles and development of fueling infrastructure. Today, the

Table I-1 The cumulative target value of introduction of H_2 fuel cell vehicle and stationary H_2 fuel battery by METI.

years	2010	2020	2030
H_2 fuel cell vehicle	50 thousand pounds	5 million pounds	15 million pounds
Stationary H_2 fuel battery (containing household and institutional use)	2.1 million kW	10 million kW	12.5 million kW

amount of H_2 production in the world is ~500 billion Nm^3 per year, and 150 Nm^3 of those is produced in Japan. Ministry of Economy, Trade, and Industry (METI) sets the cumulative target value of introduction of H_2 fuel cell vehicle and stationary H_2 fuel cell as shown in **Table I-1**. The H_2 requirement is estimated at 38.7 billion Nm^3 per year in 2020, which exceeds greatly the current amount of H_2 production. There is little doubt but that H_2 will become the "key energy" for the co-existence of nature and humankind, and the H_2 market will get larger. In the future, H_2 fuel cell may raise the "Second Industrial Revolution".

I-1.3 Actuality of Hydrogen Utilization [7]

H_2 utilization is classified into three processes as follows: H_2 production and supply, H_2 separation and purification, and H_2 storage and transportation. In particular, the storage and transportation of H_2 at moderate conditions are key factor in establishing a new and earth-conscious society sustained by H_2 energies. In this section, the summary of these processes is simply mentioned.

Production and supply of H_2

One of H_2 advantages is that it is found in a great variety of compounds including water, hydrocarbon fuels, and inorganic substances. Hence, H_2 can be produced from a multitude of sources and in many different ways. The two conventional methods of producing H_2 are the reforming of hydrocarbon fossil fuels and electrolysis of water. The least expensive, most common process in the United States is catalytic steam reforming of natural gas (mostly methane), while some European nations use nuclear power for electrolysis.

Gas reforming:

Natural-gas reforming has the advantages of high efficiency and low cost as well as the option

of recovering and using waste heat in a cogeneration system. Natural gas is easy to handle and it has the highest hydrogen-to-carbon ratio (H / C) of any fossil fuels, so it produces relatively moderate CO_2 emissions. In the first step of reforming natural gas, CH_4 reacts with steam at temperatures of about 1100-1200 K, accelerated by a nickel catalyst. This reforming step produces a synthesis gas composed of H_2 (typically 75 %), CO (15 %), and CO_2 (10 %). Then a reaction with additional steam (called the water-gas shift reaction) converts the CO to CO_2 and produces more H_2. H_2 can be separated from these syngas and purified (mention later). Overall, the methane steam reforming process can be represented by:

$$CH_4 + 2H_2O \rightarrow 4H_2 + CO_2$$

Two variations of catalytic steam reforming are used: partial oxidation and autothermal reforming. In partial oxidation, some of the feedstocks are burned as fuel to generate the heat required for the subsequent reactions. However, combustion reaction is quenched before it is complete. Generally, oxygen for the fuel is introduced into the gas reactor by cryogenic separation from air, which is an expensive part of this system. Partial oxidation is better suitable for the reforming coal or heavier hydrocarbon fuels such as diesel and gasoline because the initial high-temperature combustion step breaks these large molecules into structures that are simpler to process.

Steam reforming is endothermic reaction, while partial oxidation is exothermic. The autothermal process becomes possible by combining the two methods, which is the autothermal reforming method. In this method, the autothermal process becomes only slightly hot overall, which results in a small, quickly starting, and quickly responding system. Many of the newest onsite reformers apply the autothermal technology.

Electrolysis of water:

In water electrolysis, an electrical current passes through water and decomposes it into hydrogen and oxygen. Traditionally, two types of electrolyzers have been operated in industry (both using liquid electrolytes). One is the tank type (unipolar) with electrodes suspended in a tank of electrolytes. The other is the filter type (bipolar), which uses two separate cells and is better suitable for high pressures and temperatures. The efficiency of these systems has improved from the 70 %-75 % range in the 1970s to 80 %- 90 % today, but essentially the concept hasn't changed for more than 50 years. Recently, however, electrolysis using PEMs has attracted attention. The technology is the reverse of that used in PEM-FC. A solid polymer electrolyte (thin plastic sheet) becomes conductive when soaked in water. PEM electrolyzers reach efficiencies similar to conventional types. In addition, they generate H_2 at very high purities and high pressures, and consequently compression costs are reduced. Moreover, there are some other potential methods for the decomposition of water: water pyrolysis, using Solar or nuclear

power.

$$2H_2O \rightarrow 2H_2 + O_2$$
$$2H_2 + O_2 \rightarrow 2H_2O$$

Biomass and waste feedstocks:
Most recently, biomass has attracted much attention as a technology for the prevention of global warming because it's organic resource from botanical origin, which can absorb the CO_2 by photosynthesis. Biomass and waste include a great variety of materials as follows: inedible plants, undesirable species that create a nuisance, plants grown specifically as biomass crops, leftovers from agricultural crops, organic industrial waste, animal waste, and so on. In the case of production of electricity and heat by gasification of biomass, CO_2 is generated in the gasification process. However, these CO_2 are equivalent to the CO_2 absorbed from atmosphere by the original plant. That is, the usage of biomass does not increase CO_2 in atmosphere overall. This property is called as "carbon neutral". Biomass can be considered a renewable energy source in the sense that it was created with solar energy and can be replaced by growing more plants.

Separation and purification of H_2

As stated above, H_2 is produced by various methods. However, some of impurities with H_2 are included in the reaction products with either method. For example, syngas generated from reforming of fossil fuels includes carbon monoxide (CO), CO_2, water, CH_4, etc. with H_2. The CO is toxic, and in many cases, these impurities are impeditive for the storage and transportation. Therefore, purification of H_2 up to desired level is essential. Separation and purification processes of H_2 are categorized as absorption, cryogenic separation, adsorption, and diffusion. Details are as follows:

H_2 absorption:
Gas mixture is contacted directly with absorbing liquid, and then more soluble components can be absorbed and eliminated. Two methods are well-known, physical and chemical absorption. In the former, soluble gases are dissolved physically in absorbing liquid. On the other hand, in the latter, soluble gases are reacted chemically with reactant in absorbing liquid, and then their products are dissolved. In the case of H_2 purification, absorption using amine is usually adopted in order to eliminate CO_2 that is main impurity in syngas.

Cryogenic separation:
Gases containing H_2 are cooled down by repeating compression and expansion processes, and consequently transformed into liquids. Then, H_2 can be separated from obtained liquid mixture

by distilling in the distillation column. The boiling point of H_2 is ~20.3 K, which is lower than other gases except for Helium. This difference in boiling point is available in the cryogenic separation method.

H_2 adsorption (PSA method):

Pressure swing adsorption (PSA) method is a separation and purification technology that is used to separate some species from gas mixture under pressure using the difference of these species' molecular characteristics and affinity for an adsorbent material. It operates at near-ambient temperatures and so differs from cryogenic distillation techniques of gas separation. Special adsorptive materials (e. g., zeolites) are used as a molecular sieve, preferentially adsorbing the undesired gases at high pressure. The process then swings to low pressure in order to desorb the adsorbent material. As shown in **Fig. I-4**, the simplest equipment requires two fixed-bed adsorption towers. Using two adsorbent vessels allows near-continuous production of the target gas. It also permits so-called pressure equalization, where the gas leaving the vessel being depressurized is used to partially pressurize the second vessel. The results in significant energy savings, and is common industrial practice. One application of PSA is the separation of CO_2 from biogas to increase the CH_4 content. Through PSA the biogas can be upgraded to a quality similar to natural gas. Absorbed amount of H_2 is almost independent of pressure and very small. Gases except for H_2 are adsorbed at high pressure by use of the difference of affinity for an adsorbent material and H_2 can be purified. In PSA method, mole fraction purity 0.999999 of H_2 is achievable.

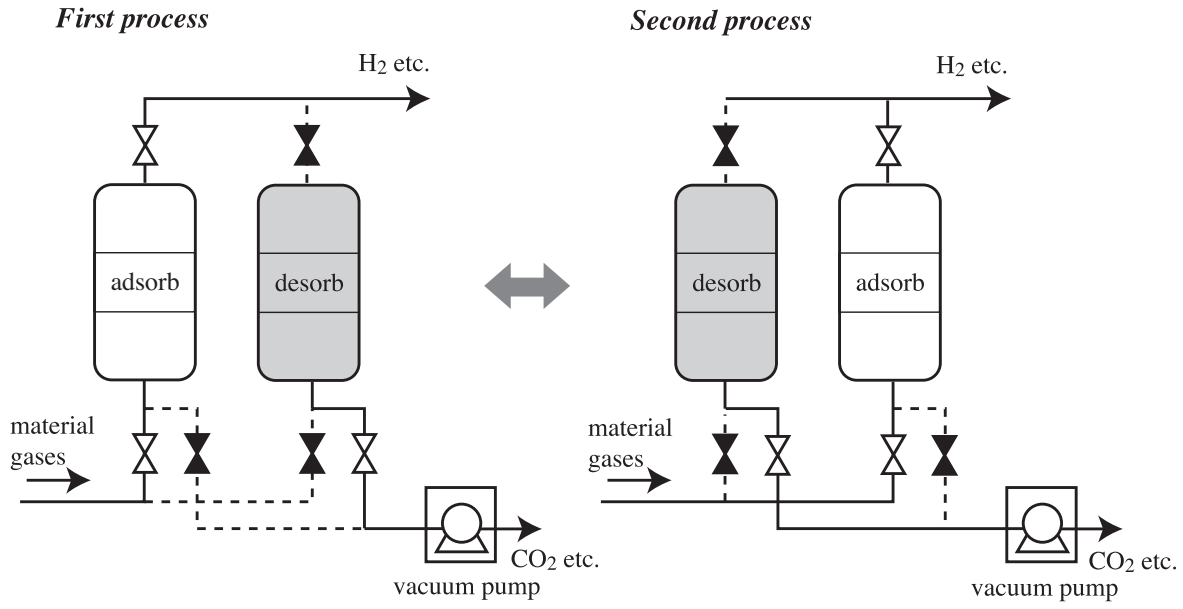

Figure I-4 Schematic illustration of overall processes for the PSA method.

H_2 diffusion (membrane separation method):
Membrane separation is carried out by use of the velocity difference in gas permeability through membrane. This method generally requires less energy than other methods and can be operated at mild conditions. In addition, the maintenance of equipment is very easy because the equipment is composed of very simple and small system. Gas mixture containing H_2 is introduced into the upper side of membrane. Then H_2 diffuses and transmits through the membrane by the driving force obtained from the pressure difference of H_2 between upper and lower sides, and consequently highly-pure H_2 can be recovered. As a membrane, polymer membrane or metallic membrane is often used.

In general, these methods are combined efficiently for the H_2 purification.

Storage and transportation of H_2

Futural H_2 energy societies of our future will depend on the developments of safe, reliable ways in order to store and transport H_2 after H_2 production. Although H_2 is more advantageous in bulk storage than electricity, technical innovation for efficient storage technology of H_2 has been still essential. The biggest challenge will be storing enough H_2 on fuel cell vehicles to allow the same travel range as their gasoline of hybrid counterparts (at least 300 miles (500 km)). Therefore, the compact and lightweight storage method is required as soon as possible. Recently, H_2 is stored and transported by carry containers of compressed H_2 gas. However, H_2 accounts for very large volume (~11.2 m^3 / kg) at room temperature and various alternatives have been proposed.

Compressed H_2 tanks:
Most compressed H_2 tanks operate at ambient temperatures and store the gas at pressures from 35 to 70 MPa. Compression of H_2 to this range requires roughly 10 % of the gas's energy content. Compressed H_2 tanks (usually cylinders with rounded ends) have been certified by standards agencies worldwide. They are used for the onboard fuel cell vehicles, the portable and onsite power generators, and the uninterruptible power supply systems, where fuel cells replace batteries. The atomic diameter of H_2 is smaller than that of most metallic materials, and H_2 is easy to break into metallic materials. Therefore, conventional steel tanks are made of the premium steel in order to prevent metal fatigue and leakage, and consequently too heavy for the H_2 storage in fuel cell vehicles. Researchers and manufacturers have explored lightweight cylinders that use various other materials such as polymer liners, multiple shells, and composite fiber wraps to minimize the amount of metal required.

Liquefied H_2 tanks:
H_2 liquefies at super-cooled (cryogenic) temperatures, ~20.3 K. In its liquefied state, H_2 takes

up just 1 / 700th as much volume as the gaseous form. An important advantage is that the storage tank can be compact. Liquefied H_2 has a higher energy density than the compressed form, so a tank containing the same amount of fuel is very smaller. Therefore, liquefied H_2 would boost the driving range of a vehicle. It allows about 2-3 times the distance of compressed H_2 tank. However, liquefaction of H_2 requires much more energy than compression. Liquefaction process consumes at least 30-35 % of H_2's energy content or 11 to 12 kWh of electricity per kilogram H_2. In addition, the other weak point of liquefied H_2 is evaporation. Whenever the H_2 isn't used (for example, when a fuel cell car is parked), the liquid naturally tends to return to its gaseous state due to the heat exchange between the cold tank and the warmer atmosphere. The boiled-off gas must be vented. Therefore, cryogenic tanks for storage require insulation and other special materials.

Chemical hydrides (containing organic and inorganic compounds):
A chemical slurry or solution can store H_2 as a hydride. In this method, the stored H_2 is released through a reaction with water, which gives off heat. These systems require heat management and they are irreversible because the storage medium must be regenerated before it can be recharged with more H_2. The most advanced chemical storage material is sodium borohydride, the familiar laundry detergent Borax (sodium borate) combined with H_2. This chemical creates a nontoxic and nonflammable solution with water and produces H_2 when exposed to a catalyst.

$$NaBH_4 + 2H_2O \rightarrow NaBO_2 + 4H_2$$

When the catalyst and solution are separated, the system stops generating H_2. The spent solution is recyclable. However, it becomes one of problems that this regeneration of solution requires large energy.

In another type of chemical hydride, the H_2 storage using a liquid organic compound (organic chemical hydride) at room temperature has become the object of much attention. For example, cyclohexane or methylcyclohexane is popular as follows:

$$C_6H_{12} \rightarrow C_6H_6 + 3H_2$$
$$C_6H_{11}CH_3 \rightarrow C_6H_5CH_3 + 3H_2$$

These organic chemical hydrides enable efficient H_2 storage at normal pressures and temperatures. However, they require large energy to release H_2 and toxic liquid such as benzene is generated after reaction. The regeneration system of these toxic media should be build for the application.

Carbon materials:
Carbon materials have attracted attention in the promise that they can hold H_2 in minuscule structures called nanotubes or nanofibers. Theoretically, these forms of carbon could store and release relatively huge quantities of H_2, if practical structures and systems can be developed. In nanotubes, carbon atoms are linked together in hexagons like chicken wire and rolled into single-layer tubes. Carbon nanotubes are known to attract H_2 molecules. The huge surface area afforded by the carbon atoms would offer potential for the H_2 storage, and the carbon atom is lightweight. The ideas is that carbon nanotubes might draw in H_2 just as water is sucked into a straw. Tube bundles might serve as light H_2 sponges ideal for fuel cell vehicles. In addition, nanotubes are extremely stiff and strong, and plenty of carbon is available to manufacture them. However, researchers haven't figure out how to control its uptake and release. They also have no clue yet how to mass-produce the tubes. From now on, further investigations are required about the interaction between hydrogen and carbon atoms.

Metal hydride (containing H_2 absorbing alloys):
Originally, metal hydrides were designed to control reactions and output in nuclear power plants. Their development for the H_2 storage was promoted by their safety advantage. In this method, a pure metal or an alloy forms a stable hydride when it absorbs the hydrogen atoms by pressurizing the metal and then gives off heat. On the contrary to this absorption process, the hydride releases the hydrogen atoms when heat is applied or the system is depressurized as follows:

$$M + xH_2 = MH_{2x} + \Delta Q \text{ (pure metal)}$$
$$AB_z + xH_2 = AB_z(H_2)_x + \Delta Q \text{ (alloy)}$$

H_2 absorbing alloys are composed of the metal A that is easy to generate hydrides and the metal B that is difficult to do so. They are categorized AB_5 and AB_3 type depending on the ratio of A to B. Ti and Ni is well known as the metal of A and B site, respectively. In this method, it would be advantageous that heat given off by a fuel cell can be used to release the H_2. When incorporated in a metal hydride, the H_2 takes up no additional space, which results in a compact and high-density storage medium. Compared with compressed H_2 tanks holding the same amount of H_2, metal hydride are only 1 / 3 - 1 / 4 as large. In addition, they operate at relatively low pressures. However, metal hydrides are heavy, and a tradeoff is involved in selecting materials. The metals with the highest storage capacity require high temperatures to release the H_2. This is not suitable for using the low-temperature exhaust heat from PEM fuel cells in vehicles. But lower temperature hydrides hold less energy, and consequently they have to be larger and heavier to carry as much H_2 fuel. Therefore, scientists are working on new alloys that optimize the hydride's temperature and energy density characteristics. In addition, aluminum

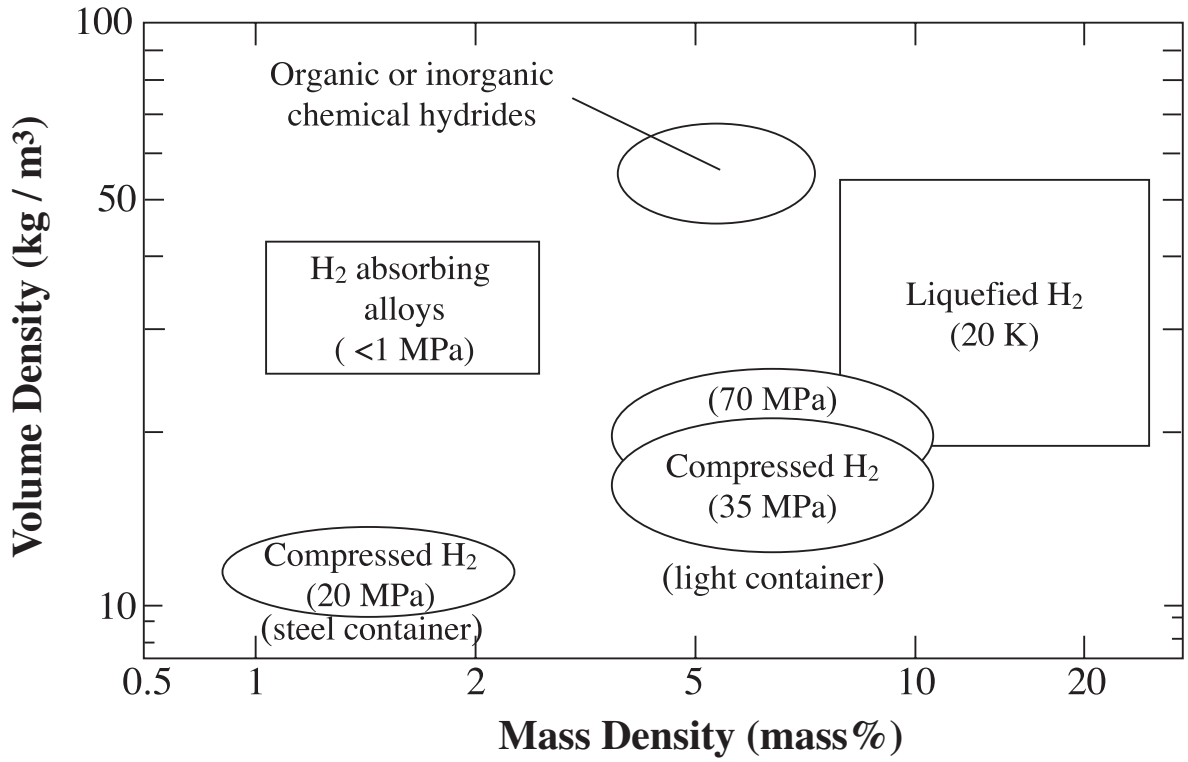

Figure I-5 Comparison of H_2 storage density for the various storage technologies.

compounds called alanates are considered to be the most promising of the complex metal hydrides. Several research projects are under way to investigate their storage mechanisms.

The relation between mass density (mass%) and volume one (kg / m^3) for the various storage technologies of H_2 is shown in **Fig. I-5**. According to Zuttel, there are no methods that fulfill all of storage efficiency, compactness, lightweight, low cost, and safety at the same time. Further studies about innovative technology for the H_2 storage are required.

I-2 Gas Hydrate

I-2.1 Structure of Gas Hydrate [8]

Gas hydrates are one of clathrate hydrates, which are crystalline inclusion compounds. They are ice-like solid crystals and are composed of the frameworks that are constructed by the hydrogen-bonded water molecules. In these frameworks, the relatively small "guest" molecules are enclosed. As shown on **Fig. I-6**, the guest molecules in the cavities have a van der Waals interaction with water molecules, and consequently the presence of the guest molecule stabilizes the structure of gas hydrates. The cavity constructed by hydrogen-bonded water molecules is generally called as "hydrate cage". So far, several cages are well known as shown in **Fig. I-7**. Circles represent the oxygen atoms of the water molecules. The hydrogen atoms of the water molecules lie among the oxygen atoms, though they haven't been drawn. The smallest cage consists of pentagonal dodecahedron (5^{12}), which is called as S-cage. Middle and large cages consist of tetrakaidecahedron, $5^{12}6^2$ and hexakaidecahedron, $5^{12}6^4$, which is called as M-cage and L-cage, respectively. The other cages are called as S'-(dodecahedron, $4^3 5^6 6^3$) and U-cage (icosahedron,

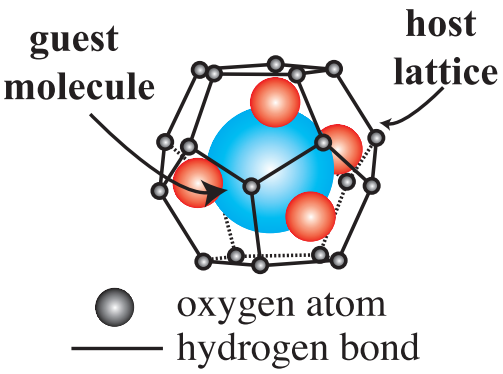

Figure I-6 Summary of gas hydrate.

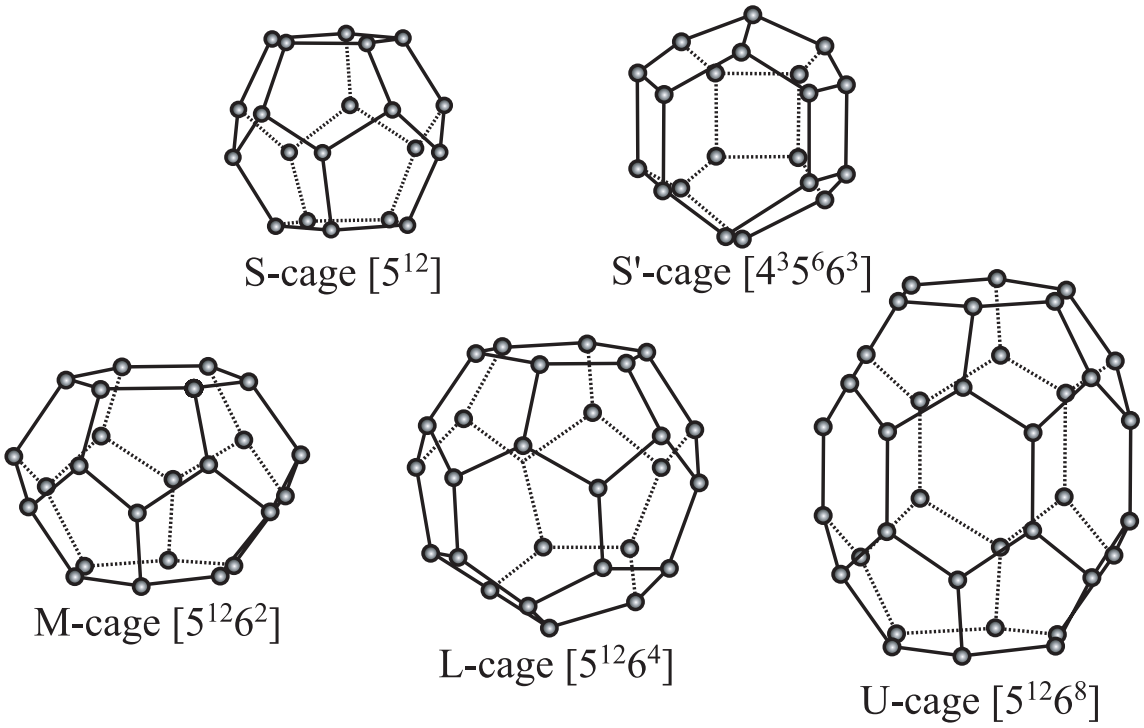

Figure I-7 Schematic illustration of five hydrate cages constructing unit-cell structures.

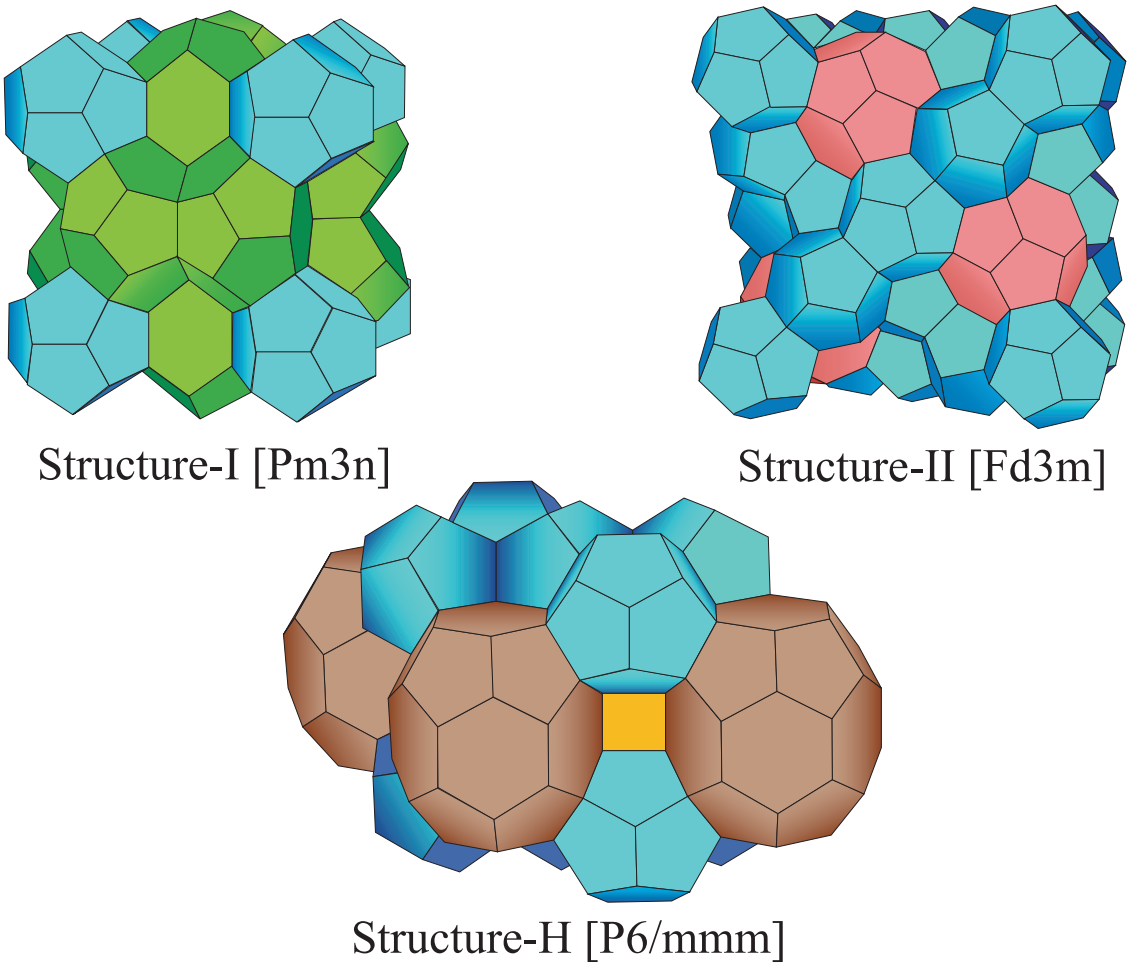

Figure I-8 Schematic illustration of hydrate unit-cell structures, structure-I, -II, and -H.

$5^{12}6^{8}$). The S'-cage is slightly larger than the S-cage, and the U-cage is much larger than the one. The cage size becomes larger in the order of S-, S'-, M-, L-, U-cage. Several cages configure the unit-cell structures of gas hydrates. There are three structures of hydrate unit-cell, structure-I (s-I), structure-II (s-II), and structure-H (s-H). As shown in **Fig. I-8**, all the structures have S-cage in common. The s-I and s-II hydrates are composed of two types of hydrate cage, the former consists of two S-cages and six M-cages and the latter sixteen S-cages and eight L-cages. On the other hand, the s-H hydrate is composed of three types of hydrate cage, three S-cages, two S'-cages, and one U-cage. The characteristics of these unit-cell structures are summarized in **Table I-2** [9, 10].

I-2.2 Stability of Gas Hydrate

Generally, it is well-known that the stability, structure, and hydration number of gas hydrate mainly depend on shapes, sizes, and physical properties of enclathrated guest species, temperature, pressure, and composition of guest species. **Figure I-9** shows the relation between

Table I-2 Summary of hydrate unit-cells and cages.

Structures of gas hydrates							
type of unit-cell	Structure-I		Structure-II		Structure-H		
water molecules in a unit-cell	46		136		34		
types of cages forming unit-cell	5^{12}	$5^{12}6^2$	5^{12}	$5^{12}6^4$	5^{12}	$4^3 5^6 6^3$	$5^{12}6^8$
tag of cages in this thesis	S	M	S	L	S	S'	U
number of cages	2	6	16	8	3	2	1
diameter of cages / nm	0.795	0.860	0.782	0.946	0.782	0.812	1.142
coordination number	20	24	20	28	20	20	36
diameter of free cavities / nm	0.51	0.58	0.50	0.67	0.50*	0.53*	0.86*
crystal type	Cubic		Cubic		Hexagonal		
lattice constant *a* / nm	1.20		1.73		1.23		
lattice constant *c* / nm	-		-		1.02		

* Subtract the diameter of water molecule from that of cage for the structure-H.
** Lattice constant for the structure-I and -II from Parrish and Prausnitz (1972), for the structure-H from Mehta and Sloan (1996).

molecular diameter and hydrate structures or cage occupancy. Normally, the better the guest species fit the cages, the more stable the hydrate structure is. For example, in the case of noble gases, the hydrate becomes more stable in the order of Argon (Ar), Krypton (Kr), and Xenon (Xe) hydrates, which agree with the order of guest molecular size (Ar: 0.38 nm, Kr: 0.40 nm, Xe: 0.43 nm). In the case of guest species whose size is larger than the free volume of S-cage, they generate the stable hydrate lattice in the presence of perfectly vacant S-cages. However, in the high-pressure region, the larger guests than S-cage can be entrapped with S-cages, which is reported as "Compressed Occupation" phenomenon [11]. In the case of guest species whose size is larger than the free volume of L-cage, double hydrate is generated. Double hydrate, which is also called "compartmentally-occupied type", can be generated from small molecule such as methane as well as large guest molecule. Details are mentioned later.

In general, gas hydrates form at low-temperature and high-pressure conditions. The thermodynamic stability of gas hydrates is an important knowledge in order to investigate its physical property.

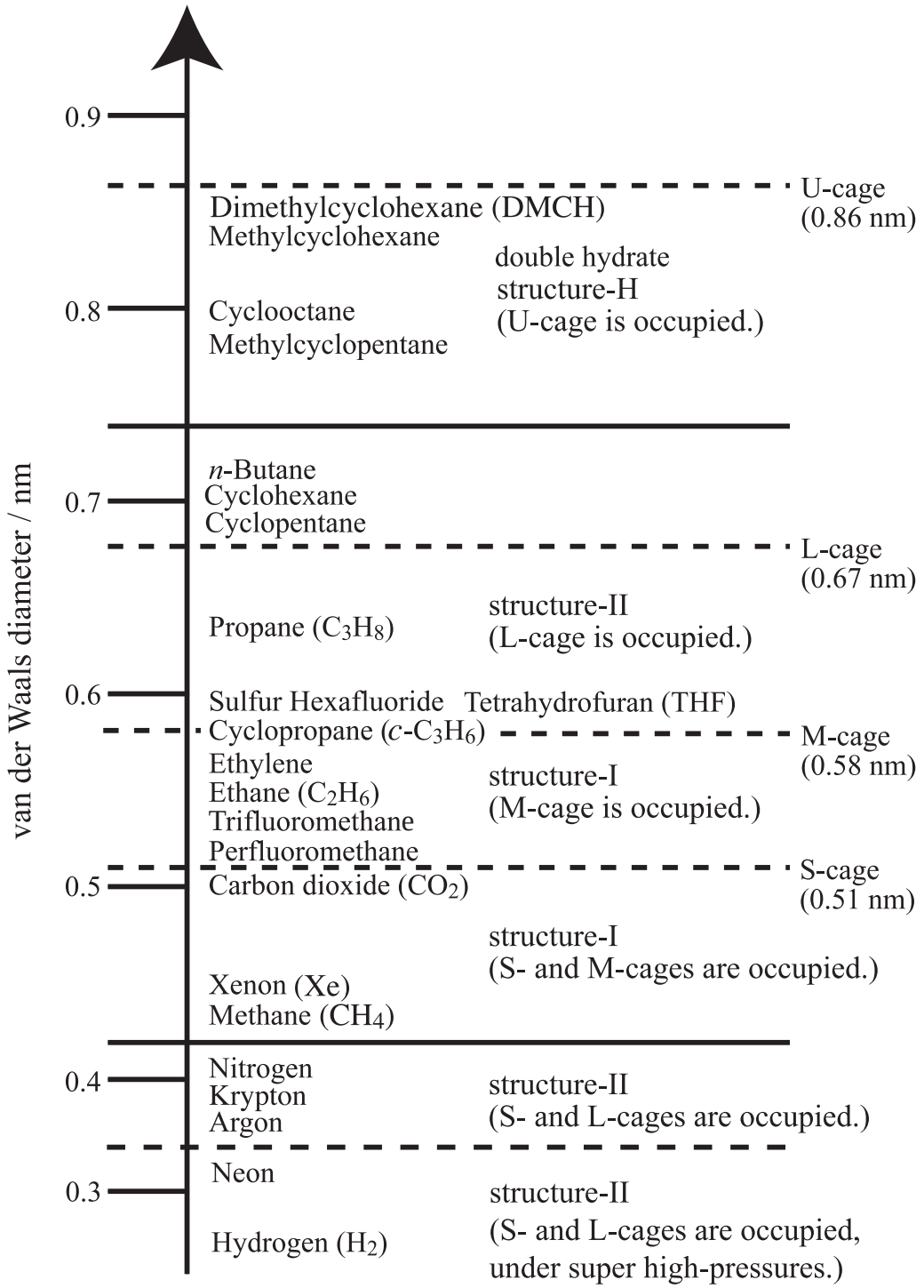

Figure I-9 Molecular diameter dependency of hydrate structures and cage occupancies.

I-2.3 Mixed Gas Hydrate

Mixed-gas hydrates are defined as the gas hydrates containing two or more guest species (for example, CH_4 + CO_2 mixed-gas hydrate) [12]. Since the first discovery of gas hydrate in 1810 [13], a lot of researches about pure (single-gas) hydrates have been reported. However, there is less information about mixed-gas hydrate systems and researches about them have been

performed little by little in the world.

Mixed-gas hydrates can construct three types of hydrate unit-cell structures, the s-I, -II, or -H, depending on temperature, pressure, composition and kind of guest species. Mixed-gas hydrate systems are classified into two types of group by their cage occupancy. One is "competitive occupation system", and the other is "compartmental occupation system". In the former system, cages of the same kind are occupied by two of more types of guest species, where only one molecule can be occupied in a cage. The s-I and -II hydrates are formed in this system. On the other hand, in the latter system, every cages are preferentially occupied by the guest molecules that optimally fit the free volume of cages. In this system, the s-II and -H hydrates are usually constructed. Details are mentioned as follows:

Competitive Occupation System

In this system, the equilibrium composition and pressure can be controlled by the initial composition of guest molecules. Initial composition also affects the cage occupancy of guest species. Some interesting behaviors for the competitive occupation mixed-gas hydrate system have been reported. The one of characteristic behaviors for this system is the "hydrate-structural phase transition" depending on the composition of guest mixture. According to the recent reports, the CH_4 + ethane (C_2H_6) [14], CH_4 + cyclopropane (*c*-C_3H_6) [15], and CH_4 + perfluoromethane (CF_4) [16] mixed-gas hydrates generate the s-II hydrate for a certain composition region, nevertheless each guest molecule generates the s-I hydrates. The structural phase transition greatly affects thermodynamic properties of mixed-gas hydrates. However, the mechanism of structural phase transition is still unclear and many scientists have investigated it.

Compartmental Occupation System

In this system, the equilibrium composition and cage occupancies of guest species are suggested to be almost invariant. However, the size and substitutional group of guest species have much effect on the equilibrium pressure. The s-H hydrate, which is typical case of compartmental occupies hydrates, was discovered in 1987 [17] and it is relatively new subject of research. Two kinds of guest species are essential to form s-H hydrate: one is small guest-species such as CH_4, nitrogen (N_2) and Xenon (Xe) etc., the other is large guest-species (LGS) like methylcyclohexane. The small guest-species are called "help gas" and it assist the formation of s-H hydrate for the LGS. The LGS cannot be enclosed in hydrates without coexistence of the help gas molecule. It is commonly believed that the help gas molecule occupies the S- and S'-cages, while the LGS occupies only the U-cage [8]. In this system, four-phase (gas, aqueous solution, oily LGS, and hydrate) equilibrium curve (pressure-temperature relation) is usually measured.

I-3 Natural-Gas Hydrate

I-3.1 Distribution of Natural-Gas Hydrate

Natural-Gas Hydrate (NGH) is one of mixed-gas hydrates that occupies natural gas containing CH_4, C_2H_6, C_3H_8, and so on. In the 1930s, NGH was firstly discovered as a nuisance material that blocked the natural-gas transport in pipe lines [18]. The natural gas containing water generated hydrates by pressurized and cooled in pipe lines. This problem was solved by drying the gas prior to transport or mixing inhibitors.

In general, it has been confirmed that the velocity of elastic wave through NGH layers is twice as fast as that of normal stratums. In case the elastic wave goes through the stratum containing NGH, acoustic discontinuous surfaces are generated between NGH layer and normal stratum. These interfacial boundaries are detected as strong reflection surface, and the existence of NGH can be recognized. This reflection surface is called "Bottom Simulating Reflector (BSR)" and has become the important clue for the search of oceanic NGH fields. In the 1960s, a lot of NGH fields were discovered in the subterranean permafrost regions and in the sediments under deep ocean floor at various locations world wide [19] as shown in **Fig. I-10**. In these regions, enormous quantities of natural-gas generated by methanogenic or thermogenic processes exist in the form of the gas hydrate. The composition and kind of natural gas depend on the production area and condition, but the major component of natural gas is CH_4 and there are some impurities such as C_2H_6, C_3H_8, C_2H_4, CO_2, H_2, and so on. The structure of NGH is generally considered to be s-II. In the special case that the guests consist of only methane or

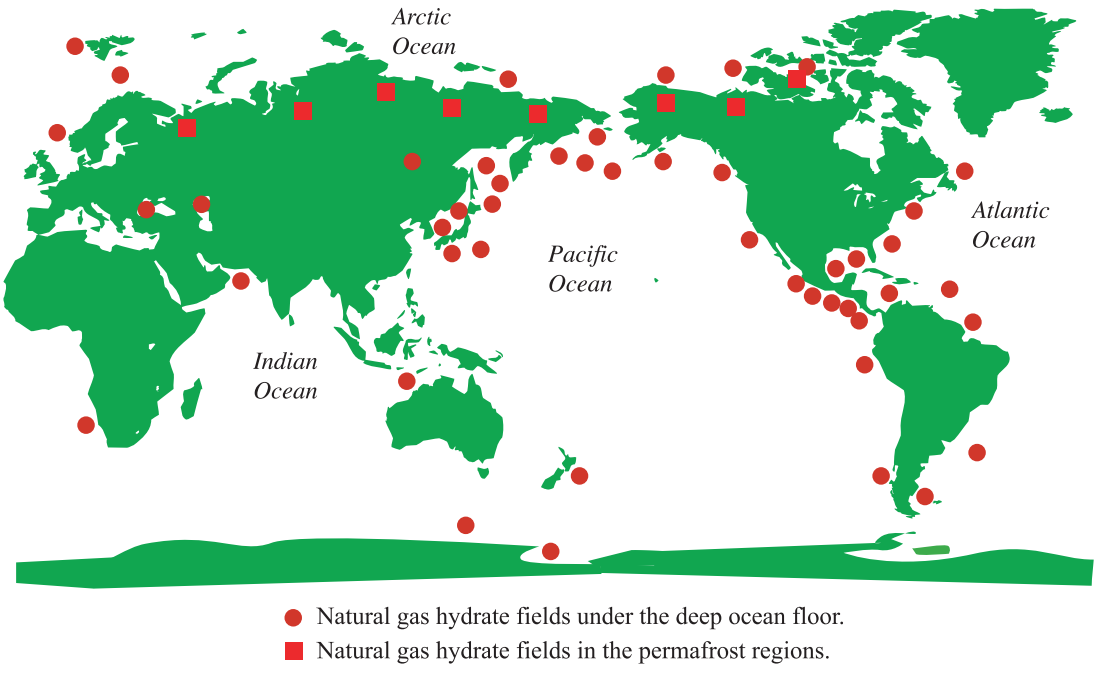

Figure I-10 NGH distribution in the world.

some large guest species such as hexane, the structure of NGH can be s-I or s-H. The NGH receives much attention as a promising unconventional energy resource instead of fossil fuels. In addition, NGH can become the source of H_2 energy, which is obtained from reforming of natural gas. However, it is not well-known that NGH has spontaneously dissociated and large quantities of gaseous methane is emitted into the atmosphere under the influence of the global warming. The global Warming Potential (GWP) of CH_4 is about twenty times as much as that of CO_2, so we have to exploit these NGH urgently in order not to make environment on the earth worse.

In order to obtain the natural gas from NGH fields, it is necessary to decompose NGH efficiently. Several methods for the recovery of natural gas from NGH fields are proposed as follows: depressurization, thermal stimulation, and inhibitor injection [20, 21]. In the depressurization, the NGH fields are depressurized below equilibrium conditions and consequently the NGH decomposes. This depressurization process is usually performed by sucking natural gas from free gas layers under the NGH fields. In the thermal stimulation, the NGH fields are heated beyond hydrate formation temperatures. Heated vapor is injected into the NGH fields and consequently the NGH decomposes. In the case of inhibitor injection, an inhibitor such as methanol (CH_3OH) is injected into the NGH fields in order to shift the hydrate equilibrium conditions to its unstable side. CH_3OH can hydrogen-bond with water molecules and consequently inhibit the hydrate formation. The most economically promising method is considered to be the depressurization technique. Recently, the innovative and potential method for the NGH exploitation is proposed, which is substituting CH_4 in the NGH fields for another guest species such as CO_2 by the difference of thermodynamic stabilities [22, 23]. The further researches have been still required and continued for developing the NGH fields as a future energy resource.

I-3.2 Medium for Natural-Gas Storage and Transportation

The NGH has also attracted much attention as a medium for the natural-gas storage and transportation technology. In Japan, liquefied natural gas (LNG) is mainly used for the long distance natural-gas transportation. However, medium- or small-scale natural-gas wells remain undeveloped because the LNG is not economical transportation method to develop these wells. The amount of natural gas reserved in these wells is considered to be more than 40 % of the total amount of natural gas. As the economical transportation method of this huge amount of natural gas, the new technique using the natural-gas hydrate pellet (NGHP, shown in **Fig. I-11**) as a medium for the natural-gas storage and transportation is proposed [24]. The NGHP is very useful for the development of medium- or small-scale wells because its initial costs are much lower than that of LNG. In addition, the NGHP can store and transport natural gas more

economically by virtue of the "self-preservation effect". This effect enables gas hydrate to reserve guest molecules for a very long period of time, nevertheless it is left under dissociation conditions [25]. As shown in **Table I-3**, the conditions of production and transportation for the NGHP are much milder than those of LNG, although the amount of transportation for the NGHP decreases because of containing water. There is little doubt but that NGHP is the potential technique in point of safety and low cost.

Figure I-11 Photo of natural-gas hydrate pellets (offered by Mitsui Engineering & ShipBuilding, Co., Ltd.).

Table I-3 Properties of natural-gas hydrate pellet (NGHP) and liquefied natural gas (LNG).

	NGHP	LNG
Transport (storage) form	Solid	Liquid
Condition of production	~MPa, > 273 K	Atmospheric pressure, 111 K
Condition of transportation	Atmospheric pressure, ~263 K	Atmospheric pressure, 111 K
Component / m^3	water: 0.8 m^3 Natural gas: 165 Nm^3	Natural gas: 600 Nm^3

As mentioned in this section, NGH is naturally occurring mixed-gas hydrate which consists of guest species of variable size and shape. For the applied techniques using gas hydrates, it is important to obtain the fundamental information about the thermodynamic properties, cage occupancies, and structures of mixed-gas hydrates containing various guest species.

I-4 Outline and Objective of This Thesis

I-4.1 Hydrogen Hydrate

H_2 hydrate is one of relatively new research themes among various studies about gas hydrates. It has long been thought that H_2 is too small to support hydrate cages by itself. In the late 1990s, Dyadin *et al.* [26] have revealed that H_2 hydrate is stable at 100-360 MPa in the

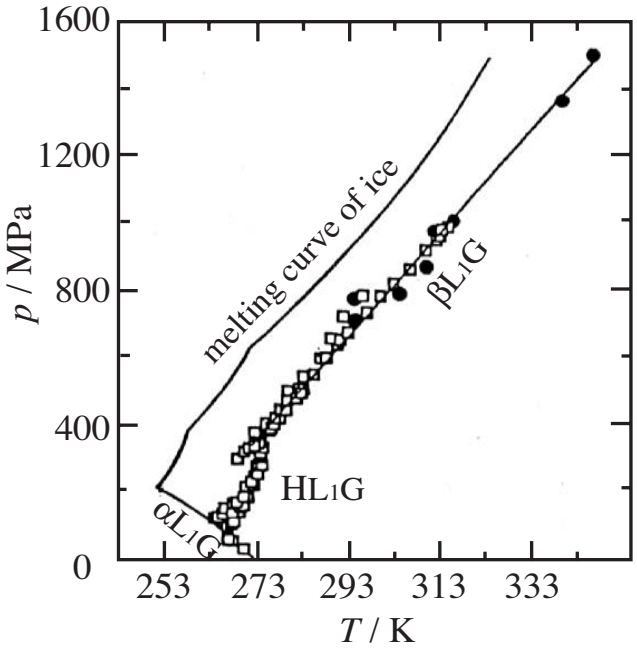

Figure I-12 Phase equilibrium relation for the H_2 + water mixed system.

vicinity of freezing point. **Figure I-12** shows the phase equilibrium (pressure - temperature) relations for the H_2 + water mixed system. The diameter of H_2 molecule is so small (0.27 nm, as shown in **Fig. I-9**) that H_2 can form interstitial solid-solution. As shown in **Fig. I-12**, the solid solution originated in the ice Ih is generated in the pressure region up to 100 MPa, while that originated in the ice II is generated in the pressure region above 360 MPa. The pure H_2 hydrate is generated only in the pressure region between two solid solution. In addition, Mao *et al.* [27] have revealed from the structural analyses using X-ray that H_2 hydrate is structure-II hydrate. In the H_2 hydrate, as shown in **Fig. I-13**, the hydrate cages are multiply occupied with a cluster of two H_2 molecules in the S-cage and four H_2 molecules in the L-cage. However, it has been recently reported from neutron diffraction that only one H_2 molecule can be encaged in the S-cage of s-II hydrate [28]. The cage occupancy of H_2 is still unclear.

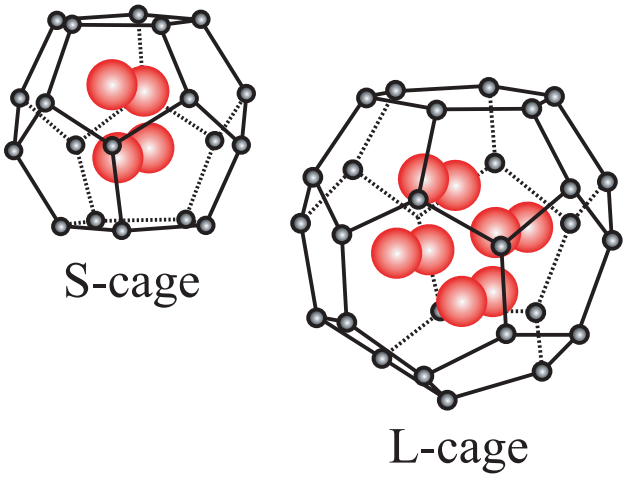

Figure I-13 Cage occupancy of H_2 in the s-II hydrate.

I-4.2 Main Objective of the Present Study

In the present study, I aim to use gas hydrates as a medium for the gas storage and transportation. As shown in **Fig. I-9**, there are a wide variety of small and large guest species which can generate clathrate hydrate by themselves or with help molecule. H_2 molecule is the smallest among various guest species. H_2 forms clathrate hydrate at high-pressure condition and diffuses freely through polygonal surfaces of hydrate cages at relatively low pressures. On the other hand, dimethylcyclohexane is one of the largest guest molecules, which requires a help gas for the hydrate formation. The thermodynamic properties on mixed gas hydrate systems which consist of these guest species are very interesting not only industrially but also scientifically.

An additive as the promoter that makes the high equilibrium pressure of pure H_2 hydrate milder is essential for the H_2 storage using gas hydrates. For the establishment of these technologies, basic thermodynamic properties (thermodynamic stability, cage occupancy and selectivity etc.) on H_2-containing hydrates were investigated by use of static and spectroscopic methods.

In this thesis, six chapters (Chapters II-VII) are divided into two parts according to the basic concept, Part A is "Thermodynamic Properties of Mixed Gas Hydrates", and Part B is "Thermodynamic Stability of Hydrogen-containing Mixed Gas Hydrates for Hydrogen Storage". The Part A consists of four chapters (Chapters II-V), and The Part B is composed of two chapters (Chapters VI and VII).

Part A: "Thermodynamic Properties of Mixed Gas Hydrates"

In the Chapters II-V, I aim to obtain the basic information for mixed gas hydrate systems containing various guest species which vary in from smallest (H_2) to largest (Dimethylcyclohexane (DMCH)). In the Chapter II, the isothermal phase equilibria containing gas hydrates for the H_2, CO_2, and water ternary system were measured by use of gas chromatography. In addition, the single crystal generated from this gas mixture was analyzed under three-phase (gas, aqueous, and hydrate phases) coexisting condition by Raman spectroscopy.

In the Chapter III, various hydrocarbons were adopted as mixed components with H_2: C_2H_6, *c*-C_3H_6, and propane (C_3H_8). The isothermal phase equilibrium relations containing gas hydrates for the three ternary system of H_2, each hydrocarbon, and water were measured by use of gas chromatography. In addition, the cage occupancies of these molecules in the hydrates were investigated under three-phase equilibrium condition by Raman spectroscopy.

In the Chapter IV, the s-H hydrate systems which are composed of DMCH stereo-isomers helped by Xe or CH_4 were studied. The stability boundaries for Xe + 1,1-, *cis*-1,2-, *trans*-1,2-, and *cis*-1,4-DMCH and CH_4 + 1,1-DMCH mixed s-H hydrate systems were measured under the four-phase (gas, aqueous, LGS, and hydrate phases) equilibrium condition. The limit of

U-cage occupancy was estimated by comparison of thermodynamic stabilities.

In the Chapter V, the measurements were carried out for the quaternary systems of H_2, CO_2, Tetrahydrofuran (hereafter, THF) or Tetra-*n*-butyl ammonium bromide (hereafter, TBAB), and water. For example, THF is well known as a additive that reduces the formation pressure of other gas hydrate systems. The effect of adding THF or TBAB to the H_2 + CO_2 + water ternary system on the equilibrium condition of the ternary system of H_2, CO_2, and water was investigated.

The important topics of these chapters are (1) the phase equilibria and stability boundaries of mixed-gas hydrates, (2) the cage occupancies of guest species, and (3) the effect of additives or LGS on the equilibrium condition. These findings have been reported in six publications, {1, 2, 3, 4, 7, 10} (see "List of Publications").

Part B: "Thermodynamic Stability of Hydrogen-containing Mixed Gas Hydrates for Hydrogen Storage"

In the Chapters VI and VII, I aimed to obtain the fundamental information for H_2 storage and transportation using gas hydrates. In the Chapter VI, THF was adopted as an additive. THF is familiar as the additive which reduces the equilibrium pressure of other gas hydrate systems. The thermodynamic stability of gas hydrate system for the ternary mixture of H_2, THF, and water were measured. The single crystals of H_2 + THF mixed gas hydrate were measured under three-phase equilibrium condition by use of Raman spectroscopy. Both measurements were carried out at the various concentrations of aqueous solutions. In addition, the effect of pressure on the cage occupancy of H_2 in mixed gas hydrate was investigated in the high-pressure regions more than 20 MPa. THF was adopted as a mixed component which is familiar as the assistant additive. Phase equilibrium measurements and Raman spectroscopic analyses were carried out for these mixed gas hydrate systems in the pressure range of 20-200 MPa. Finally, the storage capacity of H_2 in the THF hydrate was estimated by the data obtained from Raman spectroscopy.

In the Chapter VII, TBAB was adopted as an novel additive. The thermodynamic stability of H_2 + TBAB mixed gas hydrate system was measured. The cage occupancies of H_2 and TBAB were analyzed by use of Raman spectroscopic measurements. Both measurements were carried out at the various concentrations of aqueous solutions.

The important topics of this chapter are (1) dependence of thermodynamic stability and cage occupancies of each guest species on the concentrations of aqueous solutions, (2) cage selectivity of H_2, (3) pressure dependence of thermodynamic stability, cage occupancies of each guest species, and structure of H_2 + THF mixed gas hydrate. This chapter consists of four publications, {5, 6, 8, 9} (see "List of Publications").

Finally, in the final chapter (Chapter VIII), the general conclusion of the present study is summarized.

Literature Cited

[1] Lorius, C.; Jouzel, J.; Raynaud, D.; Korotkevich, E. S.; Kotlyakov, V. M. "Greenhouse Warming, Climate Sensitivity and Vostok Data.", *IAHS Publication*, **208** (Glaciers-Oceans-Atmos. Interact.), 29-47 (1991).

[2] Raynaud, D.; Jouzel, J.; Barnola, J. M.; Chappellaz, J.; Delmas, R. J.; Lorius, C. "The Ice Record of Greenhouse Gases.", *Science*, **259** (5097), 926-934 (1993).

[3] Aya, I.; Yamane, K.; Yamada, N. "Stability of Clathrate-Hydrate of Carbon Dioxide in Highly Pressurized Water.", *HTD (American Society of Mechanical Engineers),* **215**(Fundamentals of Phase Change: Freezing, Melting, and Sublimation 1992), 17-22 (1992).

[4] Shindo, Y. " Recovery and Disposal of Carbon Dioxide." *Kagaku Kogyo,* **43(8)**, 635-639 (1992).

[5] Ohgaki, K.; Hamanaka, T. "Phase-Behavior of CO_2 Hydrate-Liquid CO_2-H_2O System at High Pressure.", *Kagaku Kogaku Ronbunshu*, **21(4)**, 800-803 (1995).

[6] Ohgaki, K.; Inoue, Y. "A Proposal for Gas Storage on the Ocean Floor Using Gas Hydrates.", *Kagaku Kogaku Ronbunshu*, **17(5)**, 1053-1055 (1991).

[7] Bysby, L. R. "Hydrogen and Fuel Cells (a comprehensive guide).", PennWell Corporation (2005).

[8] Sloan, E. D., Jr. "CLATHRATE HYDRATE OF NATURAL GASES: *Second Edition, Revised and Expanded.*", MARCEL DEKKER, NEW YORK· BASEL (1998).

[9] Parrish, W. R.; Prausnitz, J. M. "Dissociation Pressures of Gas Hydrates Formed by Gas Mixtures.", *Industrial & Engineering Chemistry Process Design and Development*, **11(1)**, 26-35 (1972).

[10] Mehta, A. P.; Sloan , E. D. "Improved Thermodynamics Parameters for Prediction of Structure H Hydrate Equilibria.", *American Institute of Chemical Engineers Journal*, **42(7)**, 2036-2046 (1996).

[11] Morita, K.; Nakano, S.; Ohgaki, K. "Structure and Stability of Ethane Hydrate Crystal.",

Fluid Phase Equilibria, **169**, 167-175 (2000).

[12] Ohgaki, K.; Takano, K.; Sagawa, H.; Matsubara, T.; Nakano, S. "Methane Exploitation by Carbon Dioxide from Gas Hydrates -Phase Equilibria for CO_2-CH_4 Mixed Hydrate System-.", *Journal of Chemical Engineering of Japan*, **29(3)**, 478-473 (1996).

[13] Davy, H., "On a Combination of Oxymuriatic Gas and Oxygen Gas.", *Philosophical Transactions of the Royal Society*, **101**, 155 (1811).

[14] Subramanian, S.; Kini, R. A.; Dec, S. F.; Sloan Jr., E. D. "Evidence of Structure II Hydrate Formation from Methane + Ethane Mixtures.", *Chemical Engineering Science*, **55**, 1981-1999 (2000).

[15] Makino, T.; Tongu, M.; Sugahara, T.; Ohgaki, K. "Hydrate Structural Transition Depending on the Composition of Methane + Cyclopropane Mixed Gas Hydrate.", *Fluid Phase Equilibria*, **233**, 129-133 (2005).

[16] Kunita, Y.; Makino, T.; Sugahara, T.; Ohgaki, K. "Raman Spectroscopic Studies on Methane + Tetrafluoromethane Mixed-Gas Hydrate System." *Fluid Phase Equilibria*, **251**, 145-148 (2007).

[17] Ripmeester, J. A.; Tse, J. S.; Ratcliffe, C. I.; Powell, B. M. "A New Clathrate Hydrate Structure.", *Nature*, **325**, 135-136 (1987).

[18] Hammerschmidt, E. G. "Formation of Gas Hydrates in Natural Gas Transmission Lines.", *Industrial and Engineering Chemistry*, **26**, 851 (1934).

[19] Kvenvolden, K. A. "Methane hydrate - A Major Reservoir of Carbon in the Shallow Geosphere?", *Chemical Geology*, **71**, 41-51 (1988).

[20] Vially, R. "Les Hydrates de Gaz.", *Petrole et Techniques*, **434**, 7-10 (2001).

[21] Krason, J.; Ciesnik, M. "*Geological Evolution and Analysis of Confirmed or Suspected Gas Hydrate Localities: Gas Hydrates in the Russian Literature*.", U. S. Department of Energy, DOE/MC/21181-1950, Vol 5 (1985).

[22] Ohgaki, K.; Takano, T.; Moritoki, M. "Exploitation of CH_4 Hydrates under the Nankai Trough in Combination with CO_2 Storage.", *Kagaku Kogaku Ronbunshu*, **20(1)**, 121-123

(1994).

[23] Hirohama, S.; Shimoyama, Y.; Wakabayashi, A.; Tatsuta, S.; Nishida, N. "Conversion of CH_4-Hydrate to CO_2-Hydrate in Liquid CO_2.", *Journal of Chemical Engineering Japan*, **29(6)**, 1014-1020 (1996).

[24] Gudmundsson, J. S.; Borrehaug, A. "Frozen Hydrate for Transport of Natural Gas.", *Proceedings of 2nd International Conference of Natural Gas Hydrate*, Toulouse, France, November 29, 415 (1996).

[25] Stern, L. A.; Circone, S.; Kirby, S. H.; Durham, W. B. "Temperature, Pressure, and Compositional Effects on Anomalous of "Self" Preservation of Gas Hydrates.", *Canadian Journal of Physics*, **81(1-2)**, 271-283 (2003).

[26] Dyadin, Y. A.; Larionov, E. G.; Aladko, E. Y.; Manakov, A. Y.; Zhurko, F. V.; Mikina, T. V.; Komarov, V. Y.; Grachev, E. V. "Clathrate Formation in Water-Noble Gas (Hydrogen) Systems at High Pressures.", *Journal of Structural Chemistry*, **40**, 790-795 (1999).

[27] Mao, W. L.; Mao, H.; Goncharov, A. F.; Struzhkin, V. V.; Guo, Q.; Hu, J.; Shu, J.; Hemley, R. J.; Somayazulu M.; Zhao, Y. "Hydrogen Clusters in Clathrate Hydrate." *SCIENCE*, **297**, 2247-2249 (2002).

[28] Lokshin, K. A.; Zhao, Y.; He, D.; Mao, W. L.; Mao, H. -K.; Hemley, R. J.; Lobanov, M. V.; Greenblatt, M. "Structure and Dynamics of Hydrogen Molecules in the Novel Clathrate Hydrate by High Pressure Neutron Diffraction.", *Physical Review Letters*, **93**, 125503-1-125503-4 (2004).

Part A

Thermodynamic Properties of Mixed Gas Hydrates (Chapters II-V)

Preliminaries

Thermodynamic properties of mixed gas hydrates depend on the composition of guest molecules as well as temperature, pressure, and the size and shape of guest species. The dependency on temperature and pressure are relatively well known, because single-gas hydrates have been studied for ~200 years by a lot of researchers. However, in mixed gas hydrate systems, some unique phenomena could happen. For example, mixed gas hydrate can form the different structure, which each guest molecule cannot generate by itself, depending on the mixed composition. Therefore, we cannot predict composition dependency from investigation of only single-gas hydrates. It is very important to study mixed-gas hydrate systems which are composed of small and large guest species.

In Part A, the objective is to obtain the fundamental information about thermodynamic properties for mixed gas hydrate systems containing various guest species. These mixed systems are composed of H_2 + CO_2 + water (Chapter II), H_2 + various hydrocarbons + water (Chapter III), DMCH stereo isomers + CH_4 or Xe + water (Chapter IV). In Chapter V, two hydrosoluble molecules (THF and TBAB) are added to the ternary system of H_2 + CO_2 + water. The Chapter V plays an important role as the bridgebuilder between Part A and B.

Chapter II

Isothermal Phase Equilibria for Hydrogen + Carbon Dioxide + Water Mixtures Containing Gas Hydrate

Abstract

Isothermal phase equilibrium (pressure - composition in the gas phase) relations for the ternary system of hydrogen + carbon dioxide + water were investigated in the presence of gas hydrate phase by use of gas chromatography, which were performed at 274.3, 276.5, 280.1, and 281.9 K in a pressure range up to 10 MPa. Three-phase (gas, aqueous, and hydrate phases) equilibrium pressure increases monotonically with the hydrogen composition of gas phase at all temperature conditions. A hydrate single-crystal generated from the hydrogen + carbon dioxide + water mixture was analyzed by use of Raman spectrometer. The Raman spectra suggest that hydrogen is not enclathrated in the hydrate cages and behaves only like the diluent gas toward the formation of structure-I carbon dioxide hydrate. This fact is also supported by the thermodynamic analysis using Soave - Redlich - Kwong equation of state.

Keywords: gas hydrate; phase equilibria; gas purification; Raman spectroscopy; hydrogen; carbon dioxide

II-1 Introduction

H_2 has attracted much attention as a clean and coming energy resource. The steam reforming of hydrocarbons is well known as the H_2 production processes. The gas generated by the steam reforming is a mixture composed of CO and CO_2 as well as H_2. The Pressure Swing Adsorption (PSA) has been often used as one of the H_2 separation methods for such mixtures. In PSA method, mole fraction purity 0.999999 of H_2 is achievable. However, in the case that the on-site manufacture of H_2 is taken into consideration, a smaller-scale method is also required for H_2 separation. A new H_2 separation process using the function of gas hydrates, instead of PSA having large-scale plants, is one of the potentialities because it is possible to sieve and separate the target gas efficiently by the difference of size at relatively large pressure ranges. It is well known that H_2 is too small to generate any hydrates by itself except for a high pressure region of the GPa order [1], that is, H_2 almost never contribute to the stability of hydrate cage. On the other hand, CO_2 generates structure-I hydrate easily in the moderate condition [2, 3]. A new H_2 separation using gas hydrates [4, 5] owes to this distinction of hydrate-cage stability. This new H_2 separation technique requires the investigation of thermodynamic stability and cage occupancy on gas hydrates generated from the H_2 + CO_2 + water mixture.

In the Chapter II, the isothermal phase equilibria (pressure-composition (p - y) relation) for the ternary (H_2 + CO_2 + water) system in the presence of gas hydrate phase were measured in a temperature range of 274.3 - 281.9 K and a pressure range up to 10 MPa. The obtained p - y relations have been correlated by Soave - Redlich - Kwong equation of state under the assumption of pure CO_2 hydrate formation. In order to make sure the propriety of the above assumption, the single crystal of gas hydrates prepared from gas mixtures of H_2 + CO_2 were analyzed by use of Raman micro-spectroscopy.

II-2 Experimental Section

II-2.1 Apparatus

A schematic illustration of the experimental apparatus used in the phase equilibrium measurement is shown in **Fig. II-1**. It consists of the following parts; a high-pressure cell with glass windows (manufactured by Nezu Industries Co., Ltd.), a high-pressure pump (Shimadzu LC-6A) to supply and pressurize contents, a pressure gage, a temperature control unit, a thermometer, and composition analyzing system containing TCD-gas chromatography (TCD-GC, Shimadzu GC-14B). The inner volume and maximum working pressure of the high-pressure cell were 150 cm^3 and 10 MPa, respectively. The windows of the cell were useful for visually observing the phase behavior in the high-pressure cell. All of them are immersed in a

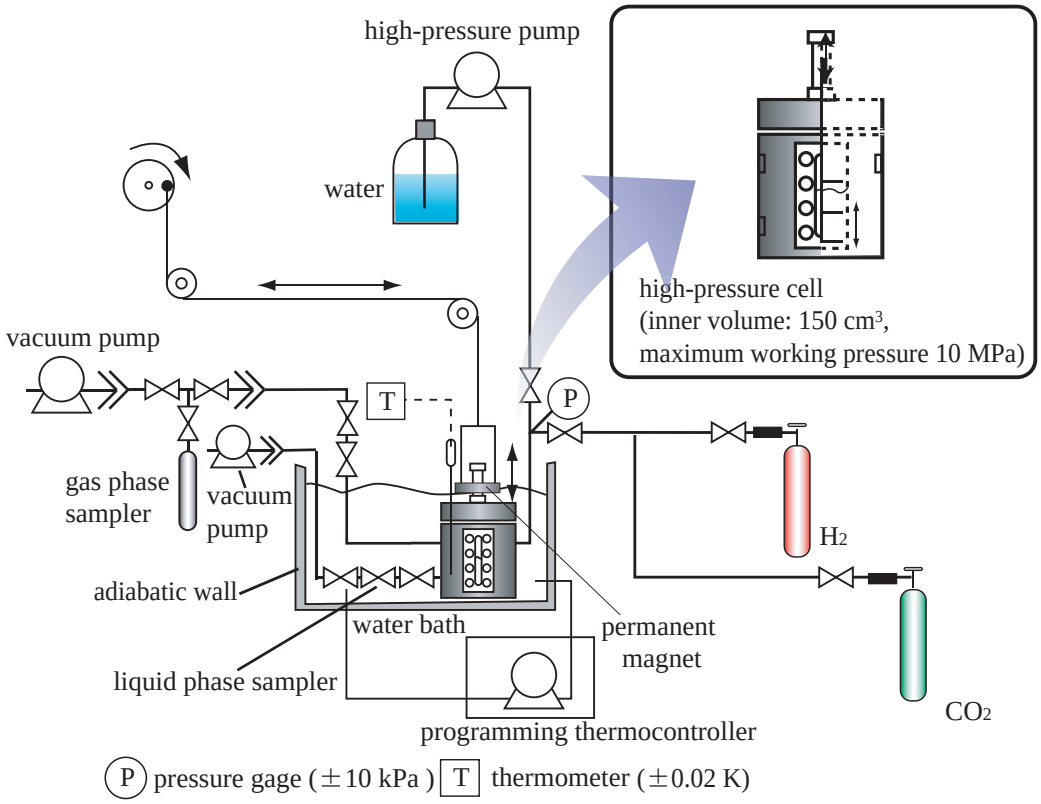

Figure II-1 Schematic illustration of experimental apparatus for phase equilibrium measurement.

temperature-controlled (by use of TAITEC coolnit CL-80R) water bath. The contents were agitated using an up-and-down mixing bar driven by an exterior permanent magnetic ring.

A schematic illustration of the experimental apparatus for Raman spectroscopic analysis is shown in Fig. **II-2**. The apparatus consists of the following parts; a high-pressure optical cell with a pair of sapphire or quartz window (manufactured by Nezu Industries Co., Ltd.), a mixing ruby-ball, a high-pressure pump to supply and pressurize contents, a pressure gage, a temperature control unit, a thermometer, a charge-coupled device (CCD) camera, and a laser Raman microprobe spectrophotometer. A schematic illustration (cross-sectional view) of the high-pressure optical cell is shown in **Fig. II-3**. The inner volume and maximum working pressure of the high-pressure optical cell were 0.2 cm^3 and 100 MPa, respectively. A pair of sapphire or quartz (highly pure) was set on both upper and lower sides (6 mm). At first, the ordinary sapphire windows were used, which the fluorescence peak derived from the impurities of sapphire window was overlapped with the H_2 vibration peaks. Therefore, the windows made of quartz (highly pure) were also adopted. Each window was sealed with a packing of Teflon type material. The thermostated water from a thermocontroller (EYELA NCB-3100) was circulated constantly in the exterior jacket of the high-pressure optical cell. A ruby ball was enclosed into the high-pressure optical cell. The contents were agitated by the ruby ball, which is rolled around by the vibration of vibrator from outside.

The system temperature was measured within an uncertainty of 0.02 K using a thermistor

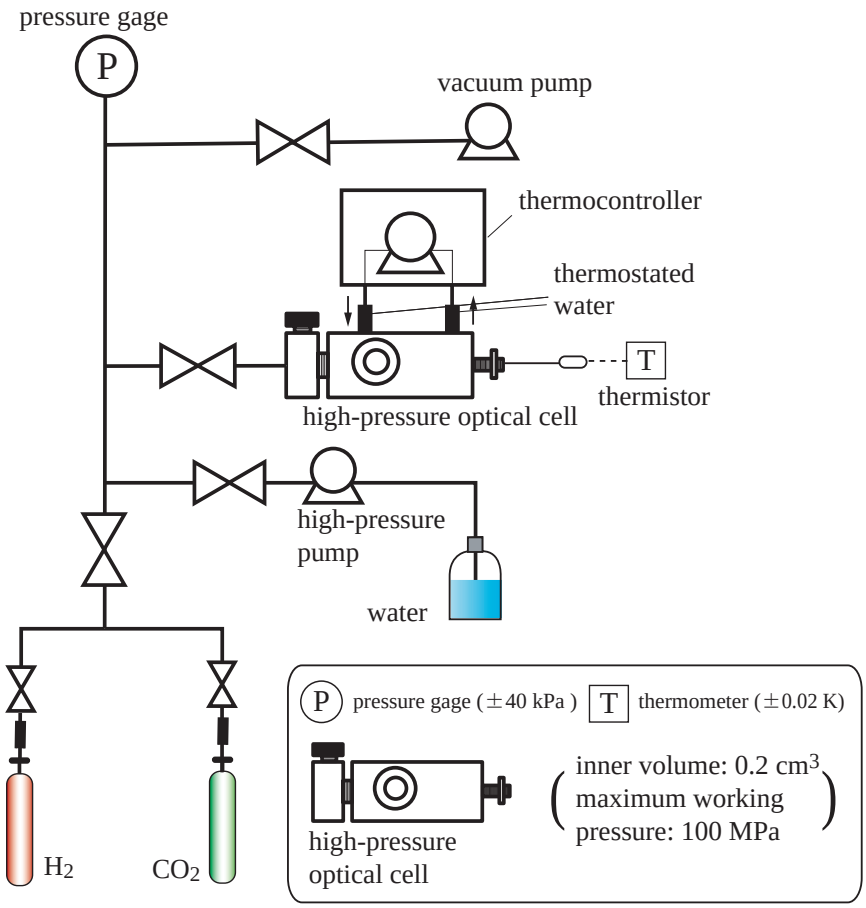

Figure II-2 Schematic illustration of experimental apparatus for Raman spectroscopic measurement.

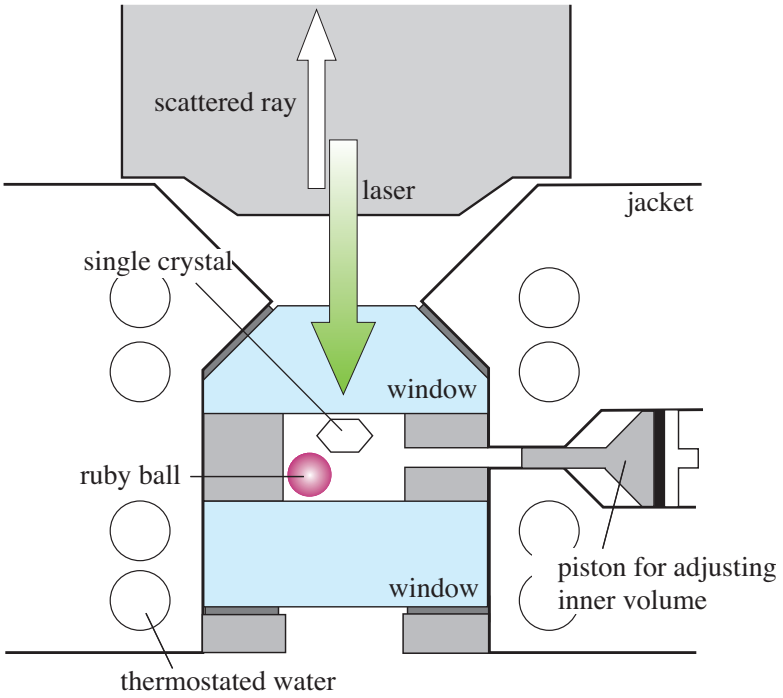

Figure II-3 Cross sectional view of high-pressure optical cell.

probe (Takara D-632), which was inserted into a hole in the cell wall. The probe was calibrated with a Pt resistance thermometer (25 Ω) defined by ITS-90. The system pressure was measured by a pressure gage (Valcom VPRT) calibrated by RUSKA quartz Bourdon tube gage (Direct Reading Pressure Gage, series 6000) with an estimated maximum uncertainty of 0.01 MPa.

II-2.2 Procedures

Phase equilibrium measurement

The H_2 and CO_2 mixture prepared at a desired composition was introduced into an evacuated high-pressure cell. The contents were pressurized up to a desired pressure by supplying water successively and then continuously agitated using the mixing bar driven by a permanent magnetic ring. After the formation of gas hydrates, the system temperature was kept constant to establish the three-phase coexisting state of hydrate + aqueous solution + gas. The phase behavior was observed straightforwardly through the window. After reaching the equilibrium state of three-phase coexistence, a small amount of gas phase was taken separately out for composition analysis. The equilibrium composition of gas phase was analyzed for H_2 and CO_2 by the TCD-Gas Chromatography (TCD-GC, Shimadzu GC-14B) as the water composition of gas phase is negligibly small under the present experimental conditions.

Thermodynamic Analysis

In the CO_2 + water binary system without H_2, the fugacity of CO_2 in the gas phase in equilibrium with the hydrate phase can be evaluated at a given temperature as:

$$f_{CO2} = \varphi_{CO2}\,(P^{e}_{CO2})\,P^{e}_{CO2} \quad (1)$$

where f_{CO2} and φ_{CO2} are the fugacity and fugacity coefficient of CO_2 at three-phase (gas + aqueous solution + hydrate) equilibrium pressure P^{e}_{CO2}, respectively. The equilibrium fugacity of pure CO_2 hydrate is correlated from experimental data by use of Eq. (2)

$$f_{CO2} = a \exp(b\,\Delta T) \quad (2)$$

where a = 0.975 MPa, b = 0.108 K^{-1}, and ΔT stands for the deviation of temperature from the quadruple point [6] of hydrate + ice + aqueous solution + gas. It is assumed that the molar volume of CO_2 hydrate is unchangeable.

In the H_2 + CO_2 + water ternary system, the equilibrium fugacity of CO_2 in the gas phase can be evaluated as:

$$f_{CO2} = y_{CO2}\, \varphi_{CO2}\,(y_{CO2}, P^{e}_{H2+CO2})\, P^{e}_{H2+CO2} \qquad (3)$$

where y_{CO2} is equilibrium composition of CO_2 in the mixed gas phase and P^{e}_{H2+CO2} stands for the three-phase (gas + aqueous solution + hydrate) equilibrium pressure.

Supposing that the generated gas hydrate is each pure CO_2 hydrate, that is, H_2 is not enclathrated in hydrate cages, the fugacity of CO_2 calculated from Eqs. (1) and (3) should coincide with each other. That is, the CO_2 hydrate cannot be generated until the fugacity of CO_2 in the gas mixture exceeds the equilibrium fugacity (Eq. (2)) of pure CO_2 hydrate system. The equation (4) is derived from Eqs. (1) and (3).

$$P^{e}_{H2+CO2} = [\varphi_{CO2}\,(P^{e}_{CO2}) \,/\, \varphi_{CO2}\,(y_{CO2}, P^{e}_{H2+CO2})]\,(P^{e}_{CO2} \,/\, y_{CO2}) \qquad (4)$$

At a given gas-phase composition, the equilibrium pressure is obtained by the trial and error method from Eq. (4) on the assumption that the equilibrium fugacity of CO_2 in gas mixture is equal to that of pure CO_2 hydrate system in the whole composition range. In the present study, the fugacity coefficient of CO_2 in the gas mixtures was calculated by use of Soave - Redlich - Kwong (SRK) equation of state [7] with the ordinary mixing rule (binary parameter: k_{12} = -0.3426) [8]. The critical constants of CO_2 and H_2 and other parameters were obtained from the reference [9].

Raman spectroscopic analysis

The H_2 and CO_2 mixture prepared at a desired composition was introduced into the evacuated high-pressure optical cell. The contents were pressurized up to a desired pressure by supplying distilled water continuously. The contents were cooled and agitated with an enclosed ruby ball to generate the gas hydrate. After the formation of hydrates, the system temperature was gradually risen to leave a few seed crystal and since then the system temperature was dropped little by little to grow the single crystal of gas hydrate under the three-phase (hydrate + aqueous solution + gas) coexisting state. A three-phase equilibrium condition with the existence of single crystal was established by keeping the temperature for more than one day. The single crystal was observed by the CCD camera through the sapphire or quartz window. The photo of single crystal is shown in **Fig. II-4**. In our laboratory, the "single crystal" was defined as the gas-hydrate crystal for which the Raman peak of intermolecular O-O vibration mode can be detected. Almost all Raman spectra were obtained from these single crystals prepared under three-phase equilibrium condition.

This single crystal of gas hydrate was analyzed by *in situ* Raman spectroscopy by use of a laser Raman microprobe spectrometer with a multichannel CCD detector. The CCD detector was maintained at ~200 K for heat-noise reduction. The argon ion laser beam (wavelength: 514.5 nm and generation power: 100 mW) and He-Ne laser beam (632.8 nm and 35 mW) condensed to 2

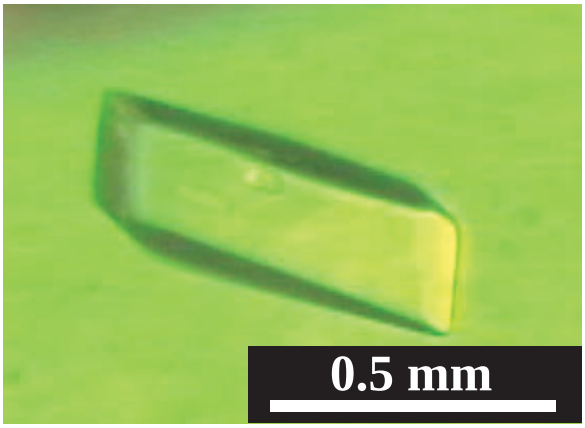

Figure II-4 A photo of hydrate single-crystal generated from H_2 + CO_2 + water mixture.

μm in spot diameter were irradiated to the single crystals from the object lens through the upper sapphire or quartz window. The backscatter of the opposite direction was taken in with the same lens. The spectral resolution was about 1 cm^{-1}. The exposed time was varied within the range 60 to 120 sec., depending on the intensity of Raman scattering. The integration number was 3 times.

II-2.3 Materials

Research grade H_2 of mole fraction purity 0.999999 was obtained from the Neriki Gas Co., Ltd. The maximum impurity was 0.2 ppm of nitrogen. Research grade CO_2 of mole fraction purity 0.9999 was obtained from the Takachiho Tradings Co., Ltd. The distilled water was obtained from the Wako Pure Chemical Industries, Ltd. All of them were used without further purifications.

II-3 Results & Discussion

II-3.1 Isothermal Phase Equilibria

The isothermal phase equilibrium (p - y) relations for the H_2 + CO_2 + water mixed system containing gas hydrate at 274.3, 276.5, 280.1, and 281.9 K are summarized in **Table II-1**, and shown in **Fig. II-5**. The three-phase equilibrium pressure increases monotonically with the composition of H_2. The variation of equilibrium pressure with the H_2 composition exhibits similar behavior in the whole temperature range of the present study. The experimental data for the pure CO_2 hydrate (left axis in **Fig. II-5**) agree well with the previous ones [2, 3]. If a gas hydrate generated from the H_2 + CO_2 mixture is the pure CO_2 hydrate, the H_2 behaves as if it is

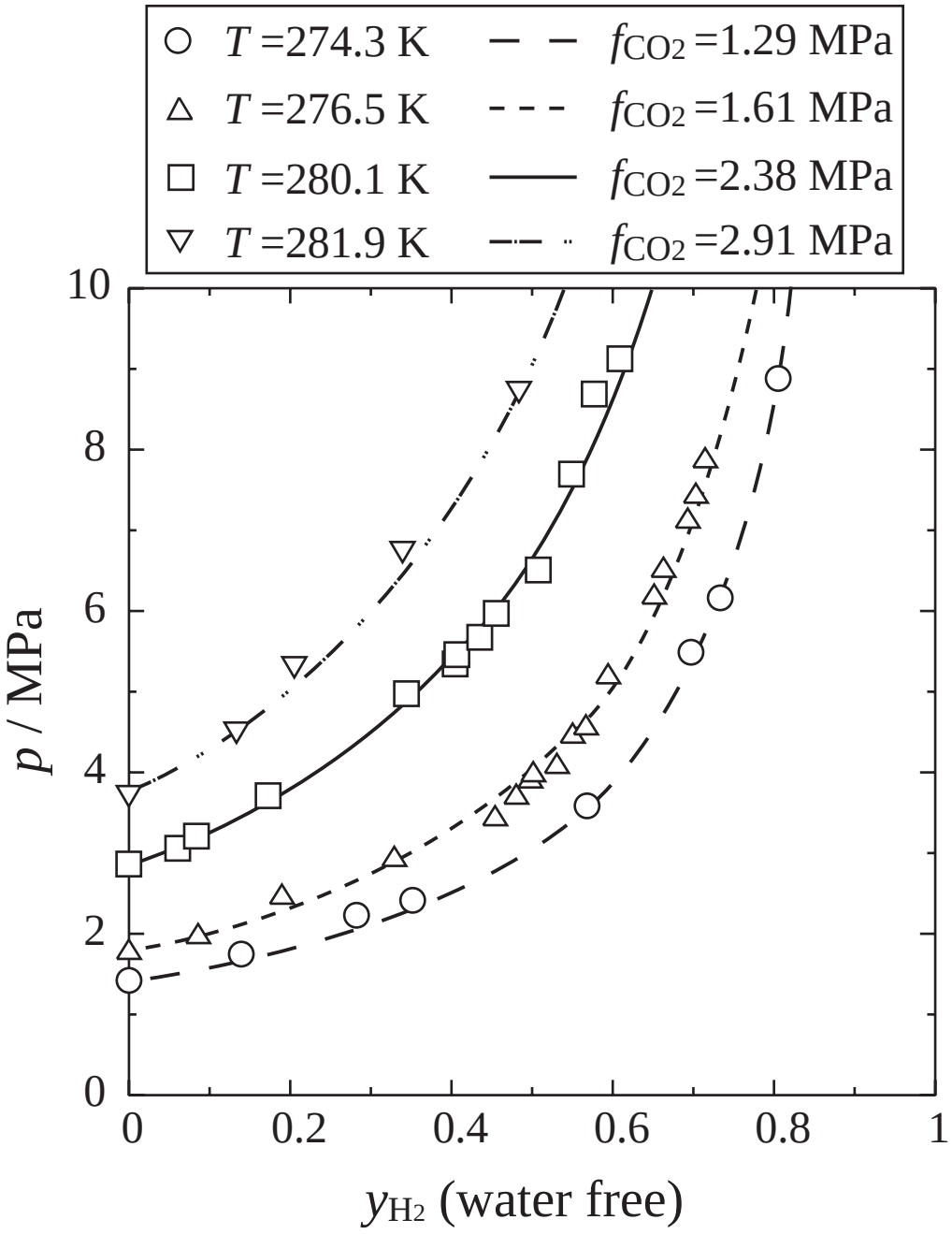

Figure II-5 Isothermal phase equilibrium (pressure - composition in the gas phase) relations for H_2 + CO_2 + water mixed system in the presence of gas hydrate phase.

only like a diluent gas. That is, the CO_2 hydrate is generated at considerably high total pressures where the CO_2 fugacity in the gas mixture exceeds the equilibrium fugacity of pure CO_2 hydrate system. At a given temperature and gas-phase composition, the total pressure is obtained by numerical calculation in order to give the equilibrium fugacity of pure CO_2 hydrate. The estimated results agree well with the experimental equilibrium pressures as shown in **Fig. II-5**.

Table II-1 Isothermal phase equilibrium data for H_2 + CO_2 + water mixed system in the presence of gas hydrate phase.

T / K	y_{H2}	p / MPa	T / K	y_{H2}	p / MPa
274.3	0.000	1.42		0.693	7.15
	0.140	1.75		0.704	7.46
	0.282	2.23		0.715	7.90
	0.352	2.42	280.1	0.000	2.86
	0.568	3.58		0.061	3.06
	0.697	5.49		0.084	3.21
	0.734	6.16		0.173	3.71
	0.805	8.89		0.345	4.98
276.5	0.000	1.81		0.405	5.35
	0.086	1.99		0.407	5.46
	0.190	2.49		0.435	5.67
	0.329	2.96		0.456	5.97
	0.455	3.46		0.508	6.51
	0.481	3.73		0.549	7.70
	0.497	3.93		0.577	8.69
	0.502	4.01		0.609	9.13
	0.530	4.10	281.9	0.000	3.70
	0.551	4.48		0.134	4.50
	0.566	4.58		0.205	5.30
	0.594	5.23		0.340	6.73
	0.651	6.21		0.484	8.71
	0.664	6.54			

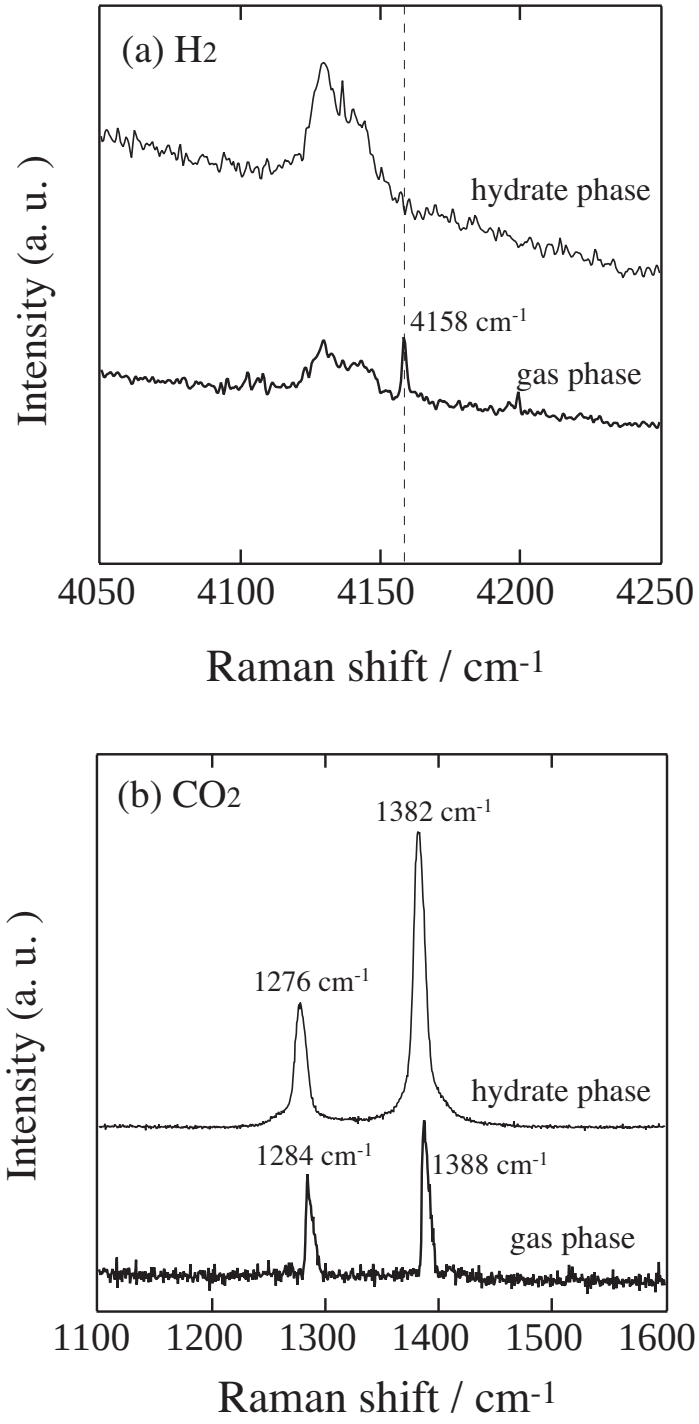

Figure II-6 Raman spectra of the intramolecular vibration for H_2 (a) and CO_2 (b) molecules in the gas and hydrate phases. Raman peaks from 4120 to 4150 cm^{-1} are due to the sapphire window of the high-pressure optical cell.

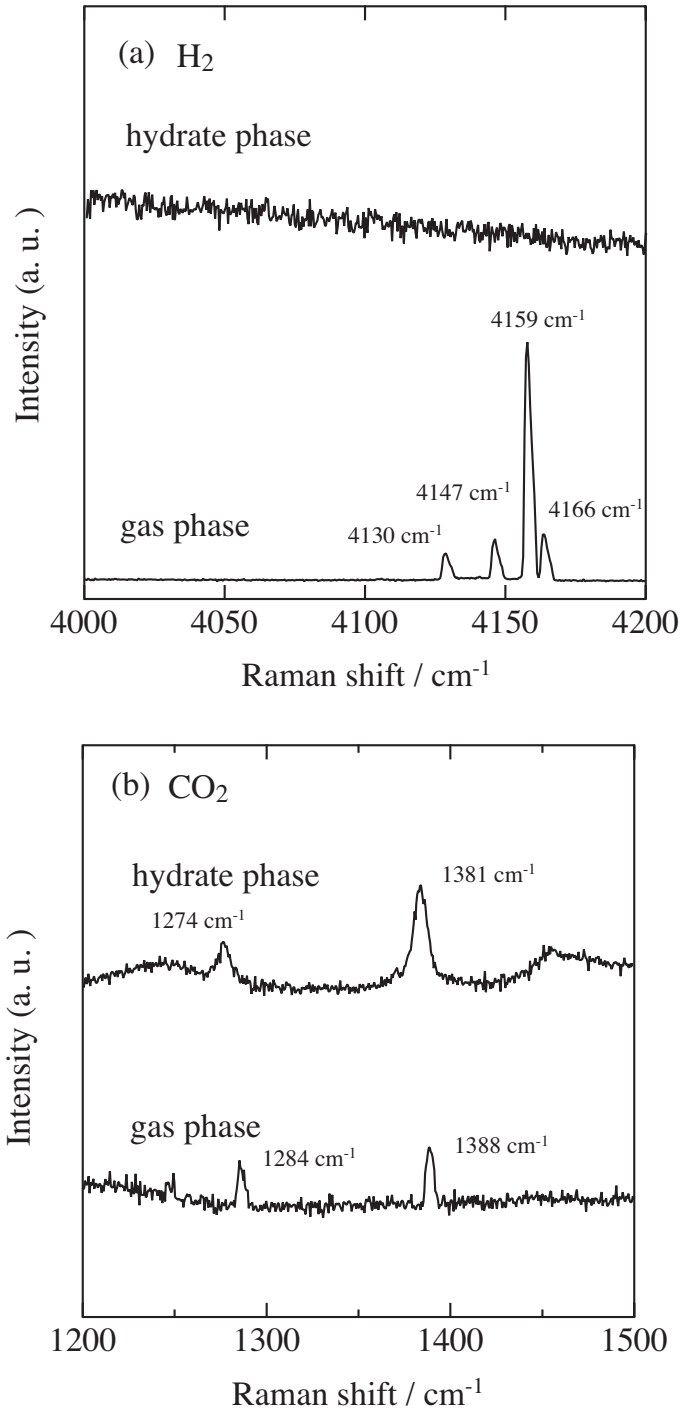

Figure II-7 Raman spectra of the intramolecular vibration for H_2 (a) and CO_2 (b) molecules in the gas and hydrate phases, which are obtained by use of quartz windows and Ar ion laser.

II-3.2 Raman Spectroscopic Analysis

Raman spectra of the intramolecular vibration of H_2 and CO_2 at 274.6 K and 15.2 MPa are shown in **Fig. II-6**(a) and (b). In order to avoid the optical effect of sapphire window, the spectra of CO_2 are given by the irradiation of the Ar ion laser, on the other hand, the spectra of H_2 are by the He-Ne laser. The Raman peaks of the intramolecular symmetric C=O stretching vibration

mode of CO_2 are detected in both gas and hydrate phases and the spectra exhibit the double peaks because of the Fermi resonance effect. There is no significant difference from the Raman shifts of pure CO_2 hydrate [10] at the same pressure. On the other hand, the Raman peak of the H-H stretching vibration mode of H_2 is detected in the gas phase, while it is not detected in the hydrate phase. In order to re-confirm it clearly, Raman spectra were measured using quartz windows instead of ordinary sapphire ones. **Fig. II-7**(a) and (b) show Raman spectra using quartz windows (Ar ion laser) in the gas phase and hydrate generated from H_2 + CO_2 + water mixture at 276.5 K and 11.2 MPa under the three-phase equilibrium condition, respectively. As shown in **Fig. II-7**(a), the fluorescence peak derived from the impurities of window materials can be eliminated by use of quartz window. The quadruplet peak derived from fluid H_2 is clearly detected, while no peak is detected in the hydrate phase. The Raman peaks of CO_2 (**Fig. II-7**(b)) agree well with those using sapphire windows. According to Mao *et al*. [11] and Mao and Mao

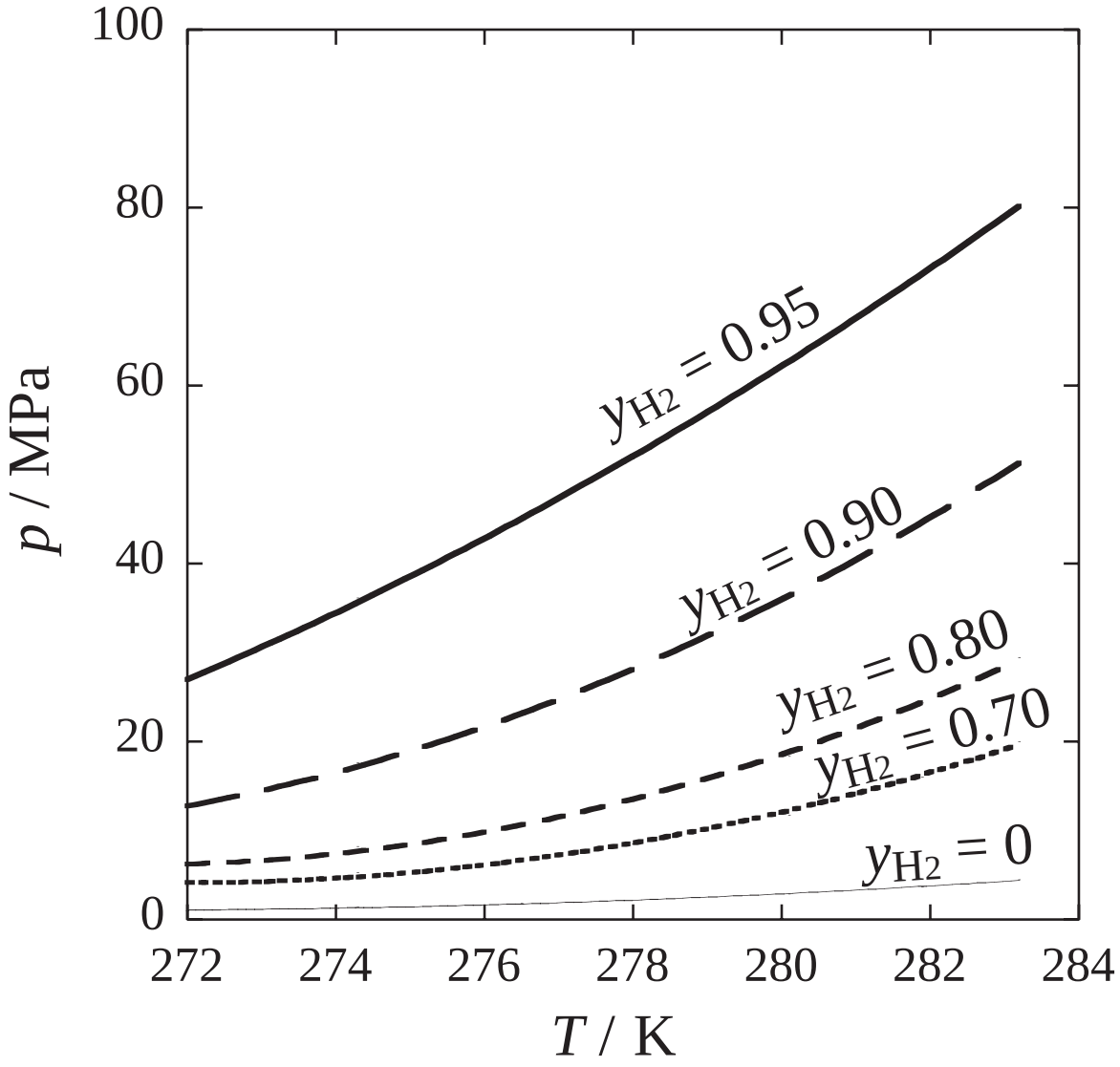

Figure II-8 Pressure - temperature projection estimated by Soave - Redlich - Kwong equation of state for H_2 + CO_2 + water mixed system in the presence of gas hydrate phase.

[12], H_2 and water mixtures generate the s-II hydrate at the high-pressure of 200 MPa or the low temperature of about 80 K, where the hydrate cages are multiply occupied with a cluster of two H_2 molecules in the S-cage and four H_2 molecules in the L-cages. The peak corresponding to such H_2 cluster is not detected in the single crystal of gas hydrate prepared from the H_2 + CO_2 mixture in the present study.

II-3.3 Development for Applied Process

The above results reveal that H_2 is not enclathrated in hydrate-cages and behaves only like the diluent gas toward the formation of CO_2 hydrate. At a given temperature, the CO_2 fugacity of gas phase in equilibrium with liquid phase and CO_2 hydrate is calculated from the three-phase coexisting curve of pure CO_2 hydrate. The equilibrium pressure of gas mixture is uniquely obtained at given temperature and mole fraction of gas phase from the above assumption. Therefore, it is possible to estimate the equilibrium pressure - temperature - composition relations by extrapolating the experimental data under the CO_2 - fugacity - constant conditions. The estimated equilibrium pressure - temperature projections in this system are shown in **Fig. II-8**. Four curves in **Fig. II-8** stand for the constant composition of gas phase. The operation temperature of separation process can be estimated under a desired pressure and composition. For example, in order to purify the H_2 + CO_2 mixture into y_{H2} = 0.90 or 0.95 at 40 MPa, the operation temperature of separation process is about 275 K or 281 K, respectively.

II-4 Summary

Isothermal phase equilibria (pressure - composition relations) and Raman spectra for the ternary system of H_2 + CO_2 + water in the presence of hydrate phase were investigated. The results of thermodynamic and Raman spectroscopic analysis reveal that H_2 is not entrapped with the hydrate cages. That is, the hydrate generated from the H_2 + CO_2 + water mixture is pure CO_2 s-I hydrate and H_2 behaves only like a diluent gas toward the formation of CO_2 hydrate. It is possible to estimate the three-phase equilibrium relations (pressure - temperature - composition) of gas hydrate prepared from the H_2 mixtures.

Notation

f: fugacity [Pa]
k: binary parameter for Soave - Redlich - Kwong equation of state [-]

p: pressure [Pa]
T: temperature [K]
y: composition of gas phase [-]
ϕ: fugacity coefficient [-]

Literature Cited

[1] Dyadin, Y. A.; Larionov, E. G.; Aladko, E. Y.; Manakov, A. Y.; Zhurko, F. V.; Mikina, T. V.; Komarov, V. Y.; Grachev, E. V. "Clathrate Formation in Water-Noble Gas (Hydrogen) Systems at High Pressures.", *Journal of Structural Chemistry*, **40**, 790-795 (1999).

[2] Robinson, D. B.; Mehta, B. R. "Hydrates in the Propane - Carbon Dioxide - Water System", *Journal of Cannadian Petroleum Technology*, **10**, 33-35 (1971).

[3] Ohgaki, K.; Makihara, Y.; Takano, K. "Formation of CO_2 Hydrate in Pure and Sea Waters.", *Journal of Chemical Engineering of Japan*, **26**, 558-564 (1993).

[4] Holder, G. D.; Stephenson, J. L.; Joyce, J. J.; John, V. T.; Kamath, V. A.; Malekar, S. "Formation of Clathrate Hydrates in Hydrogen-rich Gases.", *Industrial & Engineering Chemistry Process Design and Development* , **22**, 170-171 (1983).

[5] Zhang, S. -M.; Chen, G. -J.; Ma, C. -F.; Yang, L. -Y.; Guo, T. -M. "Hydrate Formation of Hydrogen + Hydrocarbon Gas Mixtures.", *Journal of Chemical Engineering Data*, **43**, 807-810 (2000).

[6] Anderson, G. K. "Enthalpy of Dissociation and Hydration Number of Carbon Dioxide Hydrate from the Clapeyron Equation.", *Journal of Chemical Thermodynamics*, **35**, 1171-1183 (2003).

[7] Soave, G. "Equilibrium Constants from a Modified Redlich - Kwong Equation of State.", *Chemical Engineering Science*, **27**, 1197-1203 (1972).

[8] Reid, R. C.; Prausnitz, J. M.; Poling, B. E. "The Properties of Gases and Liquids, 4th ed.", McGraw - Hill, New York, (1986).

[9] Knapp, H.; Doring, R.; Oellrich, L.; Plocker, U.; Prausnitz, J. M. "Vapor - Liquid Equilibria for Mixtures of Low Boiling Substances, Chemistry Data Series, vol. VI.", Dechema, Frankfult (1982).

[10] Nakano, S.; Ohgaki, K.; Moritoki, M. "High-pressure Phase Equilibrium and Raman Microprobe Spectroscopic Studies on the CO_2 Hydrate System", *Journal of Chemical Engineering Data*, **43**, 807-810 (1998).

[11] Mao, W. L.; Mao, H.; Goncharov, A. F.; Struzhkin, V. V.; Guo, Q.; Hu, J.; Shu, J.; Hemley, R. J.; Somayazulu, M.; Zhao, Y. "Hydrogen Clusters in Clathrate Hydrate.", *SCIENCE*, **297**, 2247-2249 (2002).

[12] Mao, W. L.; Mao, H. "Hydrogen Storage in Molecular Compounds.", *Proceedings of the National Academy of Sciences of the USA*, **101**, 708-710 (2004).

Chapter III

Thermodynamic and Raman Spectroscopic Studies on Hydrocarbon Hydrates Coexisting with Hydrogen and Aqueous Solutions

---

Abstract

Hydrogen hydration in the gas hydrates generated from three ternary mixtures of hydrogen + hydrocarbon (ethane, cyclopropane, or propane) + water have been studied by use of Raman spectroscopic analyses at 276.1 K. The Raman spectra reveal that hydrogen is enclathrated in the small hydrate cage for the mixture of hydrogen, propane, and water only. In addition, isothermal phase equilibria (pressure - composition in the gas phase) for three ternary systems of hydrogen + hydrocarbon (ethane, cyclopropane, or propane) + water have been measured at 276.1 K in the pressure range from 0.1 to 5 MPa. The thermodynamic analysis using Soave - Redlich - Kwong equation of state supports that hydrogen is enclathrated in the hydrate cage for only the mixture of hydrogen, propane, and water, even in the lower pressure than 5 MPa at 276.1 K.

Keywords: gas hydrate; phase equilibria; cage occupancy; hydrogen; hydrocarbon; gas storage

III-1 Introduction

The separation, storage, and transportation of H_2 are one of the most important techniques for developing a new society sustained by H_2 energies. The generation of pure s-II H_2 hydrate requires an extremely high pressure of 100 - 360 MPa at ambient temperatures [1]. The hydrate cages are multiply occupied with a cluster of two H_2 molecules in the S-cage and four H_2 molecules in the L-cage, respectively [2]. Recently, it has been reported that H_2 and tetrahydrofuran (hereafter, THF) can form the mixed gas hydrate at much milder condition than pure H_2 hydrate [3-5]. For the application of gas hydrates to above techniques, it is necessary to reveal the thermodynamic properties of H_2-containing mixed hydrate as well as pure H_2 hydrate.

In the Chapter II, phase equilibria containing gas hydrate for the ternary system of H_2 + CO_2 + water have been investigated at 274.3 - 281.9 K up to 10 MPa. The s-I CO_2 hydrate generated from the mixture cannot entrap the H_2 molecule. On the other hand, it has been revealed that the THF molecule occupies the L-cage completely while the H_2 occupies the S-cage of s-II hydrate (q. v. Chapter VI) [5]. Zhang *et al*. [6] and Klauda and Sandler [7] have reported that H_2 may partially fill the hydrate cages with other guest species. Hence, the H_2 occupation may depend on the mixed other component and the type of unit-cell structure as well as the pressure and temperature conditions. In order to make clear the mechanism of H_2 enclathration, it is important to investigate other H_2 mixed systems.

In the Chapter III, the hydrate-cage occupancies of each hydrocarbon and H_2 are investigated for the three ternary systems of H_2, light hydrocarbon (ethane (C_2H_6), cyclopropane (*c*-C_3H_6), or propane (C_3H_8), and water by use of *in situ* Raman micro-spectroscopy at 276.1 K in a pressure range up to 2 MPa. In addition, the isothermal phase equilibria (pressure - composition relation) for the H_2 + each hydrocarbon + water ternary system have been measured at 276.1 K in a pressure range of 0.1 to 5 MPa. Both C_2H_6 and *c*-C_3H_6 form the s-I hydrate, on the other hand, C_3H_8 generates the s-II hydrate under the present experimental conditions. These hydrocarbon hydrates have empty S-cages in a low-pressure region.

III-2 Experimental Section

III-2.1 Apparatus

The experimental apparatus for the phase equilibrium measurements were the same as the one in the Chapter II. A detail description was given in the previous chapter.

The experimental apparatus for the Raman spectroscopic analysis were the same as the one in the Chapter II except for the high-pressure optical cell. A schematic illustration (cross-sectional view) of the high-pressure optical cell is shown in **Fig. III-1**. The inner volume

and maximum working pressure of the high-pressure optical cell were 0.2 cm^3 and 400 MPa, respectively. The high-pressure optical cell for the Raman spectroscopic analysis has a pair of quartz (highly pure) windows on both the upper and lower sides (6 mm). Each window was sealed with a packing of Teflon type material. In the Chapter II, the ordinary sapphire windows were mainly used, however, the fluorescence peak derived from the impurities of sapphire window was overlapped with the H_2 vibration peaks. Therefore, the windows made of quartz (highly pure) were adopted in the Chapter III. The thermostated water was circulated constantly in the exterior jacket of high-pressure optical cell. A ruby ball was enclosed to agitate the contents by the vibration from outside.

The system temperature was measured within an uncertainty of 0.02 K using a thermistor probe (Takara D-632), which was inserted into a hole in the cell wall. The probe was calibrated with a Pt resistance thermometer defined by ITS-90. The system pressure was measured by a pressure gage (Valcom VPRT) calibrated by RUSKA quartz Bourdon tube gage (Direct Reading Pressure Gage, series 6000) with an estimated maximum uncertainty of 0.01 MPa.

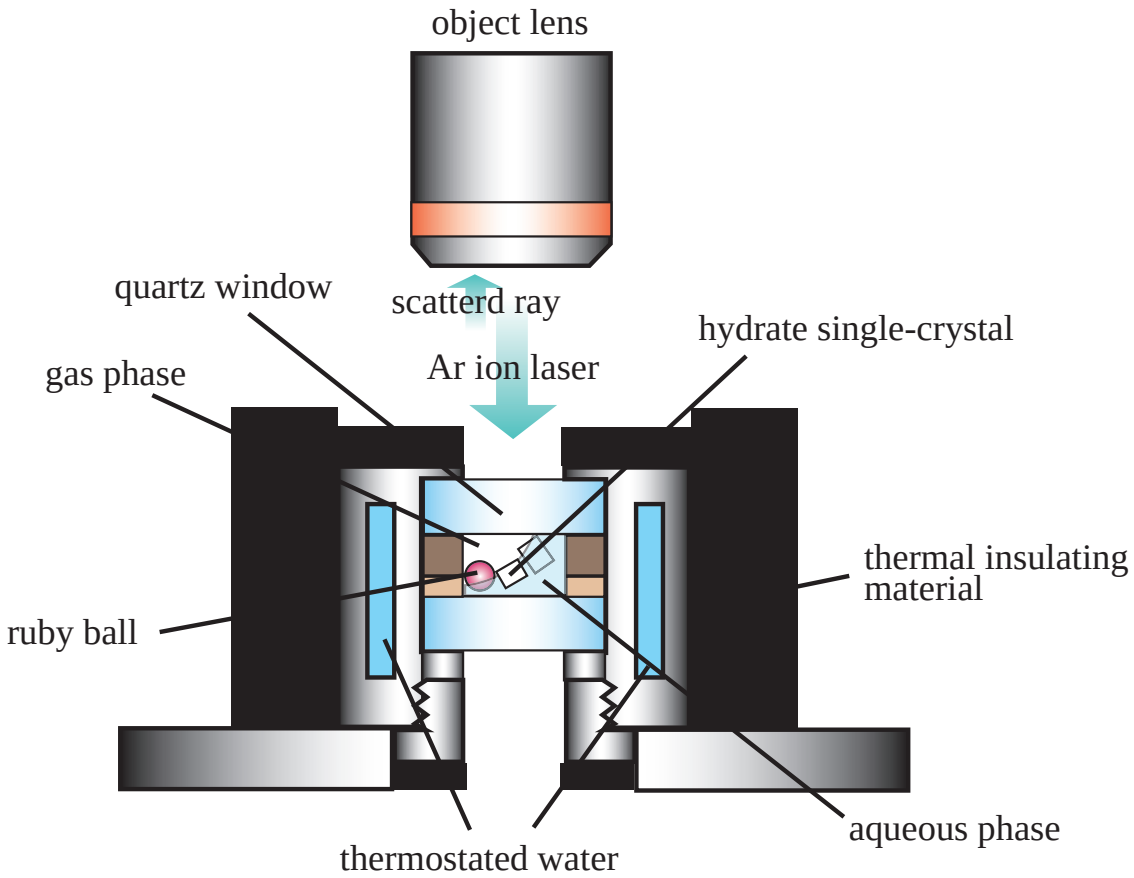

Figure III-1 Cross sectional view of high-pressure optical cell.

III-2.2 Procedures

Phase equilibrium measurement

The gas mixture of H_2 and each hydrocarbon prepared at a desired composition was introduced into the evacuated high-pressure cell. A detail description of the following procedures was given in the previous chapter.

Raman spectroscopic analysis

The distilled water was introduced into the evacuated high-pressure optical cell. The contents were pressurized up to a desired pressure by supplying H_2 and hydrocarbon mixture prepared at a desired composition continuously. The procedure for the preparation of hydrate single-crystal was similar to that of the Chapter II. The single crystal was observed by the CCD camera through the quartz window. Almost all Raman spectra were obtained from the single crystals prepared under three-phase equilibrium condition.

This single crystal of gas hydrate was analyzed by *in situ* Raman spectroscopy by use of a laser Raman microprobe spectrometer with a multichannel CCD detector. The CCD detector was maintained at ~200 K for heat-noise reduction. The argon ion laser beam (wavelength: 514.5 nm and generation power: 100 mW) condensed to 2 μm in spot diameter were irradiated to the single crystals from the object lens through the upper quartz window. The backscatter of the opposite direction was taken in with the same lens. The spectral resolution was about 1 cm^{-1}. The exposed time was varied within the range 60 to 120 sec., depending on the intensity of Raman scattering. The spectra were obtained with three or four integrations.

Thermodynamic analysis

The method used in the Chapter II were also adopted in the Chapter III to calculate the equilibrium pressure and compare the experimental results with the estimated data. The fugacity coefficient of hydrocarbon in the gas mixture was calculated by Soave - Redlich - Kwong equation of state [8] with the ordinary mixing rule (binary parameter: k_{12} = 0.1867 (H_2 + C_2H_6), 0.0 (H_2 + *c*-C_3H_6), 0.2359 (H_2 + C_3H_8)) [9]. The applicable binary parameter for the H_2 + *c*-C_3H_6 system could not be found, therefore, the value of k_{12} = 0.0 for the H_2 + *c*-C_3H_6 system is compelled to be used. The critical constants of hydrocarbons and H_2 and other parameters were obtained from the reference [10].

III-2.3 Materials

Research grade H_2 (mole fraction purity 0.999999) was obtained from the Neriki Gas Co., Ltd. The maximum impurity was 0.2 ppm of nitrogen. Research grade C_2H_6, c-C_3H_6, and C_3H_8

(mole fraction purity 0.999, 0.995, and 0.9999, respectively) were obtained from the Takachiho Tradings Co., Ltd. The distilled water was obtained from the Wako Pure Chemical Industries, Ltd. All of them were used without further purifications.

III-3 Results & Discussion

III-3.1 Isothermal Phase Equilibria

The isothermal phase equilibria for the three ternary systems containing gas hydrate at 276.1 K are summarized in **Table III-1**, and shown in **Fig. III-2**. The present experimental data on the each pure hydrocarbon hydrate (left axis in **Fig. III-2**) agree well with the previous data (C_2H_6 [11], *c*-C_3H_6 [12, 13], and C_3H_8 [14] hydrates). The three-phase equilibrium pressure

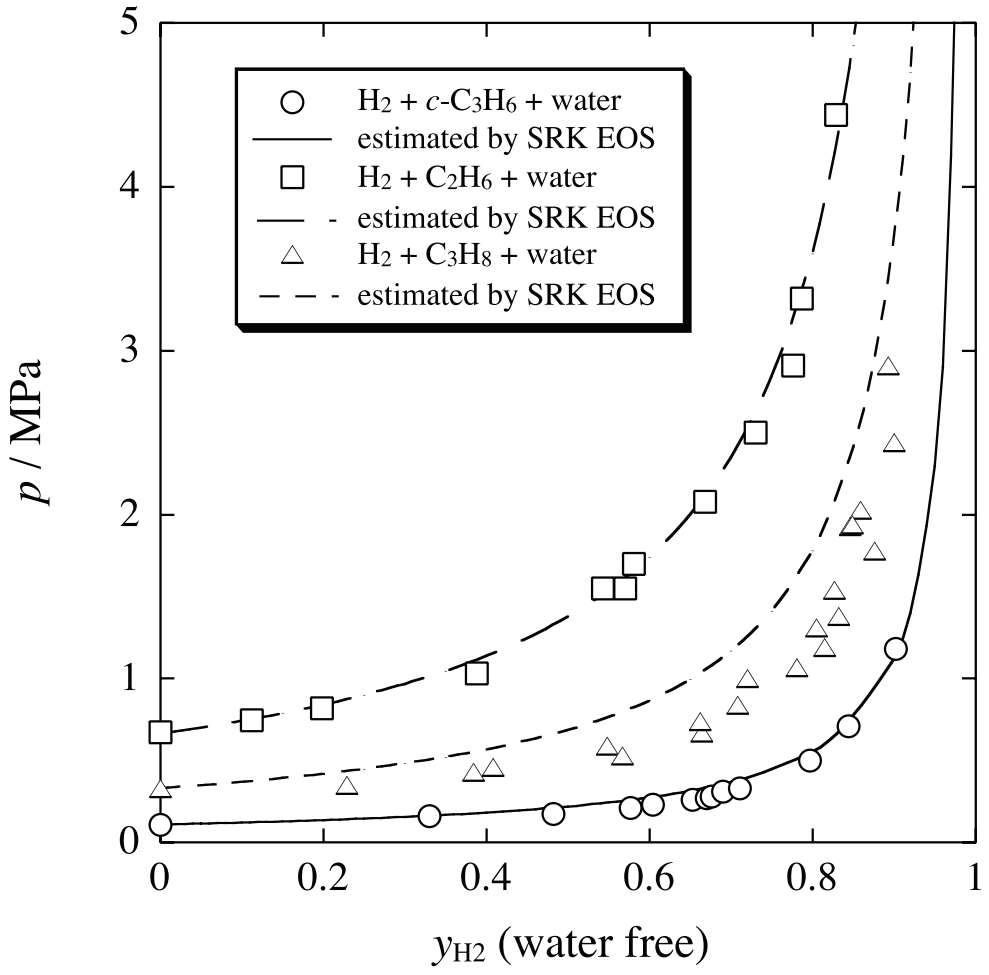

Figure III-2 Isothermal three-phase equilibrium (pressure - composition) relations for the H_2 + each hydrocarbon + water mixed systems at 276.1 K. The curves are estimated pressures by numerical calculations on the assumption that the equilibrium fugacity of hydrocarbon in gas mixture is equal to that of pure hydrocarbon hydrate system in the whole composition range.

Table III-1 Phase equilibrium data for the H_2 + hydrocarbon + water mixed system in the presence of gas hydrate.

Additive	y_{H2}	p / MPa	Additive	y_{H2}	p / MPa
c-C_3H_6	0.00	0.11		0.79	3.32
	0.33	0.16		0.83	4.44
	0.48	0.18	C_3H_8	0.00	0.33
	0.58	0.21		0.23	0.35
	0.60	0.23		0.38	0.43
	0.65	0.26		0.41	0.46
	0.67	0.27		0.57	0.53
	0.68	0.28		0.55	0.59
	0.69	0.31		0.66	0.67
	0.71	0.33		0.66	0.74
	0.80	0.50		0.71	0.84
	0.84	0.71		0.72	1.00
	0.90	1.18		0.78	1.07
C_2H_6	0.00	0.67		0.82	1.19
	0.11	0.75		0.81	1.31
	0.20	0.82		0.83	1.38
	0.39	1.03		0.83	1.54
	0.54	1.55		0.88	1.78
	0.57	1.55		0.85	1.93
	0.58	1.70		0.85	1.94
	0.67	2.08		0.86	2.03
	0.73	2.50		0.90	2.44
	0.78	2.91		0.89	2.91

increases monotonically with the increase of H_2 mole fraction. The curves in **Fig. III-2** are estimated pressures by Eq. (3) (in the Chapter II) on the assumption that the equilibrium fugacity of hydrocarbon in gas mixture is equal to that of pure hydrocarbon hydrate system in the whole composition range. In both H_2 + C_2H_6 + water and H_2 + *c*-C_3H_6 + water systems, the estimated pressures agree well with the experimental pressures as shown in **Fig. III-2**. On the

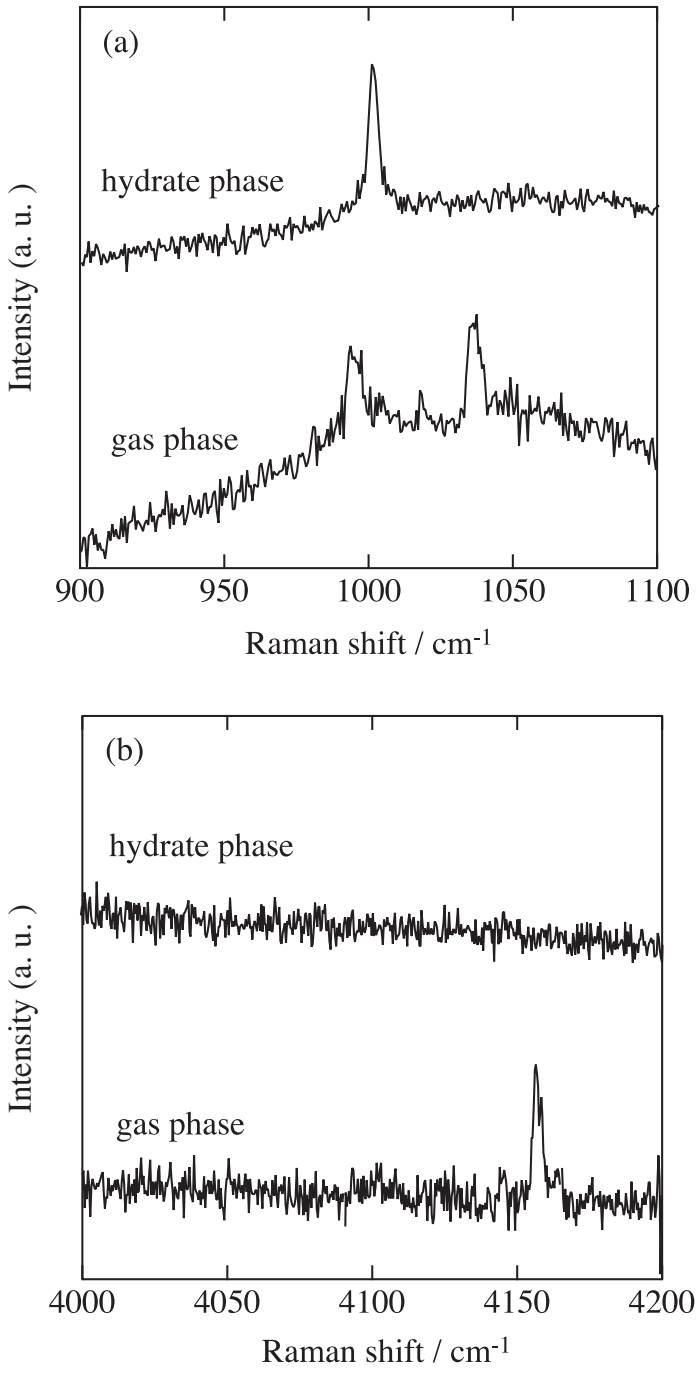

Figure III-3 Raman spectra of the intramolecular vibration for C_2H_6 (around 1000 cm^{-1}) (a), and around 4100 cm^{-1} (b) in the gas and hydrate phases for the H_2 + C_2H_6 + water mixture at 1.95 MPa, y_{H2} = 0.62, and 276.1 K. Panel (a) contains the Raman peak (around 1030 cm^{-1}) corresponding to the rotation of H_2.

other hand, the experimental pressures shift to the high-temperature or low-pressure side of the estimated pressures in the H_2 + C_3H_8 + water mixed system. This indicates that the hydrate phase would be changed from the pure C_3H_8 hydrate to the mixed C_3H_8 one. In other words, there is a possibility that H_2 can be enclathrated in the hydrate generated from H_2 + C_3H_8 + water mixture.

The hydrates prepared from gas mixtures at 276.1 K were quenched and taken out from the high-pressure cell at 243 K. After the dissociation of gas hydrate, gas sample was analyzed by use of the TCD-Gas chromatography. The mole fraction of H_2 (water free) in the dissociation gas of the hydrate generated from H_2 + C_3H_8 gas mixture is about 0.2 at 276.1 K and 1.5 MPa, which supports the above experimental data. About ten percent of S-cages in the s-II hydrate are occupied by H_2 molecule at such mild condition. In the H_2 + C_2H_6 gas mixture as a typical system of no Raman peak of H_2, the mole fraction (water free) of H_2 in the dissociation gas is less than 0.001.

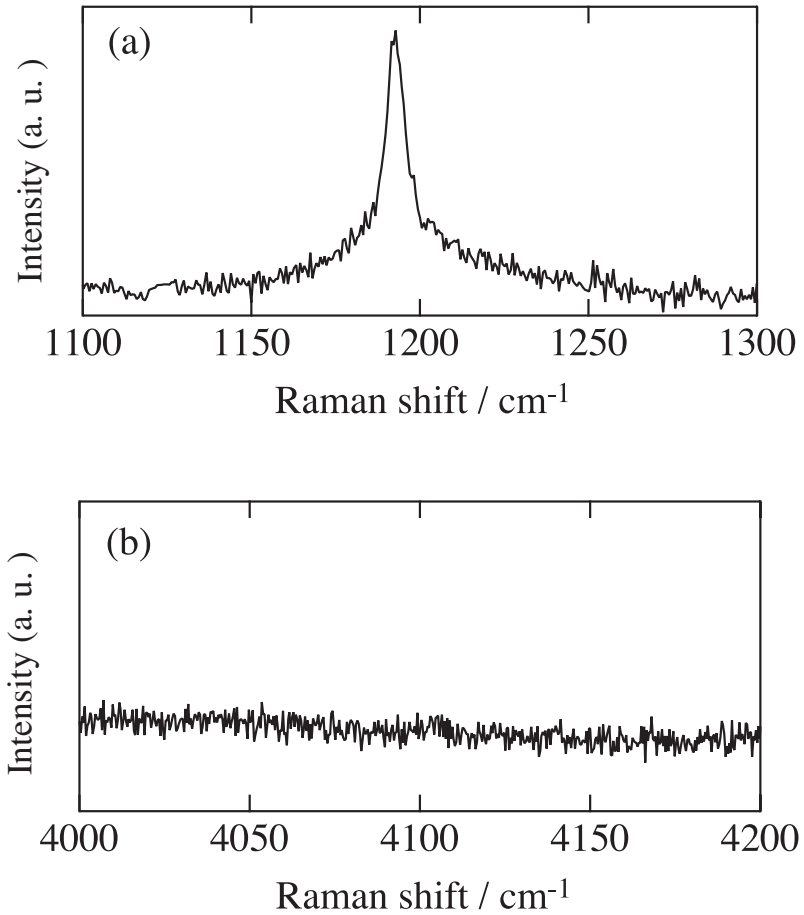

Figure III-4 Raman spectra of the intramolecular vibration for *c*-C_3H_6 (a), and around 4100 cm^{-1} (b) in the hydrate generated from the H_2 + *c*-C_3H_6 + water mixed system at 0.403 MPa, y_{H2} = 0.71, and 276.1 K.

III-3.2 Raman Spectroscopic Analysis

The Raman spectra obtained in the present study are shown in **Fig. III-3**, **-4**, and **-5**. **Figure III-3**(a) shows that the Raman peak corresponding to the intramolecular C-C stretching vibration

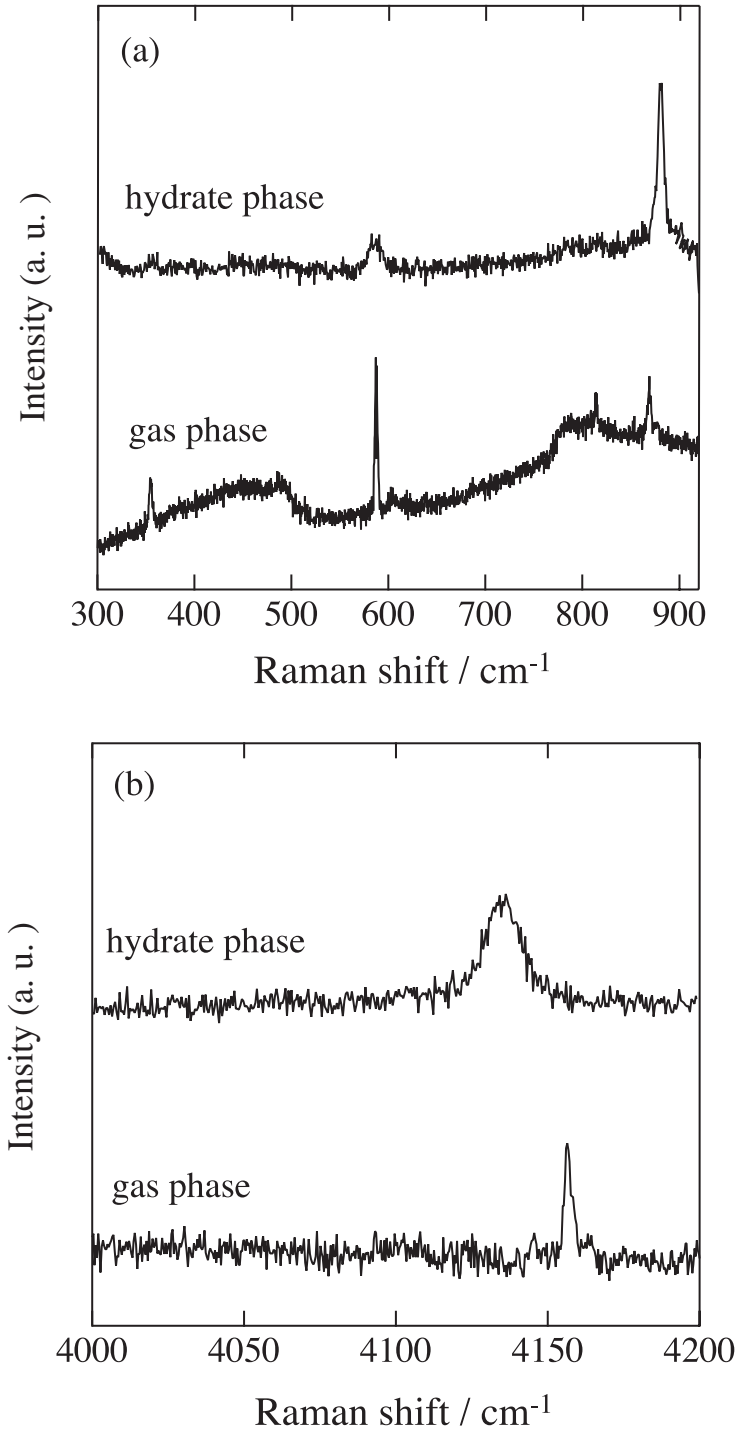

Figure III-5 Raman spectra of the intramolecular vibration for C_3H_8 (around 870 cm^{-1}) (a), and H_2 (around 4100 cm^{-1}) (b) in the gas and hydrate phases for the H_2 + C_3H_8 + water mixture at 1.50 MPa, y_{H2} = 0.82, and 276.1 K. Panel (a) contains the Raman peak (around 590 cm^{-1}) corresponding to the rotation of H_2.

mode of C_2H_6 is detected at 997 cm^{-1} in the gas phase, while at 1000 cm^{-1} in the hydrate phase. The peak corresponding to the intramolecular C-C stretching vibration mode of C_2H_6 in the M-cage of s-I hydrate is detected at 1000 cm^{-1} [11]. As shown in **Fig. III-4**(a), the Raman peak corresponding to the ring breathing mode of *c*-C_3H_6 is detected at 1193 cm^{-1} in the hydrate phase. It agrees well with that of the ring breathing vibration mode of *c*-C_3H_6 in the M-cage of s-I hydrate [12]. As shown in **Fig. III-3**(b) and **Fig. III-4**(b), no peak of the intramolecular H-H stretching vibration of H_2 in the hydrate phase is detected in both H_2 + C_2H_6 + water and H_2 + *c*-C_3H_6 + water systems (The peak should be detected around 4130 cm^{-1} if the H_2 is entrapped in the S-cage). Hence, the hydrates generated from these mixed systems are s-I hydrate originated in the pure C_2H_6 or *c*-C_3H_6 hydrates and H_2 cannot be entrapped with hydrate cages. Incidentally, the Raman peaks of H_2 rotation and vibration in the gas phase are observed around 1036 and 4159 cm^{-1} for the H_2 + C_2H_6 + water mixed system, while the peak of H_2 rotation and vibration cannot be detected in the gas phase for the H_2 + *c*-C_3H_6 + water system under the present experimental condition because of considerably low equilibrium pressure.

Figure III-5(a) shows that the Raman peak corresponding to intramolecular C-C stretching vibration mode of C_3H_8 is detected at 871 cm^{-1} in the gas phase, while at 877 cm^{-1} in the hydrate phase. It is known that the peak corresponding to the C-C stretching vibration mode of C_3H_8 in the L-cage of s-II hydrate is detected at 877 cm^{-1} [15]. **Figure III-5**(a) also shows that the Raman peak derived from the H_2 rotation is detected around 350, 590, and 820 cm^{-1} in the gas phase. On the other hand, a single peak is detected around 585 cm^{-1} in the hydrate phase, which is the most intensive peak corresponding to the H_2 rotation [16]. The peak derived from the H-H stretching vibration of H_2 is detected around 4159 cm^{-1} in the gas phase, while around 4131 cm^{-1} in the hydrate phase as shown in **Fig. III-5**(b). This Raman shift of hydrate phase agrees with that of H_2 encaged in the S-cage of s-II hydrate (Chapter IV). That is, H_2 can selectively occupy the S-cage of s-II hydrate generated from H_2 + C_3H_8 + water mixture, while C_3H_8 occupies the L-cage entirely.

In this chapter, the occupation of H_2 in the hydrate generated from H_2 + C_3H_8 + water mixture has been confirmed by use of Raman spectroscopic analysis. The cage occupancy of H_2 in various mixed systems at relatively low-pressure condition (up to 2 MPa) is summarized in **Table III-2**. H_2 molecule can occupy the S-cage of s-II hydrate even at a few MPa, while it

Table III-2 Summary of H_2 occupation for various guest molecules.

Component with H_2	Hydrate structure	Occupation of H_2
CO_2	I	-
C_2H_6	I	-
c-C_3H_6	I	-
C_3H_8	II	occupied

cannot occupy that of s-I hydrate at similar conditions. In the cases of C_2H_6 or *c*-C_3H_6 additive, H_2 cannot be enclathrated in the hydrate despite the existence of empty S-cages. The S-cage of s-II is somewhat smaller than that of s-I [17], which may causes the variation of H_2 occupation depending on the difference between s-I and -II.

III-4 Summary

Raman micro-spectroscopy reveals that the H_2 can occupy the small cage of s-II C_3H_8 hydrate. On the other hand, the small cage in the C_2H_6 and *c*-C_3H_6 hydrates cannot trap the H_2 despite all the small cages are vacant in these two gas hydrates. These facts may suggest that the H_2 does not generate any mixed hydrate of s-I. These results are also supported by Isothermal phase equilibria and the thermodynamic analysis using numerical calculation.

Notation

f: fugacity [Pa]
k: binary parameter for Soave - Redlich - Kwong equation of state [-]
p: pressure [Pa]
T: temperature [K]
y: composition of gas phase [-]

Literature Cited

[1] Dyadin, Y. A.; Larionov, E. G.; Aladko, E. Y.; Manakov, A. Y.; Zhurko, F. V.; Mikina, T. V.; Komarov, V. Y.; Grachev, E. V. "Clathrate Formation in Water-Noble Gas (Hydrogen) Systems at High Pressures.", *Journal of Structral Chemistry*, **40**, 790-795 (1999).

[2] Mao, W. L.; Mao, H.; Goncharov, A. F.; Struzhkin, V. V.; Guo, Q.; Hu, J.; Shu, J.; Hemley, R. J.; Somayazulu M.; Zhao, Y. "Hydrogen Clusters in Clathrate Hydrate.", *Science*, **297**, 2247-2249 (2002).

[3] Florusse, L. J.; Peters, C. J.; Schoonman, J.; Hester, K. C.; Koh, C. A.; Dec, S. F.; Marsh K. N.; Sloan, E. D. "Stable Low-Pressure Hydrogen Clusters Stored in a Binary Clathrate Hydrate.", *Science*, **306**, 469-471 (2004).

[4] Lee, H.; Lee, J. -W.; Kim, D. Y.; Park, J.; Seo, Y. -T.; Zeng, H.; Moudrakovski, I. L.; Ratcliffe, C. I.; Ripmeester, J. A. "Tuning Clathrate Hydrates for Hydrogen Storage.", *Nature*, **434**, 743-746 (2005).

[5] Strobel, T. A.; Taylor, C. J.; Hester, K. C.; Dec, S. F.; Koh, C. A.; Miller, K. T.; Sloan, E. D., Jr. "Molecular Hydrogen Storage in Binary THF-H_2 Clathrate Hydrates.", *Journal of Physical Chemistry B*, **110**, 17121-17125 (2006).

[6] Zhang, S. -X.; Chen, G. -J.; Ma, C. -F.; Yang, L. -Y.; Guo, T. -M. "Hydrate Formation of Hydrogen + Hydrocarbon Gas Mixtures.", *Journal of Chemical Engineering Data*, **45**, 908-911 (2000).

[7] Klauda, J. B.; Sandler, S. I. "Phase Behavior of Clathrate Hydrates: A Model for Single and Multiple Gas Component Hydrates.", *Chemical Engineering Science*, **58**, 27-41 (2003).

[8] Soave, G. "Equilibrium Constants from a Modified Redlich - Kwong Equation of State.", *Chemical Engineering Science*, **27**, 1197-1203 (1972).

[9] Reid, R. C.; Prausnitz, J. M.; Poling, B. E. "The Properties of Gases and Liquids, 4th ed.", McGraw - Hill, New York, (1986).

[10] Knapp, H.; Doring, R.; Oellrich, L.; Plocker, U.; Prausnitz, J. M. "Vapor - Liquid Equilibria for Mixtures of Low Boiling Substances, Chemistry Data Series, vol. VI.", Dechema, Frankfult

(1982).

[11] Morita, K.; Nakano, S.; Ohgaki, K. "Structure and Stability of Ethane Hydrate Crystal.", *Fluid Phase Equilibria*, 169, 167-175 (2000).

[12] Suzuki, M.; Tanaka, Y.; Sugahara, T.; Ohgaki, K. "Pressure Dependence of Small-cage Occupancy in the Cyclopropane Hydrate System.", *Chemical Engineering Science*, **56**, 2063-2067 (2001).

[13] Hafemann, D. R.; Miller, S. L. "The Clathrate Hydrates of Cyclopropane.", *Journal of Physical Chemistry*, **73**, 1392-1397 (1969).

[14] Kubota, H.; Shimizu, K.; Tanaka, Y.; Makita, T. "Thermodynamic Properties of R13 ($CClF_3$), R23 (CHF_3), R152a ($C_2H_4F_2$), and Propane Hydrates for Desalination of Sea Water.", *Journal of Chemical Engineering of Japan*, **17**, 423-429 (1984).

[15] Sum, A. K.; Burruss, R. C.; Sloan, E. D., Jr. "Measurement of Clathrate Hydrates via Raman Spectroscopy.", *Journal of Physical Chemistry B*, **101**, 7371-7377 (1997).

[16] Fink, U.; Wiggins, T. A.; Rank, D. H. Frequency and Intensity Measurements on the Quadrupole Spectrum of Molecular Hydrogen. *Journal of Molecular Spectroscopy*, **18**, 384-395 (1965).

[17] Subramanian, S.; Sloan, E. D. Jr. "Trends in Vibrational Frequencies of Guests Trapped in Clathrate Hydrate Cages.", *Journal of Physical Chemistry B*, **106**, 4348-4355 (2002).

Chapter IV

Stability Boundaries of Structure-H hydrate for Dimethylcyclohexane Stereo Isomers Helped by Xenon or Methane

Abstract

Four mixtures of 1,1-, *cis*-1,2-, *trans*-1,2-, and *cis*-1,4-dimethylcyclohexanes (hereafter abbreviated DMCH) including water and xenon were investigated in a temperature range over 274.5 K and a pressure range up to 2.7 MPa. The 1,1-DMCH and *cis*-1,2-DMCH generate the structure-H hydrate in the temperature range up to 295.2 K and 280.2 K, respectively. Especially, very large depression of equilibrium pressure was observed in the structure-H 1,1-DMCH hydrate system. On the other hand, neither *trans*-1,2-DMCH nor *cis*-1,4-DMCH generates the structure-H hydrate in the present temperature range. It is an important finding that the *cis*-1,4-DMCH does not generate the structure-H hydrate in the presence of xenon, while the mixture of *cis*-1,4-DMCH and methane generates the structure-H hydrate.

In addition, the structure-H hydrate of 1,1-DMCH helped by methane was also investigated in a temperature range of 274.6 - 289.3 K and pressure range up to 6.7 MPa. The results indicate that 1,1-DMCH is a suitable additive which makes a mild-pressure handling of natural-gas hydrate possible.

Keywords: gas hydrate; phase equilibria; pressure depression; stability; gases; transport process

IV-1 Introduction

The s-H hydrates, found out by Ripmeester *et al*. [1], consist of large guest species and help gas (CH_4, Xe, N_2 and so on) in the water host cages. There are three types of cages in the s-H hydrate, pentagonal dodecahedron (5^{12}, S-cage), dodecahedron ($4^3 5^6 6^3$, S'-cage) and icosahedron ($5^{12}6^8$, U-cage). The large guest molecules, such as adamantane [2], methylcyclohexane [3-6] or other large guest species [7-9], can be entrapped in the U-cage while help gas occupies selectively both S- and S'-cages. The structure of s-H hydrate becomes stable with the cooperative interaction between help gas and large guest species which is unable to generate s-H hydrate by itself.

Recently, a new transportation system using natural-gas hydrates (hereafter, NGH) has attracted much attention from an economical standpoint. It is regarded that the NGH transportation system is much effective in the development of small and middle-size natural-gas fields in the world. Main reason is that the initial investment in facilities for producing NGH is considerably small in comparison with the liquefied natural-gas (LNG) system. Besides that, the temperature of cargoes in a tanker is by far higher than that of LNG (it is 253 K for NGH while 111 K for LNG). However, the NGH reaction from a mixture of water and natural-gas requires high pressure conditions, for example, it becomes over 3 MPa at 275 K.

One of our objectives is to search an effective additive which is able to reduce the reaction pressures without significant reduction in the gas storage capacity. This is why we direct our attention to the s-H hydrate systems [10]. Usually, the large molecules are adopted as additives which occupy the icosahedron hydrate cage to generate the s-H hydrate crystal [1]. Some chemicals, e.g. neohexane [3, 11-13], methylcyclohexane [3-6, 14], 2,2,3-trimethylbutane [8, 11] and pinacolone [13] have been investigated as a candidate for additives. All of them show a large pressure depression from the equilibrium pressure of pure CH_4 (as a representative of natural-gas) hydrate system.

In the Chapter IV, the 1,1-DMCH, *cis*-1,2-DMCH, *trans*-1,2-DMCH and *cis*-1,4-DMCH including water and Xe were investigated using an ordinary static method. In addition, phase equilibria for the s-H hydrate system of 1,1-DMCH, water, and CH_4 was also measured. Then, the difference of function between CH_4 and Xe for the DMCH stereo isomer system has been briefly discussed and consequently we found that 1,1-DMCH gives by far the largest pressure depression in the DMCH isomers.

IV-2 Experimental Section

IV-2.1 Apparatus

The experimental apparatus used in the Chapter IV was essentially the same to the previous one [6, 15]. Two high-pressure cells were used for the phase equilibrium measurements. One was a glass cell (Hiper Glass Cylinder, purchased from Taiatsu Techno Corporation), whose inner volume was about 10 cm^3, was made of tempered glass (as shown in **Fig. IV-1**). Its maximum working pressure was 5 MPa. In the inside of the cell, a magnetic stirrer bar was controlled to move up and down by permanent magnets outside. The other was the same as the one in the Chapter II or III except for the gas and liquid sampling lines. A detail description was given in the previous chapter.

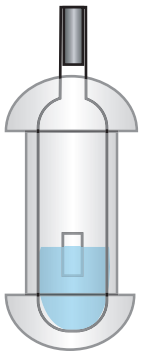

Figure IV-1 Schematic illustration of high-pressure glass cell.

The system temperature was measured within an uncertainty of 0.02 K using a thermistor probe (Takara D-632), which was inserted into a hole in the cell wall. The probe was calibrated with a Pt resistance thermometer defined by ITS-90. The system pressure was measured by a pressure gage (Valcom VPRT) calibrated by RUSKA quartz Bourdon tube gage (Direct Reading Pressure Gage, series 6000) with an estimated maximum uncertainty of 0.01 MPa.

IV-2.2 Procedures

In the measurement for the s-H hydrate system, a sufficient amount of water and DMCH was supplied to the vacuumed high-pressure cell. The contents were then pressurized carefully by the introduction of Xe or CH_4 (not to go over the equilibrium pressure of pure Xe or CH_4 hydrate which was measured in advance by an ordinary method). To generate the first gas hydrate particle of s-H, the system pressure was swung delicately just below the equilibrium pressure of help-gas hydrate (s-I) and then the agitation by the external magnetic was started. The up-and-down mixing is very important to supply fine particles of oil into water phase. In order to determine the four-phase (s-H hydrate + aqueous + liquid 1,1-DMCH + gas phases) equilibrium pressure precisely, the s-H hydrate was formed or dissociated by the pressure

control shown in **Fig. IV-2**. This procedure is quite important to prevent generating peritectic, otherwise a long time is necessary to establish the equilibrium state. When the pressure-change became within 0.01 MPa, the system was regarded as the equilibrium state. After confirming the equilibrium state of four-phase coexistence, the equilibrium temperature and pressure were measured.

V-2.3 Materials

Xe was purchased from Daido Hoxan Inc., having a stated minimum purity of 99.995 mol%. Kr was the maximum impurity of 3.78 ppm. Research grade CH_4 of purity 99.99 % was obtained from Neriki Gas Co., Ltd. The distilled water was obtained from Wako Pure Chemical Industries, Ltd.. The special grade of 1,1-DMCH (purity 99.0 %) was obtained from Aldrich. The special grade of *cis*-1,2-DMCH (purity 98.0 %), *trans*-1,2-DMCH (purity 99.0 %) and *cis*-1,4-DMCH (purity 98.0 %) were obtained from Tokyo Chemical Industry Co., Ltd.. All of them were used without further purifications.

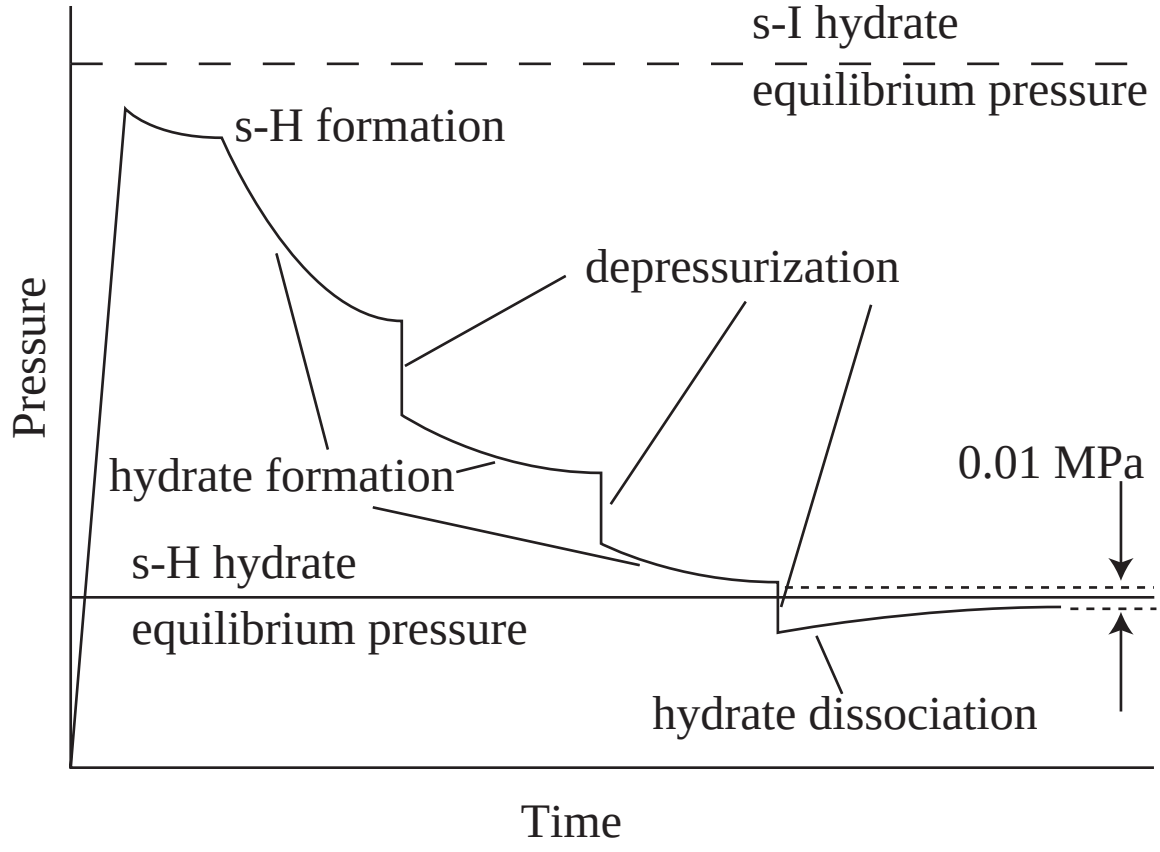

Figure IV-2 Schematic drawing of pressure controll in order to determine the equilibrium pressure for the s-H hydrate system.

Table IV-1 Four-phase equilibrium data for the s-H 1,1-DMCH hydrate helped by CH_4.

T / K	p / MPa	$\Delta_{hyd}H$ / kJmol^{-1}	T / K	p / MPa	$\Delta_{hyd}H$ / kJmol^{-1}
274.67	1.07	388	284.57	3.74	382
276.67	1.37	394	286.53	4.75	389
278.65	1.76	395	288.51	6.08	382
280.63	2.19	400	289.31	6.77	375
282.61	2.90	390			

IV-3 Results & Discussion

IV-3.1 Phase Equilibria

1,1-DMCH + CH_4 s-H hydrate system

The equilibrium data on the four-phase coexisting curve for the 1,1-DMCH + CH_4 hydrate system are summarized in **Table IV-1**. From the slope of the four-phase coexisting curve, the overall enthalpy of hydrate formation (per 1 mol of s-H hydrate), $\Delta_{hyd}H$, is evaluated by use of the Clapeyron equation under the assumption of ideal hydration ($5CH_4$ + 1,1-DMCH + $34H_2O$), where the volumetric properties of CH_4 and 1,1-DMCH are calculated from the IUPAC recommendation [16] and the Rackett equation [17], respectively. The molar volume of s-H hydrate is calculated from the hexagonal lattice constant of s-H hydrate (a =1.226 nm and c =1.017 nm) [18]. The $\Delta_{hyd}H$ of the 1,1-DMCH + CH_4 hydrate changes from 375 to 400 kJ/mol (average *ca*. 388.33 kJ / mol) in the temperature range of 274.6 - 289.3 K.

The phase equilibrium (pressure - temperature) relation obtained in the present study is shown in **Fig. IV-3**. A large depression of the equilibrium pressure from the pure CH_4 hydrate (solid line) is observed. The equilibrium pressure would be reduced from 3 to 1 MPa by adding a small amount of 1,1-DMCH, as we assume that the temperature is around 275 K for producing NGH. Thomas and Behar [11] also reported the equilibrium relations for the CH_4, 1,1-DMCH and water system at higher temperature than 280 K. The present results agree well with theirs (solid circles) in that temperature region.

It is well-known that a few water-soluble organic compounds, e.g. tetrahydrofuran [19, 20], acetone [19-22], and 1,4-dioxane [20, 23], generate the s-II hydrate crystal in the presence of CH_4 and reduce the equilibrium pressure. These additives are, however, unsuitable for our practical object because they are perfectly soluble in water. From an environmental standpoint, it is more desirable to reutilize an additive in this transport system. We try to search a candidate among hydrocarbons which would be easily separated from water after re-gasification or dissociation of NGH.

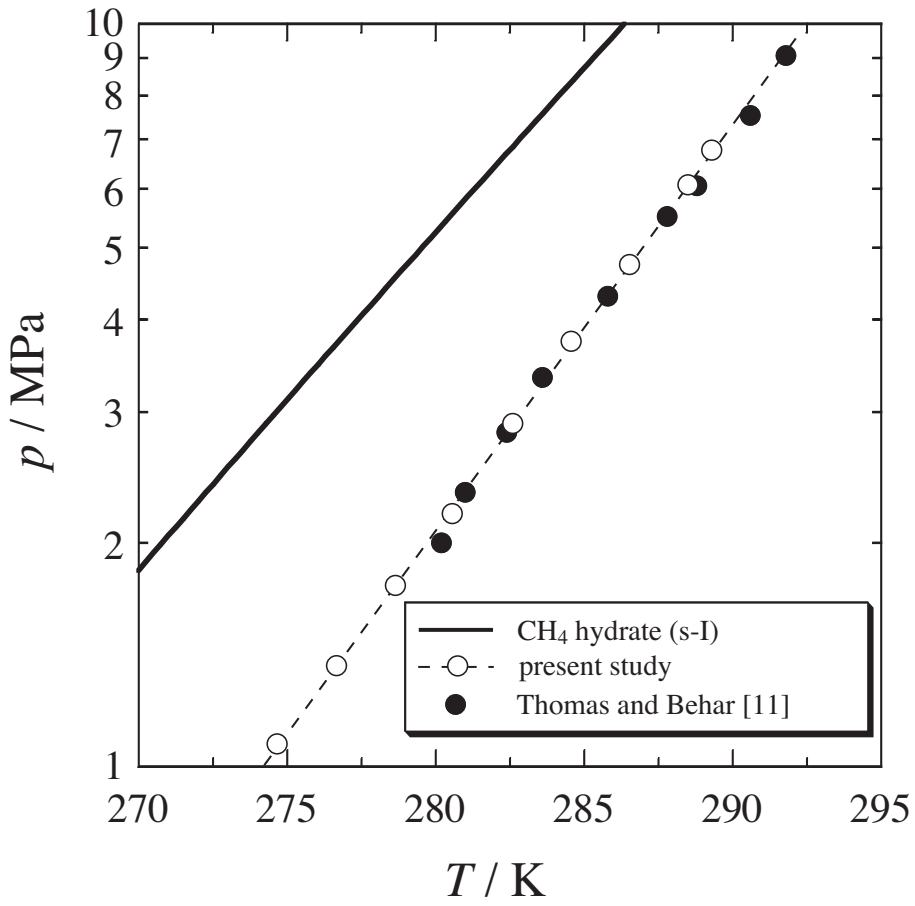

Figure IV-3 Four-phase equilinrium (pressure - temperature) relations of stability boundary for the s-H 1,1-DMCH hydrate in the presence of CH_4.

The pressure depression from the pure CH_4 hydrate system, Δp, is plotted in **Fig. IV-4** in company with some candidate systems of neohexane [13], 2,2,3-trimethylbutane [11], and pinacolone [13]. The value of Δp for all s-H hydrates, which are formed with the selected candidate as additive, increases with the temperature. The 1,1-DMCH system exhibits the largest pressure depression in the candidate systems of s-H hydrate. A further investigation using the natural gas instead of pure methane is necessary to define the validity of 1,1-DMCH.

DMCH stereo isomer + Xe mixed systems

The equilibrium data on the four-phase coexisting curve for the 1,1-DMCH + Xe and *cis*-1,2-DMCH + Xe hydrate systems are summarized in **Tables IV-2** and **-3** and shown in **Fig. IV-5**. The solid line in **Fig. IV-5** corresponds to the three-phase coexisting curve for the pure Xe hydrate [15]. The 1,1- and *cis*-1,2-DMCHs in the presence of Xe generate the s-H hydrate, while neither *trans*-1,2-DMCH nor *cis*-1,4-DMCH generates the s-H hydrate in the whole temperature range of the present study. It is noted that the 1,1-DMCH helped by Xe easily generates the s-H hydrate without special procedures which were contrived in the methylcyclohexane hydrate system [15].

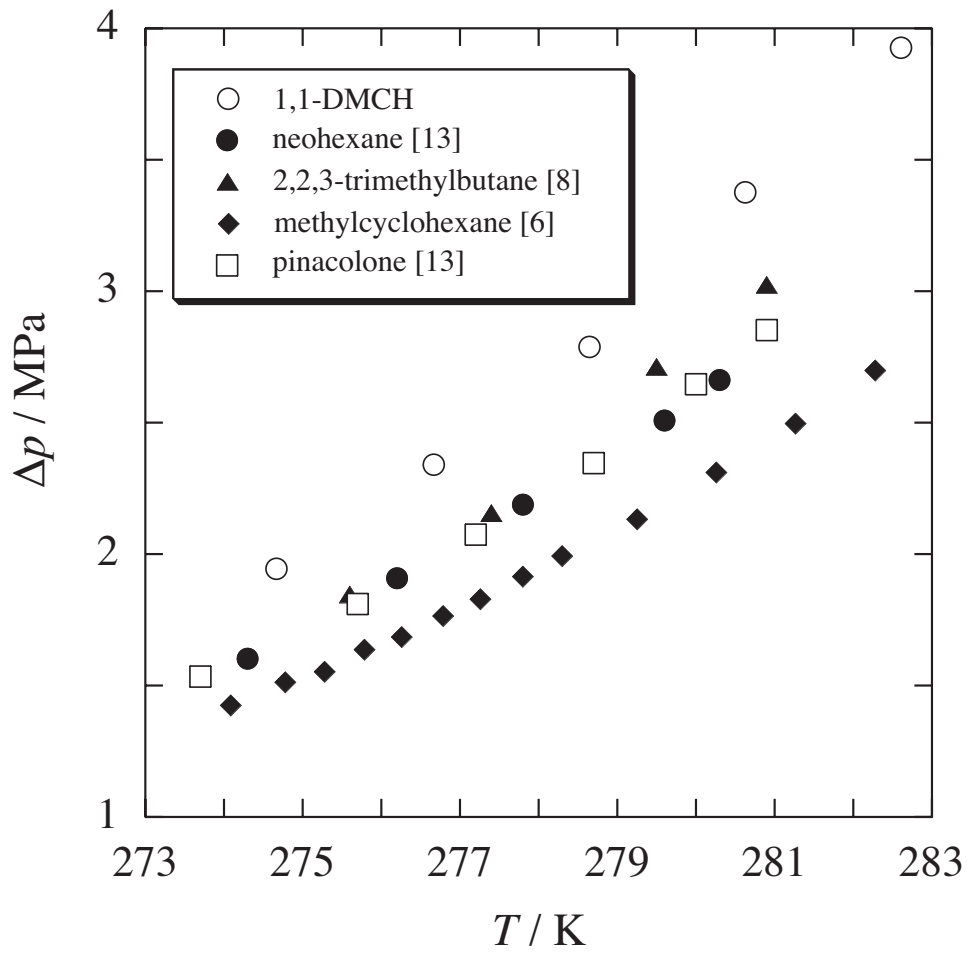

Figure IV-4 Comparison of pressure depressions in the s-H hydrates: ○: 1,1-DMCH (present study); ●: neohexane [13]; ▲: 2,2,3-trimethylbutane [8]; ◆: methylcyclohexane [6]; □: pinacolone [13].

The four-phase coexisting curves of s-H hydrates for the *cis*-1,2-DMCH and 1,1-DMCH hydrate systems intersect the three-phase coexisting curve of s-I hydrate for the pure Xe hydrate system at 280.2 and 295.2 K, respectively. In the higher temperature region, the four-phase coexisting curves of the both systems agree with the three-phase coexisting curve of Xe hydrate system. In these mixed system, the overall enthalpy of hydrate formation (per 1 mol of s-H hydrate), is also evaluated from the slope of the four-phase coexisting curve by use of the Clapeyron equation under the assumption of ideal hydration (5Xe + 1,1-DMCH or *cis*-1,2-DMCH + $34H_2O$), where the volumetric properties of fluid Xe and 1,1- and *cis*-1,2-DMCHs are calculated from the Lee-Kesler equation of state and the modified Rackett equation [17], respectively. As mentioned above, the molar volume of s-H hydrate is calculated

Table IV-2 Four-phase equilibrium data for the s-H 1,1-DMCH hydrate helped by Xe.

T / K	p / MPa	$\Delta_{hyd}H$ / kJmol^{-1}	T / K	p / MPa	$\Delta_{hyd}H$ / kJmol^{-1}
s-H hydrate			286.67	0.493	399
274.73	0.103	416	287.67	0.554	401
274.86	0.106	409	288.77	0.629	404
275.05	0.108	412	289.29	0.660	405
275.14	0.109	414	289.90	0.717	405
275.27	0.110	419	290.33	0.758	403
275.52	0.114	416	290.83	0.803	403
276.40	0.129	414	291.32	0.855	401
276.80	0.136	414	291.84	0.911	400
277.20	0.144	413	292.30	0.963	399
278.24	0.164	417	292.76	1.021	397
278.79	0.175	420	293.24	1.087	403
279.60	0.202	421	293.77	1.165	400
280.46	0.223	414	294.25	1.245	395
280.70	0.231	413	294.88	1.342	394
281.22	0.247	414	*s-I hydrate*		
281.71	0.263	414	295.34	1.420	69.3
282.26	0.280	417	295.81	1.503	68.5
282.77	0.305	410	296.21	1.563	68.5
283.29	0.323	402	296.71	1.645	68.3
283.80	0.342	404	297.18	1.725	68.1
284.24	0.362	404	297.66	1.812	67.9
284.72	0.383	405	298.69	2.017	67.1
285.22	0.407	405	299.68	2.235	66.3
285.65	0.431	403	301.64	2.759	63.4

Table IV-3 Four-phase equilibrium data for the s-H 1,2-DMCH hydrate helped by Xe.

T / K	p / MPa	$\Delta_{hyd}H$ / kJmol^{-1}	T / K	p / MPa	$\Delta_{hyd}H$ / kJmol^{-1}
s-H hydrate			279.85	0.296	392
274.51	0.153	381	280.15	0.307	393
275.42	0.171	384	*s-I hydrate*		
276.21	0.190	384	280.45	0.316	63.8
277.01	0.210	385	280.62	0.322	63.7
277.95	0.235	388	280.83	0.328	63.9
278.54	0.252	390	281.15	0.338	64.0
278.85	0.261	391	281.63	0.356	64.0
279.24	0.275	391	282.74	0.397	64.5
279.56	0.285	392	283.74	0.439	64.6

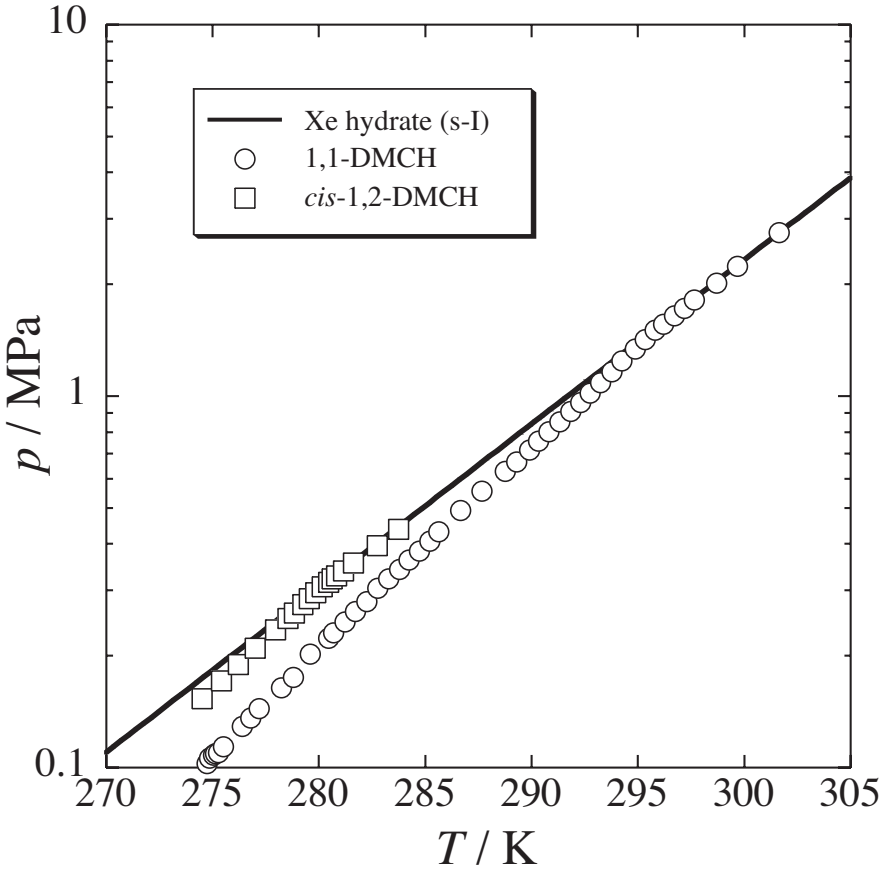

Figure IV-5 Four-phase equilibrium (pressure - temperature) relations of stability boundaries in two DMCH stereo isomers + Xe mixed systems.

from the hexagonal lattice constant of s-H hydrate (a =1.226 nm and c =1.017 nm) [18]. The details of calculation procedures are described elsewhere [24]. The $\Delta_{hyd}H$ of the 1,1-DMCH + Xe (s-H) and *cis*-1,2-DMCH + Xe (s-H) hydrates has weak temperature dependence; the value changes from 395 to 420 kJ / mol in the temperature range of 274.73 - 294.88 K and from 381 to 393 kJ / mol in the temperature range of 274.51 - 280.15 K, respectively.

IV-3.2 Icosahedron-cage Occupancy

In the comparison with the CH_4 system for the DMCH stereo isomers, we found that there is the distinction of s-H hydrate stability between the methane and Xe systems. In the CH_4 systems, 1,1-DMCH and two *cis*-isomers (*cis*-1,2- and *cis*-1,4-DMCHs) generate the s-H hydrate, while neither *trans*-DMCHs nor *cis*-1,3-DMCH generates the s-H hydrate. Exceptionally, the *trans*-1,2-DMCH generates the s-H hydrate with cooperative assistance of CH_4 and *cis*-1,2-DMCH [6, 25, 27]. On the other hand, only 1,1- and *cis*-1,2-DMCHs can generate the s-H hydrate in the Xe system as summarized in **Table IV-4**. The largest van der Waals diameter of each DMCH isomer is also listed in **Table IV-4** for reference. The value of diameter is evaluated from PM3 method of MOPAC6 [28] and a practical assumption [29]. It is difficult to draw a definite boundary line in a series of the largest van der Waals diameters, however, the transitional point would be located in the region of 0.84-0.88 nm. These results suggest that the magnitude of U-cage expansion allowed in the CH_4 system is larger than that of Xe. According to Gough [30], the distortion of hydrate cage is occasionally observed when the

Table IV-4 Summary of s-H hydrate formation for DMCH stereo isomers in the presence of CH_4 or Xe [6, 25-27].

LGS	d / nm*	CH_4	Xe
1,1-DMCH	0.84	s-H formation	s-H formation
cis-1,2-DMCH	0.84	s-H formation	s-H formation
trans-1,2-DMCH	0.84	-**	-
cis-1,3-DMCH	0.92	-	-
trans-1,3-DMCH	0.84	-	-
cis-1,4-DMCH	0.88	s-H formation	-
trans-1,4-DMCH	0.95	-	-

*The symbol d stands for the largest van der Waals diameter.

**trans*-1,2-DMCH generates the s-H hydrate with cooperative assistance of CH_4 and *cis*-1,2-DMCH [26, 27].

large guest species is entrapped in the cage. That is, the U-cage occupancy of large guest species depends on the function of help gas.

IV-4 Summary

The findings obtained in the Chapter IV are summarized as follows:

I. The s-H hydrate of 1,1-DMCH helped by CH_4 has been investigated in order to search an effective additive for natural-gas transportation system. By adding a small amount of 1,1-DMCH, it is possible that the equilibrium pressure would be reduced from 3 MPa (s-I CH_4 hydrate) to 1 MPa (s-H CH_4 + 1,1-DMCH hydrate) around 275 K for producing natural-gas hydrates.
II. The four-phase coexisting curves for the s-H hydrate of 1,1-DMCH + Xe, *cis*-1,2-DMCH + Xe have been investigated in a pressure range up to 2.7 MPa. The DMCH stereo isomers which generate the s-H hydrate helped by Xe are the 1,1- and *cis*-1,2-DMCHs. The *cis*-1,4-DMCH, which generates the s-H hydrate in the presence of CH_4, can not generate the s-H hydrate in the presence of Xe. One of the most important findings is that the U-cage occupancy limit of large guest species depends on the function of help gas.

Notation

a, c : lattice constant [m]
H : enthalpy [J / mol]
p : pressure [Pa]
T : temperature [K]

Literature Cited

[1] Ripmeester, J. A.; Tse, J. S.; Ratcliffe, C. I.; Powell, B. M. "A New Clathrate Hydrate Structure.", *Nature*, **325**, 135-136 (1987).

[2] Lederhos, J. P.; Mehta, A. P.; Nyberg, G. B.; Warn, K. J.; Sloan, E. D. "Structure H Clathrate Hydrate Equilibria of Methane and Adamantane.", *AIChE Journal*, **38**, 1045-1048 (1992).

[3] Metha, A. P.; Sloan, E. D.; "Structure H Hydrate Phase Equilibria of Methane + Liquid Hydrocarbon Mixtures.", *Journal of Chemical & Engineering Data*, **38**, 580-582 (1993).

[4] Mooijer-van den Heuvel, M. M.; Peters, C. J.; de Swaan Arons, J. "Influence of Water - Insoluble Organic Compounds on the Gas Hydrate Equilibrium Conditions of Methane.", *Fluid Phase Equilibria*, **172**, 73-91 (2000).

[5] Sun, Z. -G.; Fan, S. -S.; Guo, K. -H.; Shi, L.; Wang, R.-Z. "Equilibrium Hydrate Formation Conditions for Methylcyclohexane with Methane and a Ternary Gas Mixture.", *Fluid Phase Equilibria*, **198**, 293-298 (2002).

[6] Nakamura, T.; Makino, T.; Sugahara, T.; Ohgaki, K. "Stability Boundaries of Gas Hydrates Helped by Methane -- Structure-H Hydrates of Methylcyclohexane and cis -1,2-Dimethylcyclohexane --.", *Chemical Engineering Science*, 58, 269-273 (2003).

[7] Ripmeester, J. A.; Ratcliffe, C. I. "^{129}Xe NMR Studies of Clathrate Hydrates: New Guest for Structure II and Structure H.", *Journal of Physical Chemistry*, **94**, 8773-8776 (1990).

[8] Metha, A. P.; Sloan, E. D.; "Structure H Hydrate Phase Equilibria of Paraffins, Naphthenes, and Olefins with Methane.", *Journal of Chemical & Engineering Data*, **39**, 887-890 (1994).

[9] Makino, T.; Nakamura, T.; Sugahara, T.; Ohgaki, K. "Thermodynamic Stability of Structure-H Hydrates of Methylcyclopentane and Cyclooctane Helped by Methane.", *Fluid Phase Equilibria*, 218, 235-238 (2004).

[10] Khokhar, A. A.; Gudmundsson, J. S.; Sloan, E. D. "Gas Storage in Structure H Hydrates.", *Fluid Phase Equilibria*, **150-151**, 383-392 (1998).

[11] Thomas, M.; Behar, E. "Structure H Hydrate Equilibria of Methane and Intermediate Hydrocarbon Molecules.", *Proceedings of 73rd Gas Processors Association Convention, New Orleans*, pp. 100 (1994).

[12] Hütz, U.; Englezos, P. "Measurement of Structure H Hydrate Phase Equilibrium and the Effect of Electrolytes.", *Fluid Phase Equilibria*, **117**, 178-185 (1996).

[13] Ohmura, R.; Uchida, T.; Takeya, S.; Minagawa, H.; Ebinuma, T.; Narita, H. "Phase Equilibrium for Structure-H Hydrates formed with Methane and Either Pinacolone (3,3-Dimethyl-2-butanone) or Pinacolyl Alcohol (3,3-Dimethyl-2-butanol).", *Journal of Chemical & Engineering Data*, **48**, 1337-1340 (2003).

[14] Mehta, A. P.; Sloan, E. D. "A Thermodynamic Model for Structure-H Hydrates.", *AIChE Journal*, **40**, 312-320 (1994).

[15] Shimada, N.; Sugahara, K.; Sugahara, T.; Ohgaki, K. "Phase Transition from Structure-H to Structure-I in the Methylcyclohexane + Xenon Hydrate System.", *Fluid Phase Equilibria*, **205**, 17-23 (2003).

[16] Angus, S.; Armstrong, B.; de Reuck, K. M. "International Thermodynamic Tables of the Fluid State-5 Methane.", *PERGAMON PRESS, Oxford* (1976).

[17] Reid, R. C.; Prausnitz, J. M.; Poling, B. E. "The Properties of Gases and Liquids, 4th Ed.", *McGraw-Hill, New York* (1986).

[18] Davidson, D. W.; Gough, S. R.; Handa, Y. P.; Ratcliffe, C. I.; Ripmeester, J. A.; Tse, J. S. "Some Structural Studies of Clathrate Hydrates.", *Journal de physique*, **C1**, 537-542 (1987).

[19] de Deugd, R. M.; Jager, M. D.; de Swaan Arons, J. "Mixed Hydrates of Methane and Water-Soluble hydrocarbons Modeling of Empirical Results.", *AIChE Journal*, **47**, 693-704 (2001).

[20] Seo, Y. -T.; Kang, S. -P.; Lee, H. "Experimental Determination and Thermodynamic Modeling of Methane and Nitrogen Hydrates in the Presence of THF, Propylene Oxide, 1,4-Dioxane and Acetone.", *Fluid Phase Equilibria*, **189**, 99-110 (2001).

[21] Ng, H. -J.; Robinson D. B. "New Developments in the Measurement and Prediction of Hydrate Formation for Processing Needs.", *Annals of the New York Academy of Sciences*, **715**,

450-462 (1996).

[22] Mainusch, S.; Peter, C. J.; de Swaan Arons, J. "Experimental Determination and Modeling of Methane Hydrates in Mixtures of Acetone and Water.", *Journal of Chemical & Engineering Data*, **42**, 948-950 (1997).

[23] Jager, M. D.; de Deugd, R. M.; Peters, C. J.; de Swaan Arons, J.; Sloan, E. D. "Experimental Determination and Modeling of Structure II Hydrate in Mixtures of Methane + Water + 1,4-Dioxane.", *Fluid Phase Equilibria*, **165**, 209-233 (1999).

[24] Ohgaki, K.; Sugahara, T.; Suzuki, M.; Jindai, H. "Phase Behavior of Xenon Hydrate System.", *Fluid Phase Equilibria*, **175**, 1-6 (2000).

[25] Nakamura, T.; Sugahara, T.; Ohgaki, K., "Stability Boundaries of Structure-H Hydrate of *cis*-1,4-Dimethylcyclohexane Helped by Methane.", *Journal of Chemical & Engineering Data*, **49**, 99-100 (2004).

[26] Nakamura, T.; Makino, T.; Sugahara, T.; Ohgaki, K. "Gas Hydration of *trans*-1,2-Dimethylcyclohexane with Cooperative Assistance of Methane and *cis*-1,2-Dimethylcyclohexane.", *Chemical Engineering Science*, **59**, 163-165 (2004).

[27] Makino, T. "Thermodynamic and Raman Spectroscopic Studies on Mixed Gas Hydrates Containing Methane.", *Thesis for Doctorate* (2006).

[28] Stewart, J. J. P. "Optimization of Parameters for Semiempirical Methods. I. Method, II. Applications.", *Journal of Computational Chemistry*, **10**, 209-221 (1989).

[29] Nagao, T. "An Improved Program for a Calculation of Molecular Surface Areas and Volumes.", *Hakodate Kogyo Koto Senmon Gakko Kiyo*, **17**, 110-120 (1993).

[30] Gough, S. R. "The clathrate hydrate of 2-methylpropanal: dielectric evidence.", *Canadian Journal of Chemistry*, **56**, 2025-2028 (1978).

Chapter V

Effect of Water-soluble Additives on Hydrogen + Carbon Dioxide + Water Mixed System

---

Abstract

Isothermal phase equilibria (pressure - composition in the gas phase) for the quaternary systems of hydrogen, carbon dioxide, tetrahydrofuran or tetra-*n*-butyl ammonium bromide, and water have been measured in the presence of gas hydrate phase. In the hydrogen + carbon dioxide + tetrahydrofuran + water mixed system, the lowest three-phase equilibrium pressure is obtained under the condition that the mole fraction of tetrahydrofuran in water is 0.056. The three-phase equilibrium curves have a stepwise increase in the equilibrium pressure around 0.2 in the hydrogen mole fraction of gas phase. The Raman spectra show that the hydrogen and carbon dioxide molecules competitively occupy the small cage of structure-II in the region of hydrogen mole fraction higher than 0.2, while no hydrogen molecule is entrapped with the hydrate cage in the region of hydrogen mole fraction lower than 0.2. That is, the hydrogen molecule can be encaged in the hydrate cages with a small amount of tetrahydrofuran at considerably low pressure, which may be occurred in the region of hydrogen mole fraction higher than 0.2.

The three-phase equilibrium curve for the hydrogen + carbon dioxide + tetra-*n*-butyl ammonium bromide + water mixed system shows similar behavior to that of hydrogen + carbon dioxide + tetrahydrofuran + water mixed system.

Keywords: gas hydrate, phase equilibria, Raman spectroscopy, hydrogen, carbon dioxide, solution

V-1 Introduction

The purification of H_2 from gas mixtures is one of the most important techniques for developing new society sustained by H_2 energies. An option of H_2 separation would be an application of gas hydrates, that is, impurities in the gas mixtures are removed from the H_2 stream by generating gas hydrates where impurities are selectively entrapped in the hydrate cages. It is well known that the pure H_2 hydrate is generated only in extremely high-pressure regions [1, 2].

In the Chapter II, we have investigated the phase equilibria for the ternary mixtures of H_2, CO_2, and water. The isothermal equilibrium pressure of three-phase coexistence (gas hydrates, aqueous solution, and gas phase) has increased in proportion with the H_2 composition in the gas phase. It has been also shown that the isothermal equilibrium pressure can be estimated under a constant fugacity of CO_2 from the assumption of pure CO_2 hydrate formation. In addition, the Raman spectra for the single crystal generated from H_2, CO_2, and water mixtures suggest that hydrogen is not enclathrated in the hydrate cages. It is suggested that H_2 would behave only like the diluent gas toward the formation of s-I carbon dioxide hydrate. That is, it has been revealed that the separation of H_2 from gas mixture containing some impurities can be performed by use of gas hydrates.

In the Chapter V, quaternary mixtures including tetrahydrofuran (hereafter, THF) or tetra-*n*-butyl ammonium bromide (hereafter, TBAB) were investigated at the same temperature with the aim of reducing operation pressures. The dependence of THF composition in the aqueous solution has been also investigated near the stoichiometric THF composition. Finally, the cage occupancy of the H_2 molecules in the hydrate generated from the H_2 + CO_2 + THF + water mixture were discussed briefly by use of Raman spectroscopic analysis.

V-2 Experimental Section

V-2.1 Apparatus

The experimental apparatus for the phase equilibrium measurements were the same as the one in the Chapter II or III except for the supply line for the aqueous solutions (as shown in **Fig. V-1**). A detail description was given in the previous chapter.

A schematic illustration of the experimental apparatus for the Raman spectroscopic analysis is shown in Fig. **V-2**. The experimental apparatus for the Raman spectroscopic analysis were the same as the one in the Chapter II or III except for the supply line for the aqueous solution. The high-pressure optical cell was the same as the one in the Chapter III. A detail description of the high-pressure optical cell was given in the previous chapter.

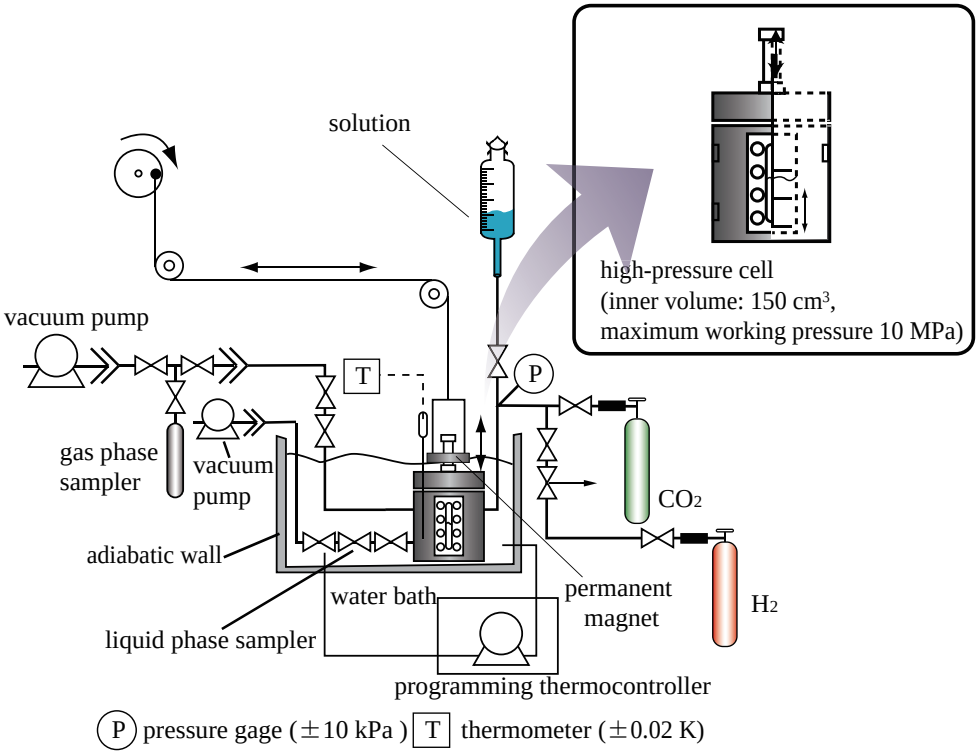

Figure V-1 Schematic illustration of experimental apparatus for phase equilibrium measurement.

The system temperature was measured within an uncertainty of 0.02 K using a thermistor probe (Takara D-632), which was inserted into a hole in the cell wall. The probe was calibrated with a Pt resistance thermometer (25 Ω) defined by ITS-90. The system pressure was measured by a pressure gage (Valcom VPRT) calibrated by RUSKA quartz Bourdon tube gage (Direct Reading Pressure Gage, series 6000) with an estimated maximum uncertainty of 0.01 MPa.

V-2.2 Procedures

Phase equilibrium measurement

The THF or TBAB aqueous solution prepared at a desired composition was introduced into the evacuated high-pressure cell. The THF molecule generates the s-II hydrate and the stoichiometric mole fraction is 0.056 for the pure THF hydrate formation [3-5]. In the present study, the THF mole fractions (x_{THF}) of 0.030, 0.056 and 0.080 were adopted. The TBAB mole fraction (x_{TBAB}) of 0.037 was adopted, which is the stoichiometric mole fraction for the tetragonal TBAB hydrate formation [6, 7]. The contents were pressurized up to a desired pressure by supplying H_2 + CO_2 mixture at a desired composition and then continuously agitated using the mixing bar driven by a permanent magnetic ring. After the formation of gas hydrates, the system temperature was kept constant to establish the three-phase coexisting state of hydrate + aqueous solution + gas. The phase behavior was observed directly through the window. After reaching

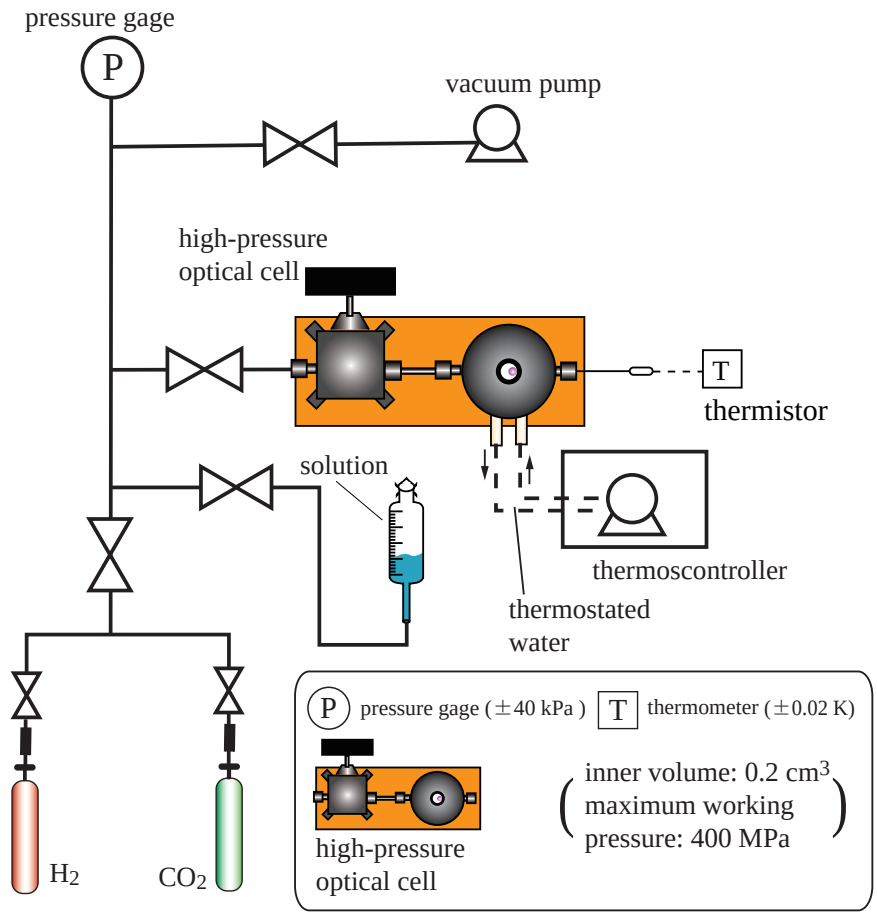

Figure V-2 Schematic illustration of experimental apparatus for Raman spectroscopic analysis.

the equilibrium state of three-phase coexistence, a small amount of gas phase was sampled for the composition analysis. The equilibrium composition of gas phase was analyzed for the H_2 and CO_2 by the TCD-Gas Chromatography (TCD-GC, Shimadzu GC-14B) as the water and THF or TBAB composition of gas phase is negligibly small under the present experimental conditions.

Raman spectroscopic analysis

The THF aqueous solution prepared at a desired composition was introduced into the evacuated high-pressure optical cell. The THF mole fractions of 0.056 were adopted, which is the stoichiometric mole fraction for the pure THF hydrate formation. The contents were pressurized up to a desired pressure by supplying H_2 + CO_2 mixture prepared at a desired composition. The procedure for the preparation of hydrate single-crystal was similar to that of the Chapter II or III. In the case that the single crystal was prepared from aqueous solution, the rate and range of temperature drop should be paid special attention in order not to grow the single crystal overly. We also paid enough attention to preparing as few single-crystals as possible. The single crystal was observed by the CCD camera through the quartz window. The photo of single crystal is shown in **Fig. V-3**.

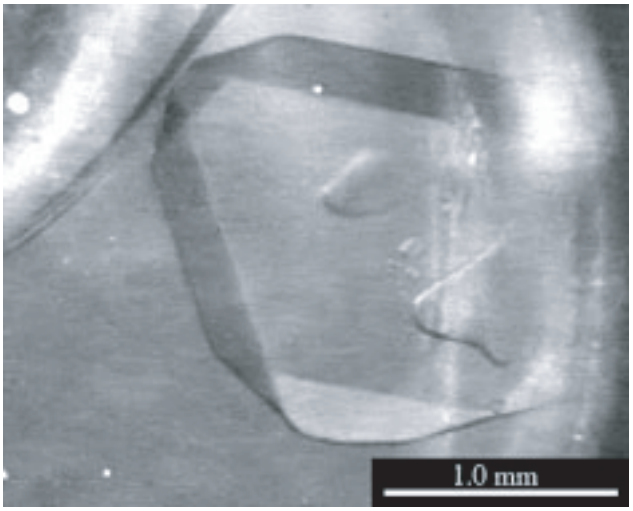

Figure V-3 A photo of hydrate single-crystal prepared from H_2 + CO_2 + THF + water mixture.

This single crystal of gas hydrate was analyzed by *in situ* Raman spectroscopy by use of a laser Raman microprobe spectrometer with a multichannel CCD detector. The CCD detector was maintained at ~200 K for heat-noise reduction. The argon ion laser beam (wavelength: 514.5 nm and generation power: 100 mW) condensed to 2 μm in spot diameter were irradiated to the single crystals from the object lens through the upper quartz window. The backscatter of the opposite direction was taken in with the same lens. The spectral resolution was about 1 cm^{-1}. The exposed time and integration number were 60 sec. and 3 times, respectively.

V-2.3 Materials

Research grade H_2 (mole fraction purity 0.999999) was obtained from the Neriki Gas Co., Ltd. The maximum impurity was 0.2 ppm of nitrogen. Research grade CO_2 (mole fraction purity 0.9999) was obtained from the Takachiho Tradings Co., Ltd. Research grade THF (mole fraction purity 0.997), TBAB (mole fraction purity 0.980) and the distilled water were obtained from the Wako Pure Chemical Industries, Ltd. All of them were used without further purifications.

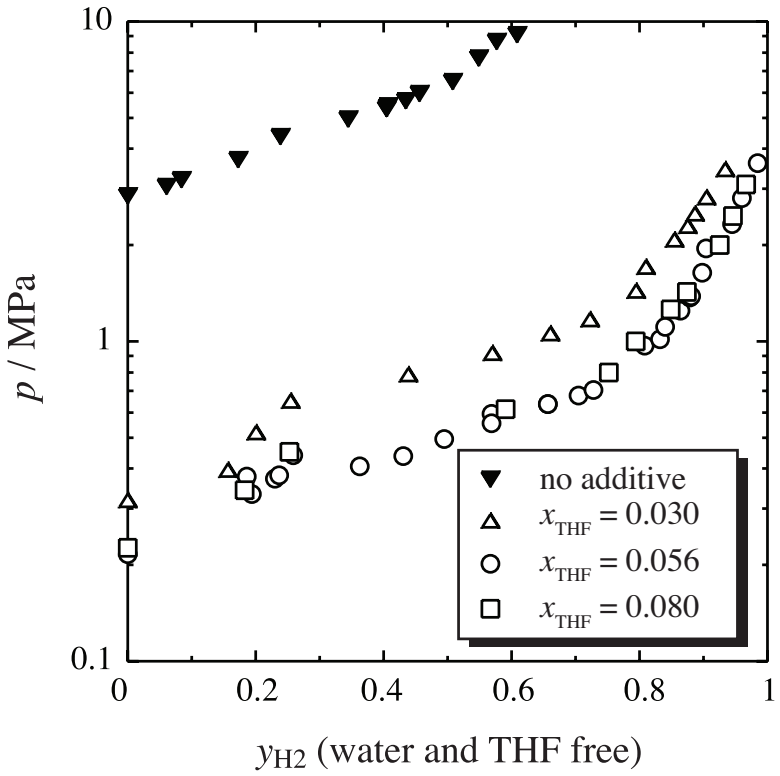

Figure V-4 Isothermal phase equilibrium (pressure - composition in the gas phase) relations for H_2 + CO_2 + THF + water mixed system in the presence of hydrate phase at 280.1 K at x_{THF} = 0.030, 0.056, and 0.080.

V-3 Results & Discussion

V-3.1 Isothermal Phase Equilibria

The isothermal phase equilibrium (p - y) relations for the H_2 + CO_2 + THF + water mixed system (x_{THF} = 0.030, 0.056, and 0.080) containing gas hydrate at 280.1 K are summarized in **Table V-1**, and shown in **Fig. V-4**. In the present study, it is assumed that the mole fraction of THF in the gas phase can be neglected. The three-phase equilibrium pressure increases monotonically with the composition of H_2. In comparison with the Chapter II, the most remarkable change is a large depression of equilibrium pressure which is caused by the addition of a small amount of THF. This pressure depression is the greatest at x_{THF} = 0.056, which is stoichiometric for the pure THF hydrate. The degree of pressure depression depends on the additive composition, that is, the additional THF depresses the equilibrium pressure till the THF composition comes up to the stoichiometric mixture. The THF composition exceeding the stoichiometric ration does not depress the equilibrium pressure any more because excess THF molecules may play the role of a inhibitor. In the present study, the isothermal phase equilibria (p - y) relation for the same mixed system was also measured at 281.9 K under the condition that the THF mole fraction in water is 0.056. The results are summarized in **Table V-2**, and

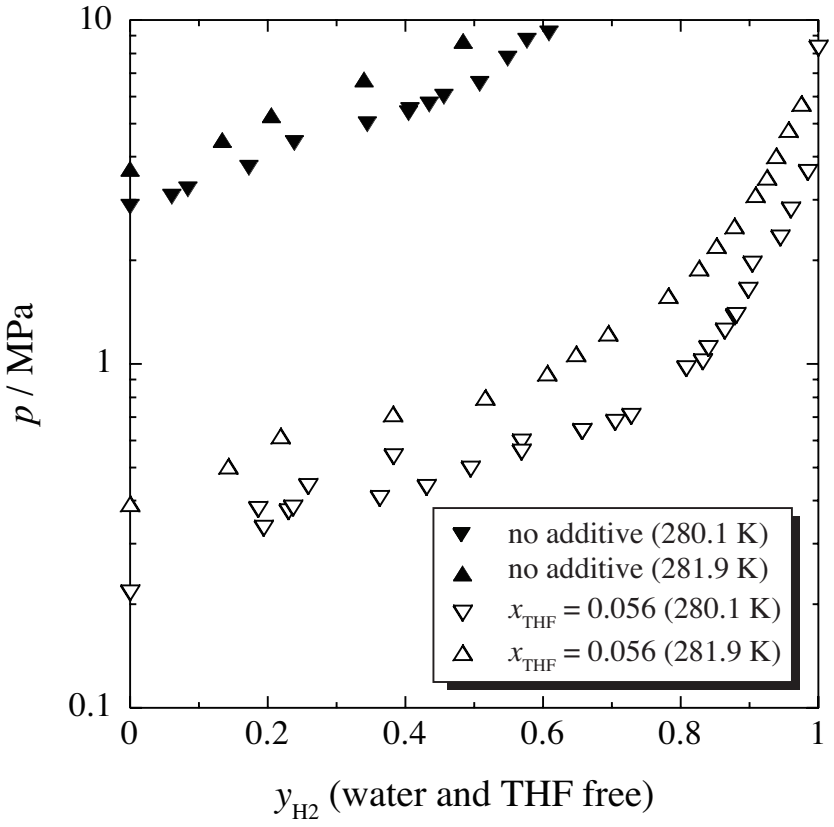

Figure V-5 Isothermal phase equilibrium (pressure - composition in the gas phase) relations for H_2 + CO_2 + THF + water mixed system in the presence of hydrate phase at 280.1 K and 281.9 K at x_{THF} = 0.056.

shown in **Fig. V-5** accompanied with the results at 280.1 K at the same THF concentration. As shown in **Fig. V-5**, the three-phase equilibrium pressure increases monotonically with the composition of H_2. The large pressure depression from the equilibrium pressure without additives is observed at each temperature condition. There is no remarkable difference of phase behavior between these results except for the equilibrium condition. That is, the effect of THF does not depend on the system temperature.

It is also notable characteristic that the unusual behavior comes into existence on the *p* - *y* curve for the quaternary mixtures including THF. A stepwise increase in the equilibrium pressure appears around 0.2 in the H_2 mole fraction of gas phase (y_{H2}) for every aqueous solution of different THF mole fractions. It is reasonable to guess that the H_2 molecule starts to occupy the S-cage of s-II in the CO_2 + THF mixed gas hydrate at y_{H2} = *ca*. 0.2.

The isothermal phase equilibrium (*p* - *y*) relations for the H_2 + CO_2 + TBAB + water mixed system (x_{TBAB} = 0.037) containing gas hydrate at 285.9 K are summarized in **Table V-3**, and shown in **Fig. V-6** accompanied with the results of H_2 + CO_2 + THF + water mixed system at the stoichiometric THF mole fraction (280.1 K). The behavior of *p* - *y* curve for the H_2 + CO_2 + TBAB + water mixed system is very similar to that of H_2 + CO_2 + THF + water mixed system. The depression of equilibrium pressure for the H_2 + CO_2 + TBAB + water

Table V-1 Isothermal phase equilibrium data for H_2 + CO_2 + THF + water mixed system in the presence of hydrate phase at 280.1 K at x_{THF} = 0.030, 0.056, and 0.080.

x_{THF}	y_{H2}	p / MPa	x_{THF}	y_{H2}	p / MPa
0.030	0.000	0.32		0.657	0.64
	0.157	0.40		0.705	0.68
	0.201	0.52		0.728	0.71
	0.255	0.65		0.808	0.97
	0.439	0.79		0.832	1.02
	0.570	0.92		0.840	1.11
	0.661	1.06		0.864	1.25
	0.723	1.17		0.879	1.37
	0.795	1.44		0.881	1.39
	0.810	1.71		0.898	1.64
	0.855	2.08		0.904	1.95
	0.875	2.30		0.945	2.32
	0.887	2.51		0.960	2.81
	0.905	2.82		0.985	3.61
	0.934	3.46	0.080	0.000	0.23
0.056	0.000	0.22		0.183	0.34
	0.186	0.38		0.253	0.45
	0.194	0.33		0.591	0.61
	0.230	0.37		0.752	0.80
	0.237	0.38		0.794	1.00
	0.259	0.44		0.849	1.26
	0.363	0.41		0.874	1.43
	0.431	0.44		0.925	2.00
	0.495	0.50		0.946	2.47
	0.569	0.55		0.967	3.10
	0.569	0.59			

Table V-2 Isothermal phase equilibrium data for H_2 + CO_2 + THF + water mixed system at 281.9 K at x_{THF} = 0.056.

x_{THF}	y_{H2}	p / MPa	x_{THF}	y_{H2}	p / MPa
0.056	0.000	0.39		0.827	1.90
	0.143	0.51		0.852	2.21
	0.219	0.62		0.878	2.52
	0.382	0.72		0.909	3.11
	0.516	0.80		0.925	3.49
	0.606	0.94		0.939	4.03
	0.648	1.07		0.957	4.80
	0.695	1.23		0.975	5.73
	0.782	1.58			

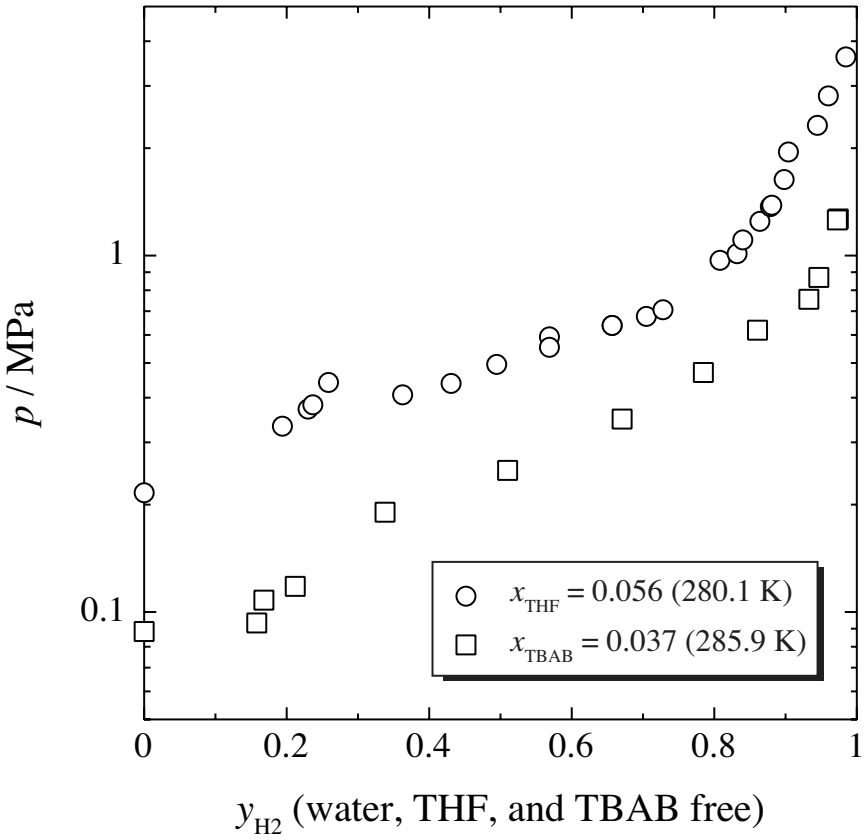

Figure V-6 Isothermal phase equilibrium (pressure - composition in the gas phase) relations for H_2 + CO_2 + THF + water (at 280.1 K and at x_{THF} = 0.056) and H_2 + CO_2 + TBAB + water (at 285.9 K and at x_{TBAB} = 0.037) mixed system in the presence of hydrate phase.

Table V-3 Isothermal phase equilibrium data for H_2 + CO_2 + TBAB + water mixed system in the presence of hydrate phase at 285.9 K at x_{TBAB} = 0.037.

x_{TBAB}	y_{H2}	p / MPa	x_{TBAB}	y_{H2}	p / MPa
0.037	0.000	0.088		0.785	0.47
	0.158	0.093		0.861	0.62
	0.168	0.11		0.933	0.76
	0.212	0.12		0.947	0.87
	0.338	0.19		0.973	1.26
	0.510	0.25		0.974	1.27
	0.671	0.35			

mixed system, in spite of higher temperature, is greater than that of H_2 + CO_2 + THF + water mixed system. In addition, a stepwise increase in the equilibrium pressure at y_{H2} = *ca.* 0.2 observed in the H_2 + CO_2 + THF + water mixed system also appears in the H_2 + CO_2 + TBAB + water mixed system.

V-3.2 Raman Spectroscopic Analysis

In order to confirm the existence of H_2 in the hydrate phase, the single crystals of gas hydrate were prepared from the H_2 + CO_2 + THF + water mixture in the higher or lower composition region than y_{H2} = 0.2. The mole fraction of THF is 0.056. Raman spectroscopic analysis was performed for these single crystals. The Raman peaks obtained in the higher composition region than y_{H2} = 0.2 (at 280.1 K and 4.3 MPa, y_{H2} = ~0.95) are shown in **Fig. V-7**(a), (b), and (c). The Raman spectra gives the characteristic signals of THF, H_2, and CO_2. As shown in **Fig. V-7**(a), the single peak detected at 919 cm^{-1} corresponds to the ring breathing mode of the THF molecules enclathrated in the hydrate phase. In addition, the quadruplet peak corresponding to the H_2 rotation in the gas phase is observed at around 350, 590, 820, and 1036 cm^{-1}. The three weak and broad peaks except for the peak around 1036 cm^{-1} are also detected at the similar position in the hydrate phase. The peak around 1036 cm^{-1} overlaps with that of THF. **Figure V-7**(c) indicates that the split peak by Fermi resonance effect corresponding to C=O symmetric stretching vibration mode of CO_2 are detected at 1286 and 1389 cm^{-1} in the gas phase, and at 1274 and 1381 cm^{-1} in the hydrate phase. These peaks are consistent with the previous study [8]. As shown in **Fig. V-7**(b), the peaks corresponding to the H-H stretching vibration mode of H_2 are observed at 4129, 4146, 4159, and 4165 cm^{-1} in the gas phase, and at

4131 cm^{-1} in the hydrate phase. These sharp peaks in the gas phase and the broad and single peak in the hydrate phase corresponding to the H-H stretching vibration mode of the H_2 molecule are consistent with the reference data [9]. These findings reveal that the THF molecules occupy L-cages and the H_2 and CO_2 molecules are competitively enclathrated in the S-cages.

Figure V-8(a), (b), and (c) show the Raman spectra of H_2 + CO_2 + THF + water mixed

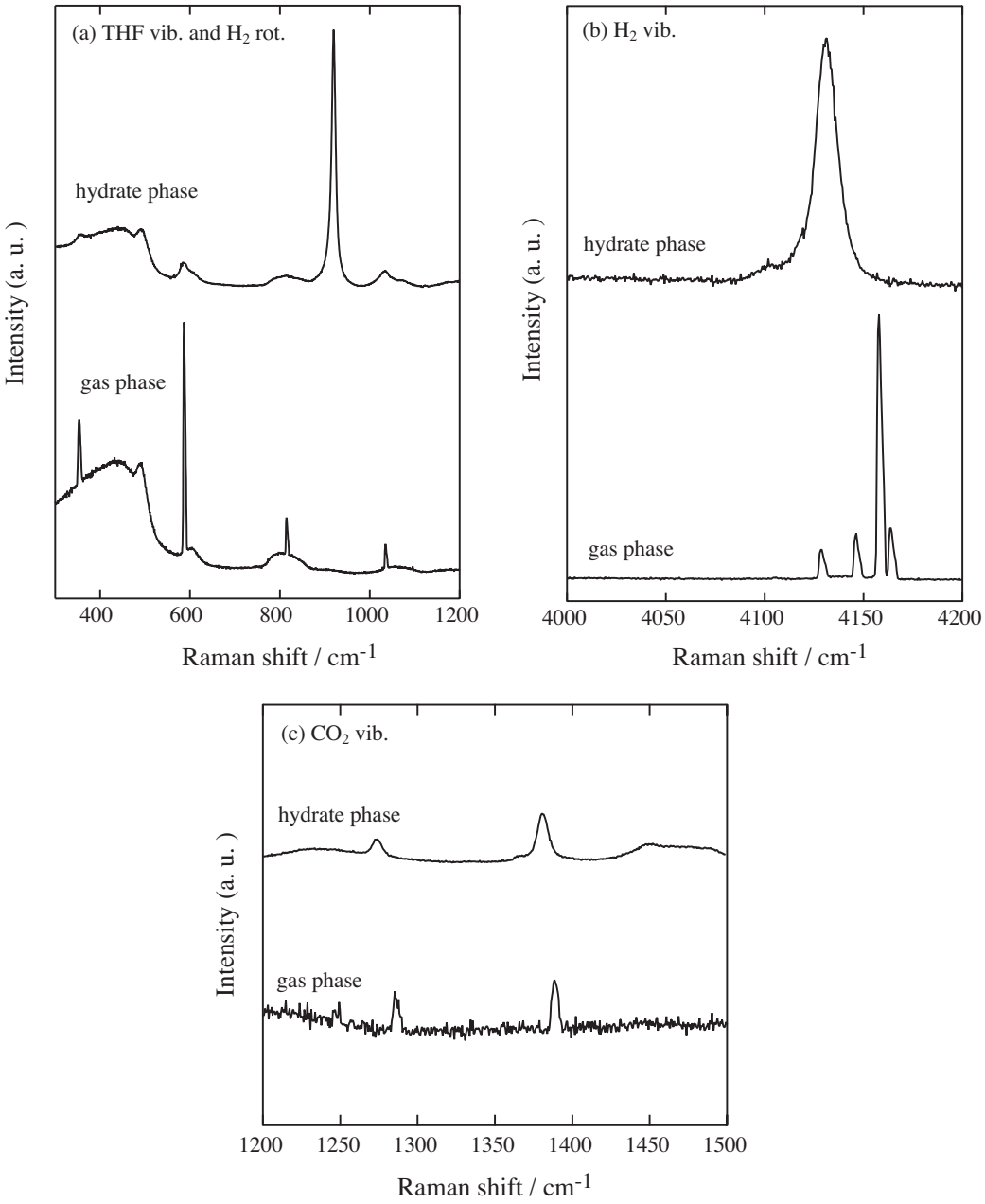

Figure V-7 (a) Raman spectra of the intramolecular vibration for THF in the gas and hydrate phases. Panel (a) contains the spectra corresponding to the rotation of H_2. The high base line less than 520 cm^{-1} is due to the quartz windows of high-pressure optical cell. (b) Raman spectra of the intramolecular vibration for H_2 in the gas and hydrate phases. (c) Raman spectra of the intramolecular vibration for CO_2 in the gas and hydrate phases. All Raman spectra were obtained at the composition region of $y_{H2} > 0.2$.

system obtained in the composition region of $y_{H2} < 0.2$ (at 280.1 K and 0.3 MPa, $y_{H2} = \sim 0.10$). As shown in **Fig. V-8**(a), the single peak detected at 920 cm^{-1} corresponds to the ring breathing mode of the THF molecules enclathrated in the hydrate phase. No peak of H_2 rotation is detected in the hydrate phase. As shown in **Fig. V-8**(c), the split peaks of CO_2 vibration are detected in the hydrate phases at the almost same position for the results of $y_{H2} > 0.2$. **Figure V-8**(b) shows that the peak is not observed in the hydrate phase. That is, in the composition region of $y_{H2} < 0.2$, H_2 molecule cannot occupy the hydrate cages and s-II CO_2 + THF mixed gas hydrate is generated. It is suggested that the H_2 cage occupancy changes depending on y_{H2} in the H_2 + CO_2 + THF + water mixed system.

In the Chapter II, it has been claimed that the hydrate generated in the ternary system of H_2, CO_2 and water (without THF) can be regarded as the pure CO_2 hydrate crystal (s-I) from Raman spectroscopic study. The author have also tried to estimate the equilibrium curve under the constant fugacity of pure CO_2. The gas hydrate crystal generated in the present study is the s-II. The S-cage of s-II is somewhat smaller than that of s-I [10]. Therefore, it is possible that the H_2 molecule occupies the S-cage to generate H_2 + CO_2 + THF mixed hydrate crystal.

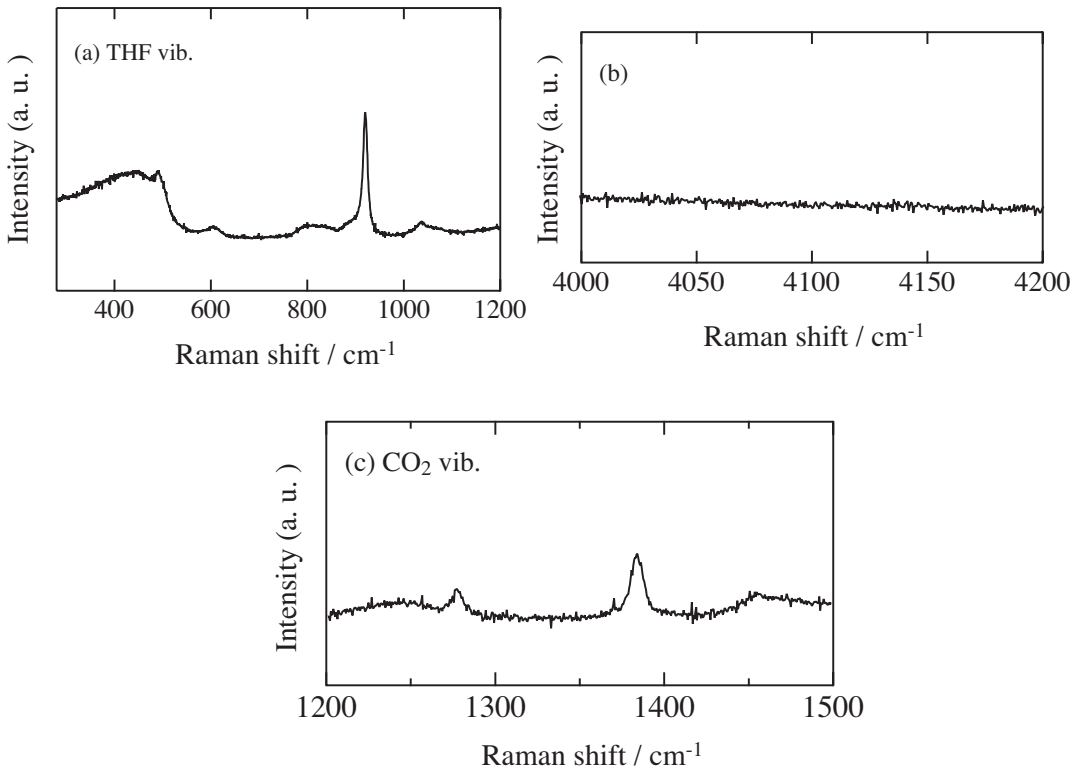

Figure V-8 (a) Raman spectra of the intramolecular vibration for THF in the hydrate phase. The high base line less than 520 cm^{-1} is due to the quartz windows of high-pressure optical cell. (b) Raman spectra obtained around 4100 cm^{-1} in the hydrate phase. (c) Raman spectra of the intramolecular vibration for CO_2 in the hydrate phase. All Raman spectra were obtained at the composition region of $y_{H2} < 0.2$.

V-4 Summary

Isothermal phase equilibria for the H_2 + CO_2 + THF or TBAB + water mixed systems were measured. The results reveal that the equilibrium pressure considerably reduces with a small amount of THF or TBAB. In the H_2 + CO_2 + THF + water mixed system, the largest pressure depression is obtained when the THF concentration is the stoichiometric composition for the pure THF hydrate formation. The pressure depression for the H_2 + CO_2 + TBAB + water mixed system is greater than that of H_2 + CO_2 + THF + water mixed system. The Raman spectroscopy for the hydrate single crystal generated from the H_2 + CO_2 + THF + water mixtures reveal that the cage occupancy of H_2 molecule changes depending on the composition of H_2 in the gas phase. In the region higher than 0.2 in the H_2 mole fraction of gas phase, the H_2 and CO_2 molecules are competitively enclathrated in the S-cages of s-II hydrate while the THF molecules occupy L-cages.

Notation

Nomenclature

p: pressure [Pa]
T: temperature [K]
x: mole fraction of aqueous solution
y: composition of gas phase [-]

Subscript

H2: H_2, THF: THF solution, TBAB: TBAB solution

Literature Cited

[1] Dyadin, Y. A.; Larionov, E. G.; Aladko, E. Y.; Manakov, A. Y.; Zhurko, F. V.; Mikina, T. V.; Komarov, V. Y.; Grachev, E. V. "Clathrate Formation in Water-Noble Gas (Hydrogen) Systems at High Pressures.", *Journal of Structral Chemistry*, **40**, 790-795 (1999).

[2] Mao, W. L.; Mao, H.; Goncharov, A. F.; Struzhkin, V. V.; Guo, Q.; Hu, J.; Shu, J.; Hemley, R. J.; Somayazulu M.; Zhao, Y. "Hydrogen Clusters in Clathrate Hydrate.", *Science*, **297**, 2247-2249 (2002).

[3] Hawkins , R. E.; Davidson, D. W. "Dielectric Relaxation in the Clathrate Hydrates of Some Cyclic Ethers.", *Journal of Physical Chemistry*, **70**, 1889-1894 (1966).

[4] Gough, S. R.; Davidson, D. W. "Composition of Tetrahydrofuran Hydrate and the Effect of Pressure on the Decomposition.", *Canadian Journal of Chemistry*, **49**, 2691-2699 (1971).

[5] Makino, T.; Sugahara, T.; Ohgaki, K. "Stability Boundaries of Tetrahydrofuran + Water System.", *Journal of Chemical Engineering Data*, **50**, 2058-2060 (2005).

[6] Shimada, W.; Ebinuma, T.; Oyama, H.; Kamata, Y.; Takeya, S.; Uchida, T.; Nagao, J; Narita, H. "Separation of Gas Molecules Using Tetra-*n*-butyl Ammonium Bromide Semi-Clathrate Hydrate Crystals.", *Japanese Journal of Applied Physics*, **42**, 129-131 (2003).

[7] Oyama, H.; Shimada, W.; Ebinuma, T.; Kamata, Y.; Takeya, S.; Uchida, T.; Nagao, J; Narita, H. "Phase Diagram, Latent Heat, and Specific Heat of TBAB Semiclathrate Hydrate Crystals.", *Fluid Phase Equilibria*, **234**, 131-135 (2005).

[8] Nakano, S.; Ohgaki, K.; Moritoki, M. "High-pressure Phase Equilibrium and Raman Microprobe Spectroscopic Studies on the CO_2 Hydrate System", *Journal of Chemical Engineering Data*, **43**, 807-810 (1998).

[9] Florusse, L. J.; Peters, C. J.; Schoonman, J.; Hester, K. C.; Koh, C. A.; Dec, S. F.; Marsh K. N.; Sloan, E. D. "Stable Low-Pressure Hydrogen Clusters Stored in a Binary Clathrate Hydrate.", *Science*, **306**, 469-471 (2004).

[10] Subramanian, S.; Sloan, E. D. Jr. "Trends in Vibrational Frequencies of Guests Trapped in Clathrate Hydrate Cages.", *Journal of Physical Chemistry B*, **106**, 4348-4355 (2002).

Part B

Thermodynamic Stability of Hydrogen-containing Mixed Gas Hydrates for Hydrogen Storage (Chapters VI and VII)

Preliminaries

Historically, the H_2 molecule was considered to be too small to contribute to the stability of clathrate hydrates. In 1999, the first pure H_2 hydrate has been demonstrated. Pure H_2 hydrate has several advantages as a H_2 storage material. Firstly, the storage material is pure water. When the H_2 is released from the hydrate, the only byproduct is harmless water which is reusable and compatible with hydrogen fuel cells. Secondly, the formation and decomposition kinetics can be very fast. Furthermore, the hydrogen storage in molecular form is possible. This means that no chemical reaction is required for the H_2 release, and the binding energy is low so heat generation will not be problematic. Finally, water is abundant and cheap. However, the H_2 requires the high pressure (~200 MPa at 273 K) for the hydrate formation, and this severe condition is clearly disadvantageous to the H_2 storage. It is necessary to reduce the high equilibrium pressure of pure H_2 hydrate. For the pressure depression of pure H_2 hydrate system, I regard the addition of other components as the most advantageous method.

In Part B, the objective is to obtain the fundamental information about the thermodynamic stabilities of mixed gas hydrates containing H_2 for H_2 storage and transportation using gas hydrates. From the contents in the Chapter V, two guest species are adopted as the assistant additive for the formation of H_2-containing mixed gas hydrate: THF (Chapter VI) and TBAB (Chapter VII).

Chapter VI

Stability Boundary and Cage Occupancy on Hydrogen + Tetrahydrofuran Mixed Gas Hydrate

---

Abstract

Phase equilibrium curves of hydrogen + tetrahydrofuran mixed gas hydrate were measured in a pressure range up to 200 MPa for the stoichiometric and non-stoichiometric aqueous solutions. Three-phase equilibrium curves for the non-stoichiometric aqueous solutions are shifted to the low-temperature or high-pressure side from that of the stoichiometric ones. Each three-phase equilibrium curve converges at the equilibrium point of the pure tetrahydrofuran hydrate for the mother aqueous solution of same mole fraction. It is directly confirmed by use of Raman spectroscopy that hydrogen is enclathrated in the hydrate cages by adding a small amount of tetrahydrofuran. Hydrogen is enclathrated in only the small cage while tetrahydrofuran occupies the large cages of each mixed gas hydrate. The selectivity of hydrate-cage occupancy by hydrogen does not change with the variation of mole fraction in the aqueous solution. Hydrogen is entrapped in the only small cages of tetrahydrofuran hydrate in the whole mole fraction ranges. The structural transition does not occur and the hydrogen gradually occupies empty small cages of structure-II tetrahydrofuran hydrate depending on the pressure.

The storage capacity of hydrogen in the tetrahydrofuran hydrate was investigated by the data obtained from Raman spectroscopic measurements. It is directly confirmed by use of Raman spectroscopy that the amount of enclathrated hydrogen molecules in the mixed gas hydrate increases as the pressure rises. The storage capacity would reach the ceiling value at about 80 MPa. This ceiling value seems to be about 1.0 mass% which is almost equal to the maximum amount of hydrogen storage in the structure-II tetrahydrofuran hydrate on the assumption that the only one hydrogen molecule can occupy the small cage of tetrahydrofuran hydrate.

Keywords: gas hydrate; phase equilibria; cage occupancy; hydrogen; solution; gas storage

VI-1 Introduction

H_2 has become the object of attention as a clean and promising energy resource. Recently, H_2 hydrate is being considered as a medium of H_2 storage and transportation. However, the pure H_2 hydrate is generated only in extremely high-pressure region of 100-360 MPa [1]. Mao *et al.* [2] and Mao and Mao [3] reveal that H_2 + water mixtures generate the s-II hydrate at high pressure of 200 MPa and low temperature of *ca.* 80 K, where the hydrate cages are multiply occupied by two H_2 molecules in the S-cage and four in the L-cage. Much milder conditions are desired to utilize H_2 hydrate as a medium of H_2 storage and transportation.

Tetrahydrofuran (hereafter, THF), well known as a common solvent, generates s-II hydrate [4] below atmospheric pressures. THF can be enclathrated in the L-cage while it cannot occupy the S-cage. The chemical formula of ideal THF hydrate is written as $THF \bullet 17H_2O$ [5]. THF has been widely used as an additive that would reduce the equilibrium pressure of other gas hydrates (for example, CH_4 and N_2 hydrates). Furthermore, the effect of THF addition was the highest among several additives (for example, acetone, 1, 4-dioxane) [6, 7]. Florusse *et al.* [8] have firstly reported that H_2 can be entrapped in hydrate cages with the existence of THF at low pressures. They have also revealed that the crystal structure of H_2 + THF mixed gas hydrate belongs to the s-II hydrate by X-ray diffraction measurement. According to Florusse *et al.* [8] and Lee *et al.* [9], one or two H_2 molecules are only enclathrated in the S-cage and one THF molecule in the L-cage. Phase behavior of H_2 + THF hydrate, however, is unclear in a low pressure region where the pure THF hydrate exist stable [10].

In addition, Lee *et al.* [9] have investigated the binary-mixed gas hydrate containing H_2 + THF at various THF concentrations by use of Nuclear Magnetic Resonance (NMR). They have claimed that the H_2 molecule can occupy the L-cage as well as the S-cage at THF mole fractions lower than 0.020, and that THF occupies the L-cage completely, while H_2 is entrapped by only the S-cage in the THF mole fraction region higher than 0.020. Recently, Strobel *et al.* [11] have reported that the cage occupancy of H_2 is independent of the THF concentration in the mole fraction range lower than 0.056 based on gas release data and H_2 does not occupy the L-cage. They have also reported that he storage capacity of H_2 in the THF hydrate reaches the ceiling value at *ca.* 70 MPa, where the peak value is about 1.0 mass% of hydrogen. The results about the L-cage occupancy of H_2 reported by Strobel *et al.* [11] are inconsistent with those of Lee *et al.* [9]. In order to reveal the storage capacity of H_2, it is necessary to verify the cage occupancy of H_2 by spectroscopic method other than NMR. Furthermore, the variation of the THF concentration results in the change of the phase equilibrium relation for mixed hydrate containing THF. For example, it is well known that phase equilibrium curves for the N_2 + THF mixed gas hydrate in non-stoichiometric THF concentration are shifted to a high-pressure or low-temperature condition compared with those of stoichiometric concentration [7]. Considering this tendency in the N_2 + THF mixed-gas hydrate system, thermodynamic stability boundary of

H_2 + THF mixed-gas hydrate in non-stoichiometric THF concentration would be also shifted to a high-pressure or low temperature condition. Therefore, it is necessary to determine both the phase behavior and cage occupancy of H_2 in the H_2 + THF mixed gas hydrate system simultaneously for H_2 storage using gas hydrates.

In the Chapter VI, thermodynamic stabilities of H_2 + THF mixed gas hydrate were measured (for the stoichiometric aqueous solution, in the lower pressure region than the previous report [8]). Raman spectra for each single crystal of H_2 + THF mixed gas hydrate were measured under the three-phase coexisting conditions. In order to confirm the results reported by Lee *et al*. [9], the effect of thermodynamic stability and H_2 occupancy on mole fraction of aqueous solution were also investigated for the H_2 + THF mixed gas hydrate system. Finally, the H_2 storage capacity of THF hydrates can be evaluated by the data obtained from Raman spectroscopic measurements under the three-phase (gas, aqueous, and hydrate phases) equilibrium and isothermal conditions.

VI-2 Experimental Section

VI-2.1 Apparatus

The experimental apparatus for the phase equilibrium measurements in the low-pressure range (up to 10 MPa) was the same as the one in the Chapter III except for the lack of gas sampling lines (**Fig. VI-1**). As shown in **Fig. VI-1**, two types of high-pressure cell were used for phase equilibrium measurements. The high-pressure cell made of stainless steel had an inner volume of *ca*. 150 cm^3. The maximum working pressure was 10 MPa. The cell had a set of windows for visually observing the phase behavior. The other was pressure-proof glass cell. The inner volume and maximum working pressure of the high-pressure glass cell were 10 cm^3 and 5 MPa, respectively. All parts of the high-pressure cell were immersed in a temperature-controlled water bath. The contents were agitated using an up-and-down mixing bar driven by an exterior permanent magnetic ring.

For the phase equilibrium measurements in the high-pressure range (up to 200 MPa) and Raman spectroscopic analyses, the high-pressure optical cell was used, which had a pair of quartz (highly pure) or sapphire (highly pure) windows on both the upper and lower sides. The apparatus containing the high-pressure optical cell was the same as the one in the Chapter III and IV, except for the pressurizing line. The schematic illustration of experimental apparatus is shown in **Fig. VI-2**. As shown in **Fig. VI-2**, the intensifier was added to the gas introducing line.

The system temperature was measured within an uncertainty of 0.02 K using a thermistor probe (Takara D-632), which was inserted into a hole in the cell wall. The probe was calibrated

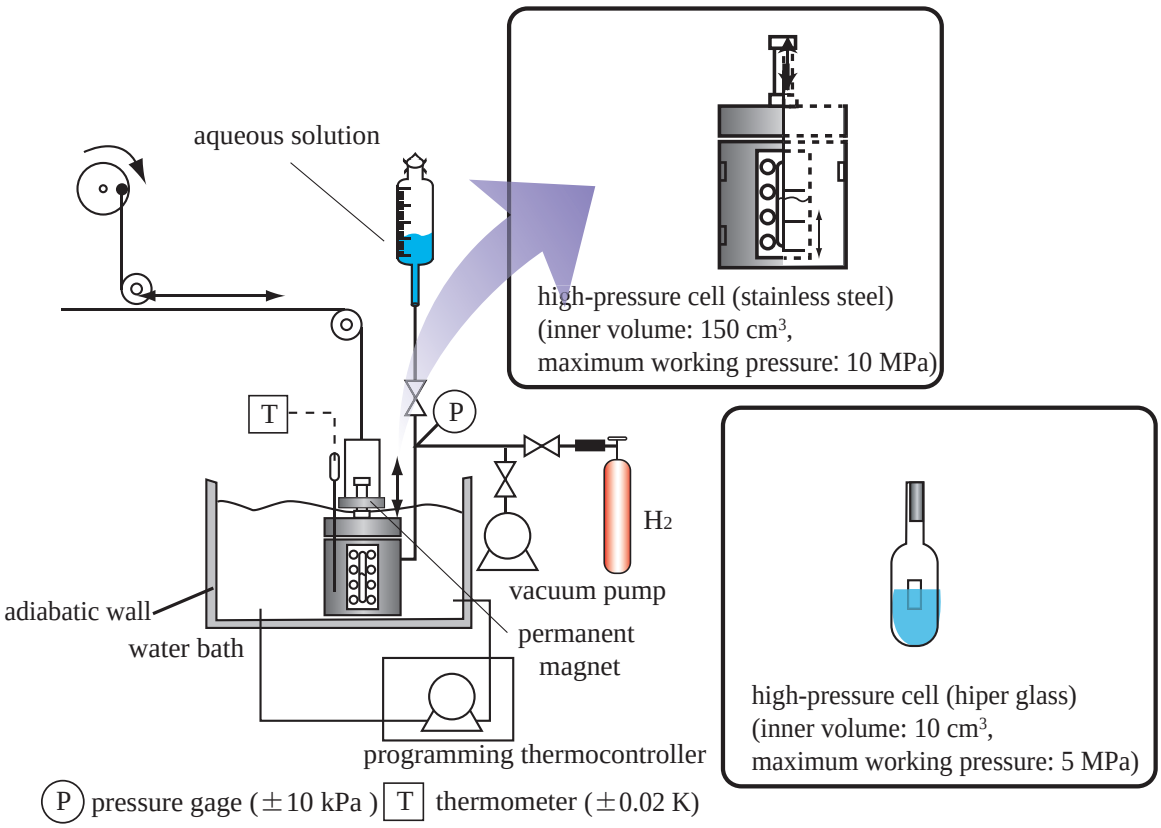

Figure VI-1 Schematic illustration of experimental appratus for the phase equilibrium measurements in the low-pressure range.

with a Pt resistance thermometer defined by ITS-90. The system pressure was measured by a pressure gage (Valcom VPRT) calibrated by RUSKA quartz Bourdon tube gage (Direct Reading Pressure Gage, series 6000) with an estimated maximum uncertainty of 0.01 MPa (low-pressure range) and 0.1 MPa (high-pressure range).

VI-2.2 Procedures

Phase equilibrium measurement

The THF aqueous solution prepared at a desired mole fraction (x_{THF} = 0.010, 0.024, 0.056 or 0.130) was introduced into the evacuated high-pressure cell. The content was pressurized up to the desired pressure by supplying H_2. In the present study, we have adopted the method similar to the "*T*-cycle method [12]" for the three-phase equilibrium measurement. At first, the system temperature was decreased and kept constant at the point of pressure depression which is caused by the H_2 + each additive mixed gas hydrate formation (the formation can be confirmed through the window of the cell). We cannot directly measure the equilibrium composition of aqueous phase under the coexistence of gas hydrate phase. Therefore, the content was heated very gradually and step by step (0.1 K each) until there was a negligibly small amount of gas

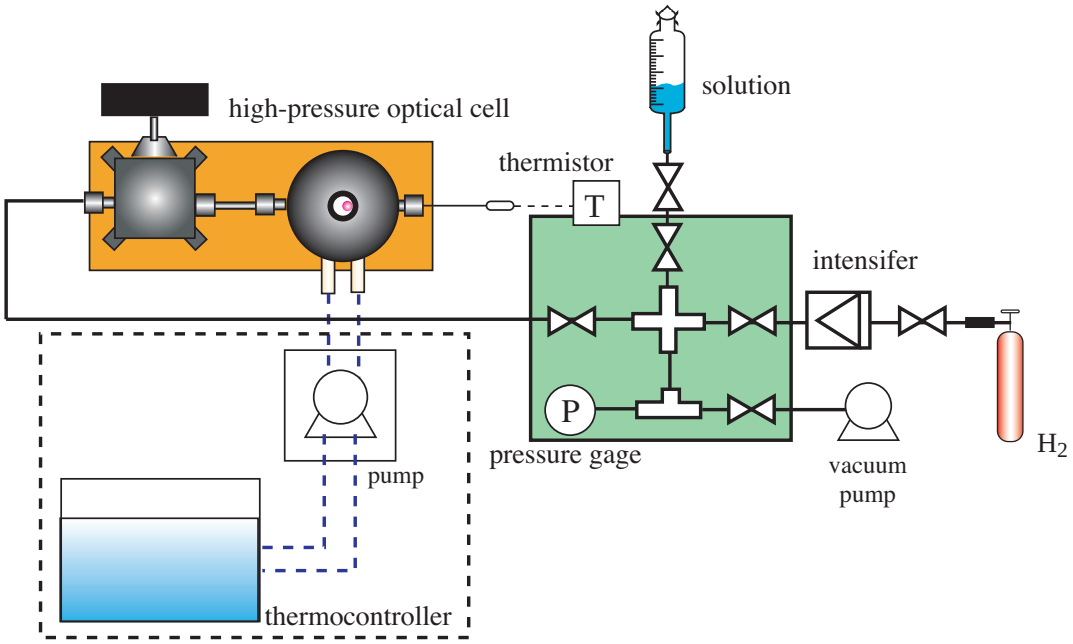

Figure VI-2 Schematic illustration of experimental apparatus for phase equilibrium measurement in the high-pressure range and Raman spectroscopic analysis.

hydrate left in order to minimize change of concentration in the aqueous solution. The interval time was taken adequately (at least one day) for establishing equilibrium state at each temperature step. When the last particle of hydrates disappeared on gradually heating, we adopted this point as the equilibrium point. In order to eliminate a hysteresis effect, we have used the annealing method (0.05 K one cycle per day) in addition to the "*T*-cycle method [12]". We never fail to repeat several times the *T*-cycle and annealing methods. In addition, we also repeated the same equilibrium measurements using the fresh solution at the same mole fraction.

Raman spectroscopic analysis

Three-phase equilibrium state

The aqueous solution prepared at a desired composition (x_{THF} = 0.024 or 0.056) was introduced into the evacuated high-pressure cell. The contents were pressurized up to a desired pressure by supplying H_2 and then cooled and agitated with an enclosed ruby ball in order to prepare the gas hydrate. The procedure for the preparation of hydrate single-crystal was similar to that of the previous chapter. A photo of single crystal for the H_2 + THF mixed gas hydrate is shown in **Fig. VI-3**. We also paid enough attention to preparing as few single-crystals as possible.

This single crystal of gas hydrate was analyzed by *in situ* Raman spectroscopy by use of a laser Raman microprobe spectrometer with a multichannel CCD detector. The CCD detector was maintained at ~200 K for heat-noise reduction. The argon ion laser beam (wavelength: 514.5 nm and generation power: 100 mW) condensed to 2 μm in spot diameter were irradiated to the

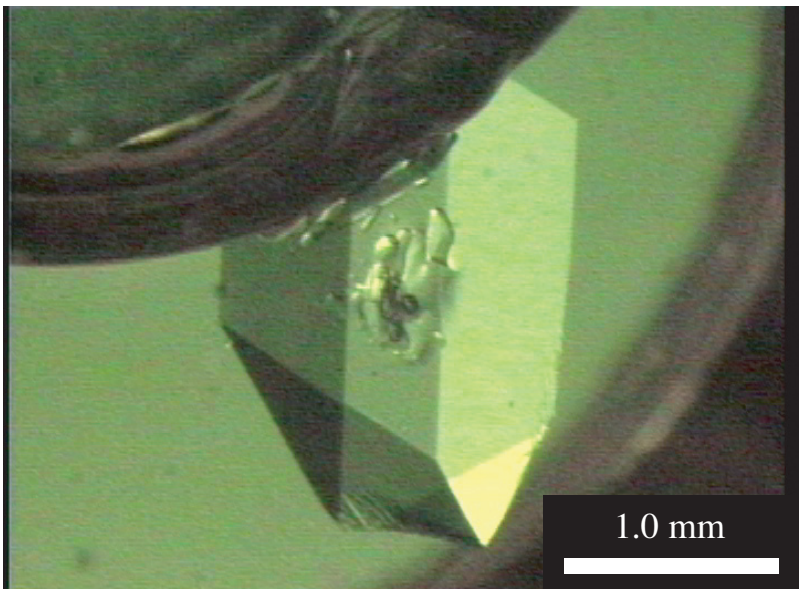

Figure VI-3 A photo of single crystal for H_2 + THF mixed gas hydrate prepared at 137.0 MPa, 294.39 K, and x_{THF} = 0.024.

single crystals from the object lens through the upper quartz or sapphire window. The backscatter of the opposite direction was taken in with the same lens. The spectral resolution was about 1 cm^{-1}. The exposed time was 60 sec. The spectra were obtained with three integrations.

Isothermal condition

The aqueous THF solution prepared at x_{THF} = 0.056 was introduced into the evacuated high-pressure cell. The contents were supercooled and agitated with an enclosed ruby ball in order to prepare the THF hydrate. After the complete formation of gas hydrates, the system temperature was kept constant for more than one day at 277 K to mature the hydrate. Then, the contents were pressurized up to a desired pressure by supplying H_2 and the cell was kept quiet in order to establish the two-phase (gas and hydrate phases) equilibrium state. After one day, the hydrate phase was analyzed through the upper quartz or sapphire window by *in situ* Raman spectroscopy. The other measurement conditions were similar to those performed under the three-phase equilibrium state.

VI-2.3 Materials

Research grade H_2 (mole fraction purity 0.999999) was obtained from the Neriki Gas Co., Ltd. The maximum impurity was 0.2 ppm of nitrogen. Research grade THF (mole fraction purity 0.997) and the distilled water were obtained from the Wako Pure Chemical Industries, Ltd. All of them were used without further purifications.

VI-3 Results & Discussion

VI-3.1 Phase Equilibria

Phase equilibria for the H_2 + THF mixed gas hydrate system at various THF concentrations are summarized in **Table VI-1** and shown in **Fig. VI-4**. The mole fractions of THF (x_{THF}) in the aqueous solutions are 0.010, 0.024, 0.056, and 0.130. The stoichiometric mole fraction of the pure THF hydrate is x_{THF} = 0.056 [10]. As shown in **Fig. VI-4**, the three-phase equilibrium curve of pure THF hydrate has a maximum temperature point at 277.45 K and 4.9 kPa [10]. The three-phase equilibrium curve of H_2 + THF hydrate, which is prepared from the THF stoichiometric aqueous solution, converges at the maximum temperature point. The three-phase equilibrium curves of H_2 + THF mixed gas hydrate, which were obtained from the THF aqueous solution of x_{THF} = 0.024 and 0.130, converge at each equilibrium point of pure THF hydrate prepared from the same mole fraction solution, (275.73 K, 2.6 kPa) and (276.21 K, 6.3 kPa) [10], respectively. Each equilibrium curve vertically rises up in the pressure up to about 2 MPa, which may be attributed to the hydrogen content in the hydrate. Each three-phase equilibrium pressure increases continuously with the temperature increase. The quadruple point of gas, aqueous solution, ice, and hydrate phases for the THF + water mixed system is located at x_{THF} = 0.0106, 272.06 K and 1.1 kPa [10]. The three-phase equilibrium line of H_2 + THF mixed

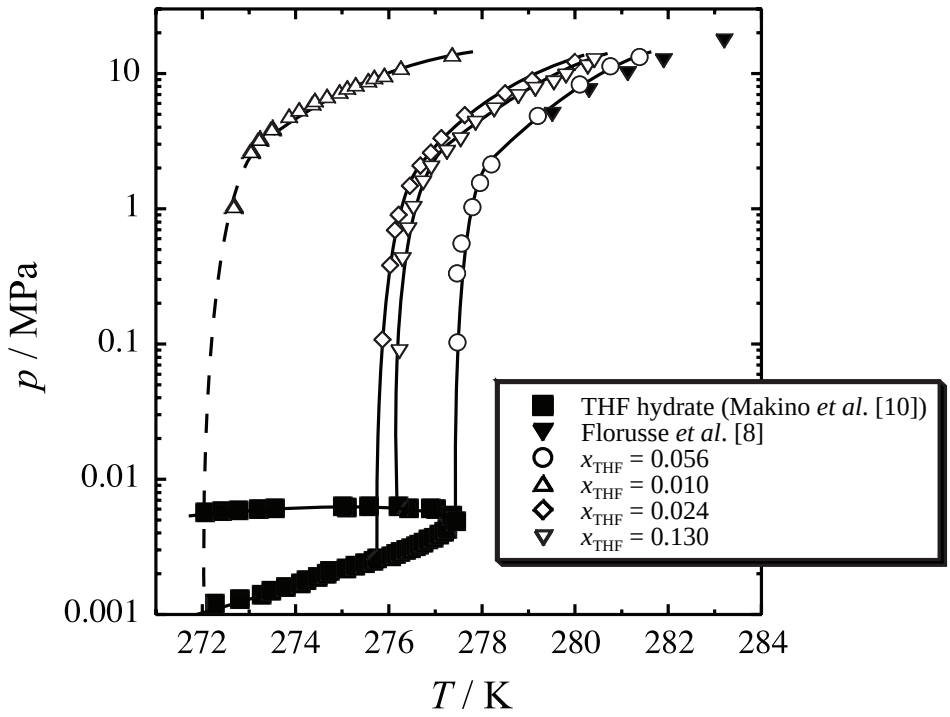

Figure VI-4 Three-phase equilibrium curves of the H_2 + THF mixed gas hydrate system. The solid lines are fitting lines for the experimental data, and broken line is an extraporated line on the assumption that three-phase equilibrium line for the THF mole fraction of 0.010 has a similar behavior as the other lines.

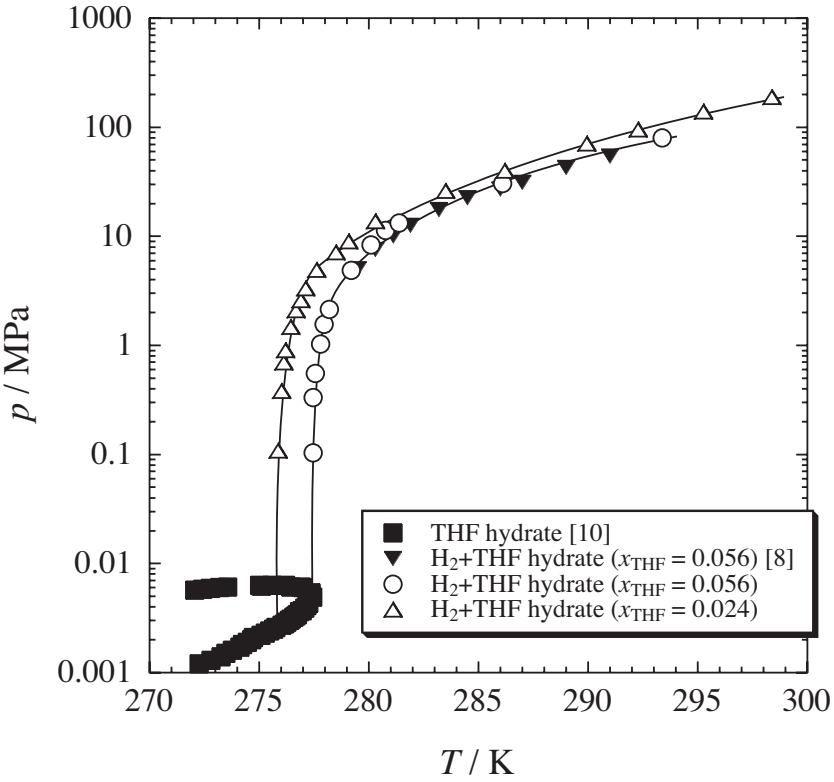

Figure VI-5 Phase equilibrium (p - T) relation for the H_2 + THF mixed gas hydrate system including the high-pressure region.

gas hydrate of x_{THF} = 0.010 would converge at the vicinity of the quadruple point as well as those of x_{THF} = 0.024, 0.056, and 0.130. The phase behaviors of all equilibrium curves agree well with one another.

Figure VI-5 shows the phase equilibrium (pressure - temperature) relations for the H_2 + THF mixed gas hydrate system including the high-pressure region. The phase equilibrium data are also summarized in **Table VI-1**. In the high-pressure region, the equilibrium curve of x_{THF} = 0.056 agrees well with that of Florusse *et al.* [8]. The three-phase equilibrium pressure increases monotonically with the temperature increase from the low-pressure to high-pressure region, and does not exhibit a stepwise variation. Therefore, it is likely that the structural transition of hydrate structure or variation of cage occupancy may not occur under the present experimental condition.

VI-3.2 Raman Spectroscopic Analysis

In situ Raman microspectroscopy was performed at x_{THF} = 0.010, 0.024, 0.056, and 0.130 under the three-phase equilibrium conditions. **Figure VI-6** shows a few typical Raman spectra derived from the THF and H_2 molecules for the H_2 + THF mixed gas hydrate system (at 294.39 K, 137.0 MPa, and x_{THF} = 0.024). As shown in **Fig. VI-6**(a), the Raman peaks corresponding to

Table VI-1 Phase equilibrium data for the H_2 + THF mixed gas hydrate system at various THF mole fractions.

	T / K	p / MPa		T / K	p / MPa
x_{THF} = 0.010	272.89	1.13		292.28	95.0
	273.25	2.78		295.25	140.0
	273.42	3.41		298.38	190.0
	273.68	4.05	x_{THF} = 0.056	277.47	0.10
	273.86	4.86		277.47	0.33
	274.08	5.43		277.56	0.55
	274.36	6.02		277.80	1.03
	274.42	6.36		277.96	1.55
	274.68	6.83		278.20	2.13
	274.94	7.36		279.20	4.87
	275.11	7.86		280.10	8.30
	275.29	8.33		280.76	11.3
	275.56	8.88		281.39	13.3
	275.69	9.38		286.10	30.5
	275.91	9.73		293.39	80.0
	276.26	11.0	x_{THF} = 0.130	276.23	0.09
	277.36	13.8		276.30	0.42
x_{THF} = 0.024	275.86	0.11		276.42	0.70
	276.03	0.38		276.53	1.01
	276.13	0.70		276.74	1.55
	276.21	0.90		276.91	2.01
	276.45	1.48		277.25	2.61
	276.68	2.09		277.54	3.24
	277.13	3.34		277.87	4.31
	277.63	4.92		278.26	5.37
	278.50	7.15		278.79	6.74
	279.08	8.94		279.15	7.64
	280.31	13.7		279.55	8.56
	283.50	26.2		279.81	9.60
	286.20	39.7		280.28	11.2
	289.94	71.2		280.41	12.5

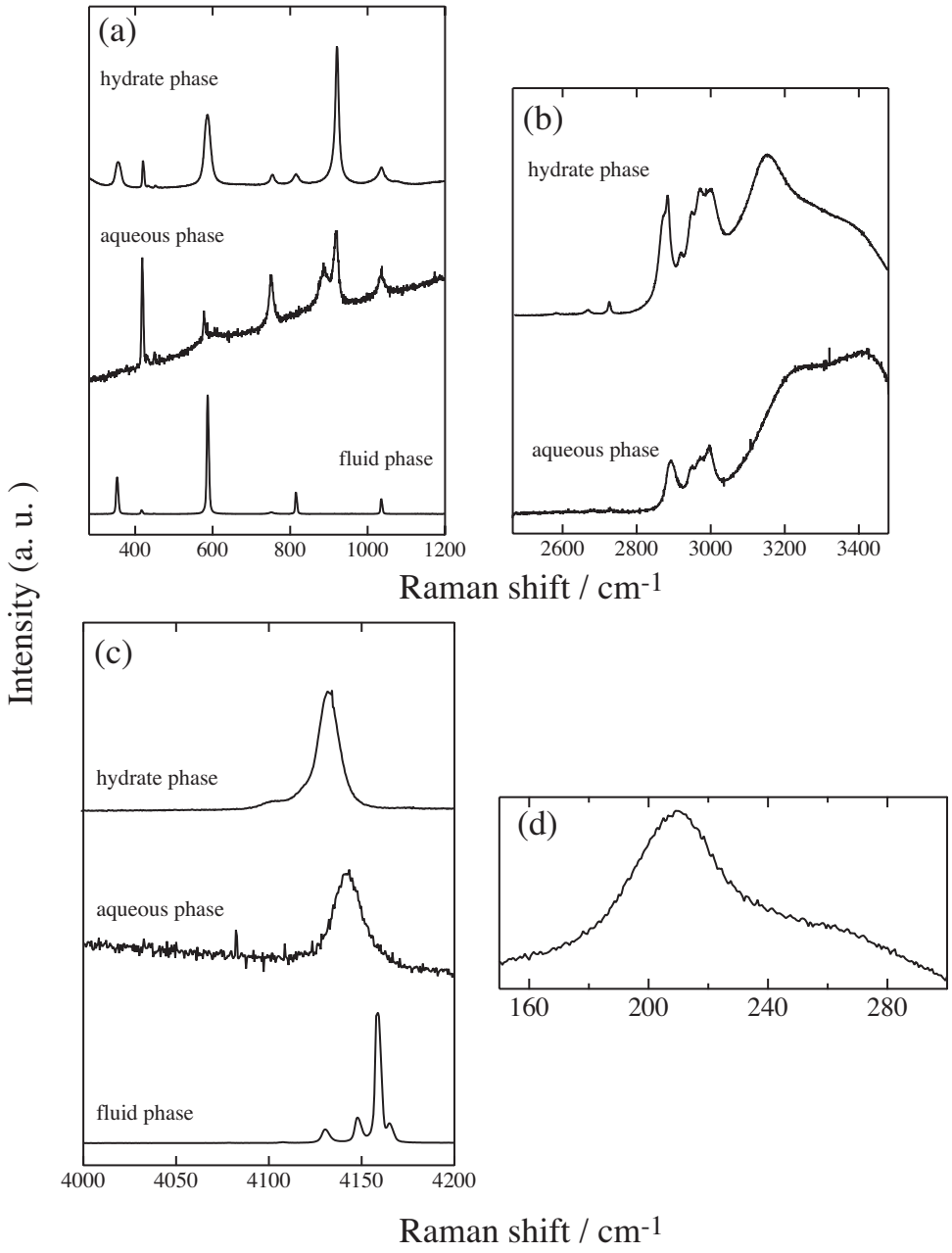

Figure VI-6 Typical Raman spectra derived from the THF, H_2, and host water molecules for the H_2 + THF mixed gas hydrate system (at 294.39 K, 137.0 MPa, and x_{THF} = 0.024).

the enclathrated THF molecule are detected at 919 and 1033 cm^{-1} in the hydrate phase, while the three peaks are detected at 883, 920, and 1036 cm^{-1} in the aqueous phase [13-15]. Therefore, it can be confirmed from the Raman spectra that the peaks of hydrate phase are not affected by the aqueous phase. The peaks corresponding to the H_2 rotation are obtained at 354, 588, 816, and 1036 cm^{-1} in the gas phase, while detected at 351, 584, and 814 cm^{-1} in the hydrate phase [16]. The peak around 1036 cm^{-1} overlaps with that of THF. As shown in **Fig. VI-6**(b), the peaks corresponding to the C-H vibration of THF are obtained around 2900 cm^{-1} in the aqueous and hydrate phases. **Figure VI-6**(b) contains the broad peaks derived from the O-H vibration of host water molecules. In this region, no peak is obtained in the gas phase. As shown in **Fig.**

VI-4(c), four peaks corresponding to the H-H stretching vibration of H_2 are detected at 4129, 4146, 4159, and 4165 cm^{-1} in the gas phase, while a broad and single peak is detected at 4139 cm^{-1} and 4131 cm^{-1} in the aqueous and hydrate phases, respectively. In addition, **Figure VI-6**(d) shows that the peak corresponding to the intermolecular O-O vibration of water is detected at 210 cm^{-1}. This indicates that the H_2 + THF mixed gas hydrate is the s-II unit-cell structure [17,

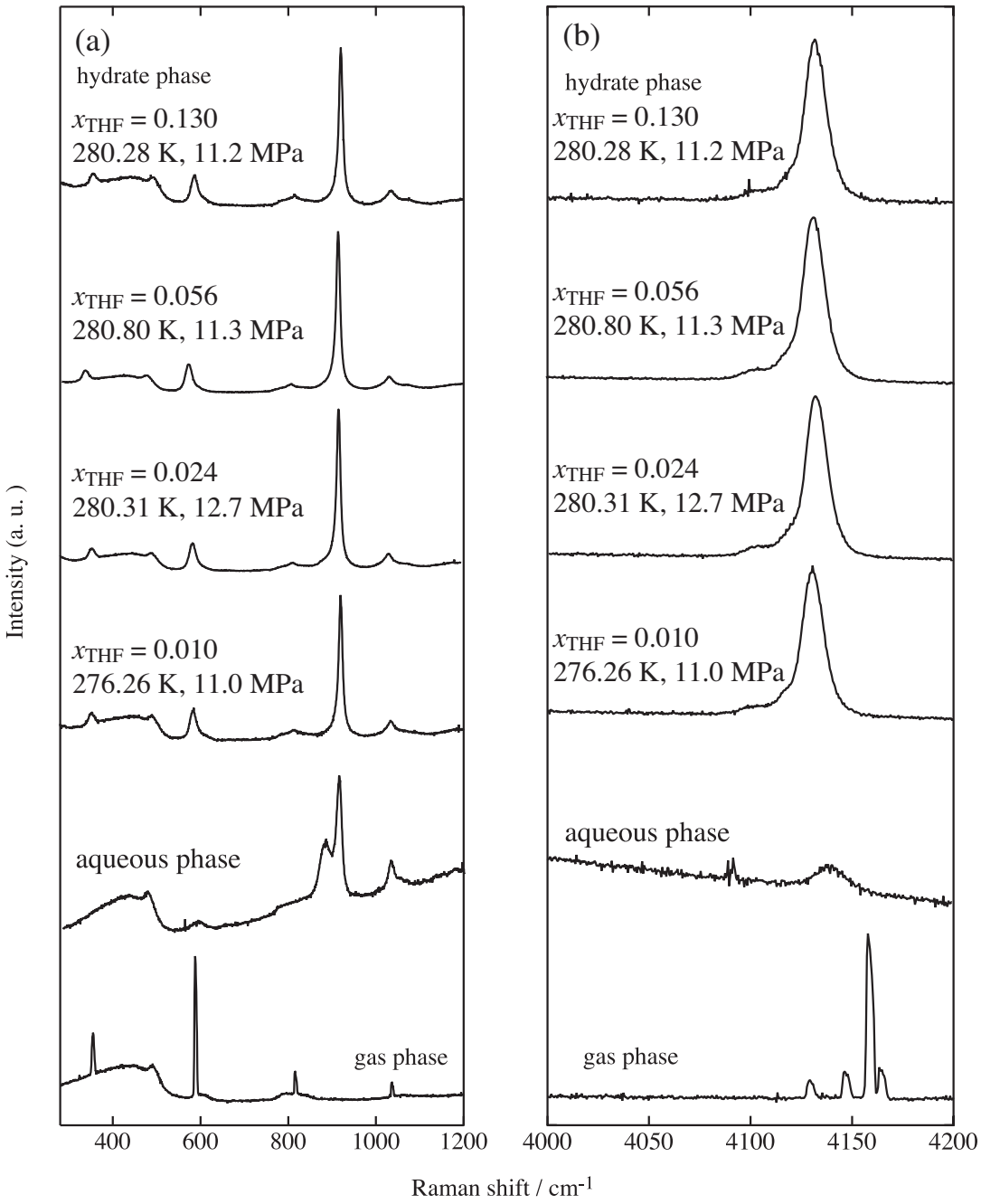

Figure VI-7 Raman spectra of the intramolecular vibration for the THF (a) and H_2 (b) molecules in the gas and hydrate phases at various THF mole fractions. Panel (a) contains the spectra corresponding to the rotation of H_2. Typical spectra obtained in the gas and aqueous solution phases at x_{THF} = 0.056 are contained. The broad signals that appear in lower than 520 cm^{-1} correspond to the quartz windows of high-pressure optical cell.

18]. Incidentally, the signals which appear around 419 and 751 cm^{-1} are due to the sapphire windows of high-pressure optical cell.

The change of Raman spectra on the THF concentration is shown in **Fig. VI-7**(a) and (b). As shown in **Fig. VI-7**, the position and shape of all peaks derived from H_2 in the hydrate phase agree well with one another. There is no remarkable change of Raman spectrum with the variations of THF concentration. Therefore, the cage occupancies of guest molecules for the H_2 + THF mixed gas hydrate are independent of THF concentrations in the aqueous solutions under the present experimental condition. That is, the THF molecule occupies the L-cage completely while the H_2 selectively occupies the S-cage of s-II hydrate. The results obtained in this study are consistent with those of Strobel *et al*. [11] on the point that the H_2 molecule cannot occupy the L-cage for the H_2 + THF mixed gas hydrate.

Figure VI-8 shows the pressure dependence of the peak derived from the H_2 molecule. In

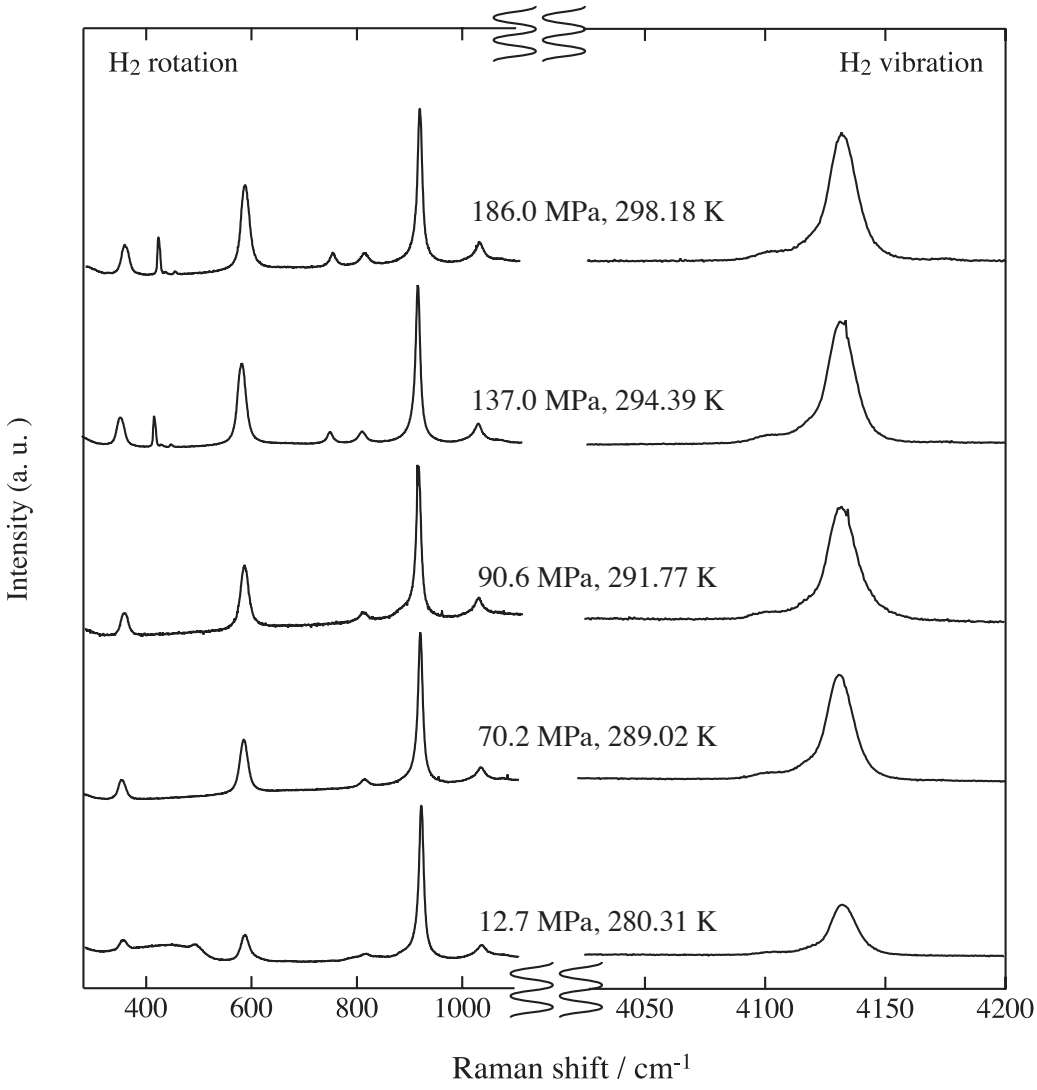

Figure VI-8 Pressure dependence of the normalized Raman peak derived from the H_2 molecule under the three-phase equilibrium state at $x_{THF} = 0.024$. The peak of H_2 is normalized by that of THF ring-breathing mode.

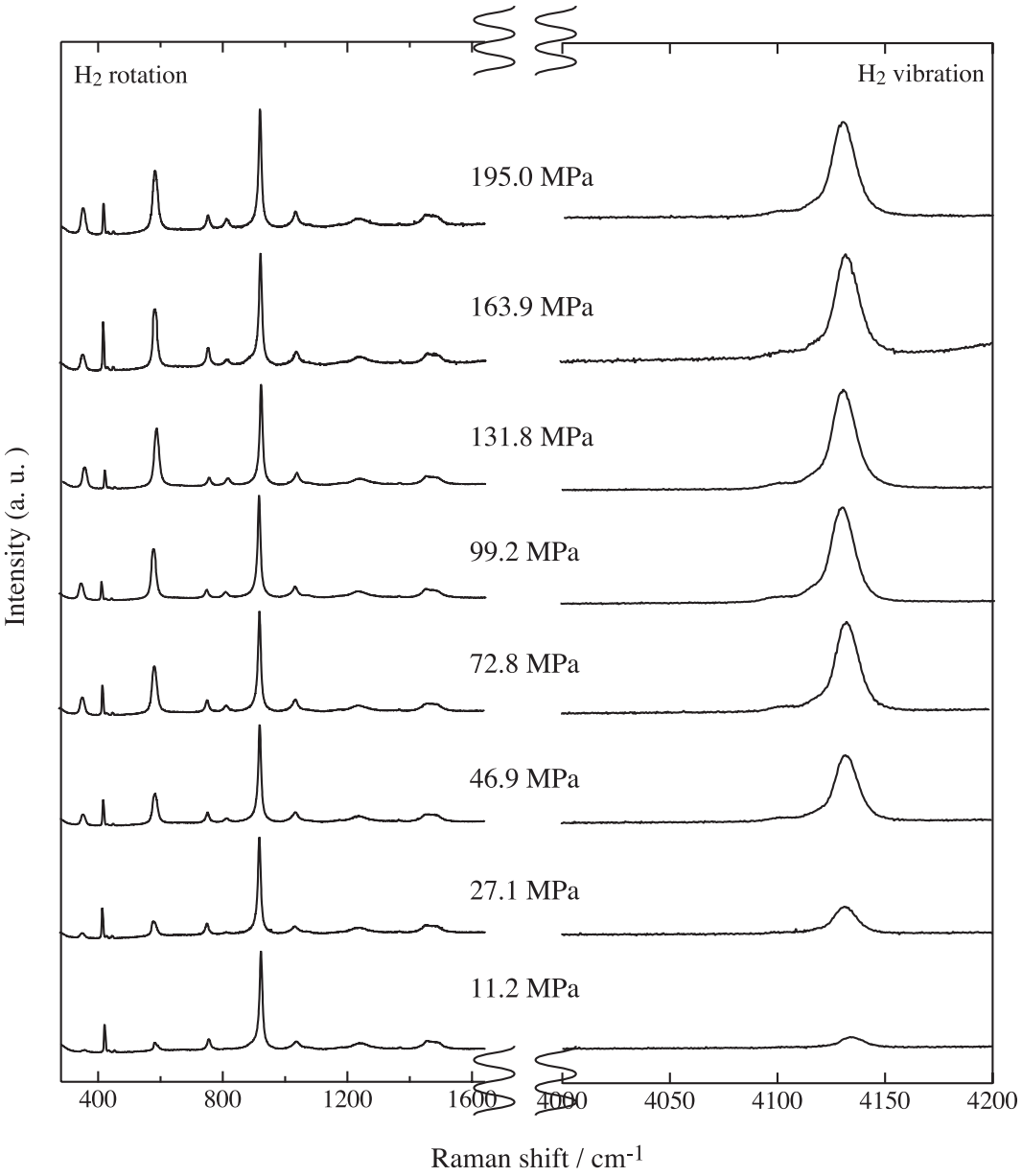

Figure VI-9 Pressure dependence of the normalized Raman peak derived from the H_2 molecule under the isothermal condition (at 277 K) and x_{THF} = 0.056. The peak of H_2 is normalized by that of THF ring-breathing mode.

Fig. VI-8, the peaks of H_2 (4131 cm^{-1}) are normalized by use of the sharp peak (920 cm^{-1}) corresponding to the ring-breathing (C-C-C-C) vibration mode of THF. As shown in **Fig. VI-8**, the peak area of H_2 increases successively with the system pressure increases. That is, the storage amount of H_2 in the THF hydrate increases with the pressure increases. In the case of pure THF hydrate, it was reported previously that the structural transition from s-II to s-I occurs at 268 K and 200 MPa [10, 13, 19]. On the other hand, Raman shift obtained in the present study does not depend on the system pressure, that is, the structural transition of hydrate structure or the variation of cage occupancy may not occur under the present experimental condition.

In the Chapter VI, Raman spectroscopy was performed at the constant temperature of 277 K and x_{THF} = 0.056 under the two-phase equilibrium conditions. **Figure VI-9** shows the pressure dependence of the peak derived from the H_2 molecule. In **Fig. VI-9**, the peaks of H_2 are normalized as well as **Fig. VI-8**. As shown in **Fig. VI-9**, the peak intensity or area of H_2 increases successively with the system pressure increases. That is, the H_2 storage in the THF hydrate may be potential by the pressurization of the THF hydrate using H_2 gas.

VI-3.3 Storage Capacity

Figure VI-10 shows the pressure dependence of normalized peak area ratio (H_2 vibration / THF ring-breathing). **Figure VI-10** indicates that the storage amount of H_2 approaches about maximum area ratio and reaches plateau in the pressure region more than 80 MPa. This maximum value seems to be *ca.* 1.05 mass%, which is almost equal to the maximum amount of hydrogen storage in the s-II THF hydrate on the assumption that the only one hydrogen molecule can occupy the small cage of tetrahydrofuran hydrate. These findings are consistent

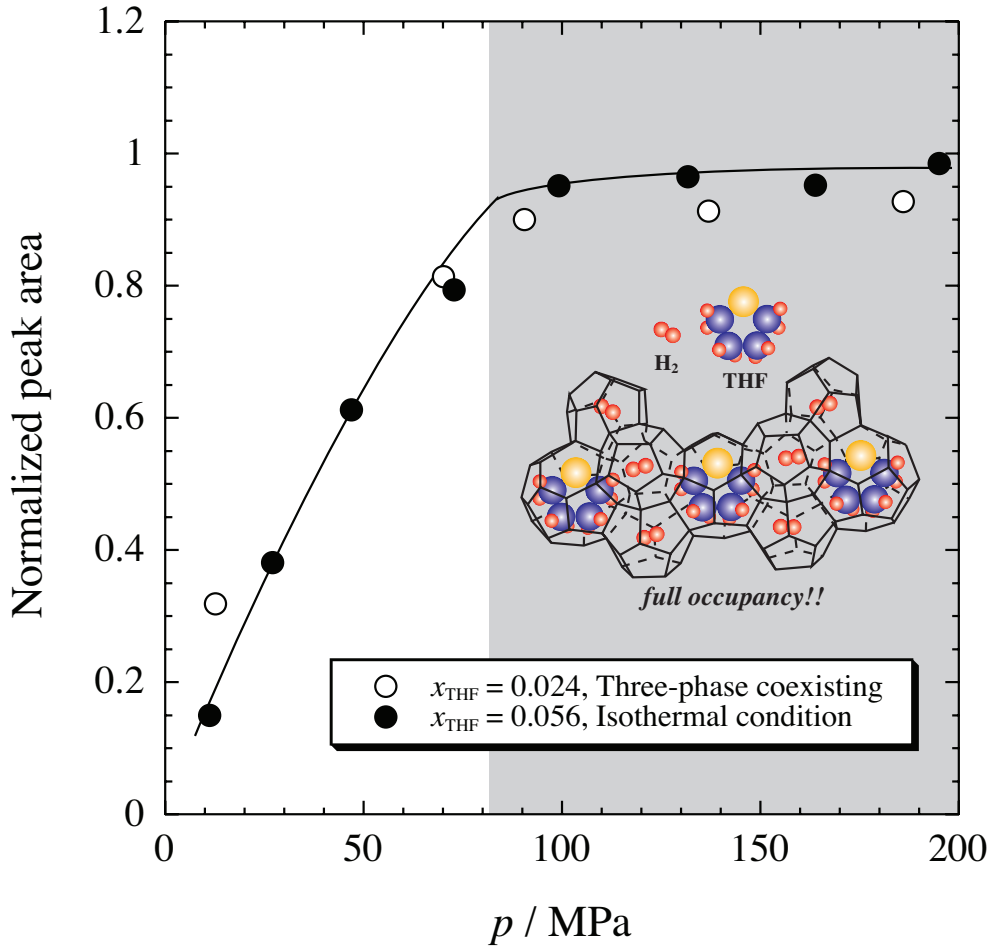

Figure VI-10 Pressure dependence of normalized Raman peak area (H_2 vib. / THF ring-breathing).

with the data reported by Strobel *et al*. [11]. In addition, as shown in **Fig. VI-10**, the H_2 storage amount does not depend on the difference of aqueous concentrations or coexisting phase. It is suggested that the storage capacity of H_2 in THF hydrate can be evaluated simply by means of Raman spectroscopic method.

VI-4 Summary

Phase equilibria for the ternary systems of H_2 + THF + water were measured at the various mole fractions of aqueous solution. The three-phase (gas, aqueous solution, and hydrate phases) equilibrium curves of each mixed gas hydrate converge at the equilibrium point of each pure THF hydrate prepared from the same aqueous solution. Three-phase equilibrium curves of H_2 + THF mixed gas hydrate changes smoothly and successively from the low-pressure to high-pressure region up to 200 MPa. From Raman spectroscopy for the single crystals of H_2 + THF mixed gas hydrates, it is concluded that the S-cages and the other large-cages are selectively occupied by H_2 and THF in all mole fraction range of aqueous solution, respectively. The Raman spectra also reveal that the amount of enclathrated H_2 molecules in the mixed gas hydrate increases as the system pressure rises and reaches plateau around *ca*. 80 MPa. On the other hand, the shift and shape of Raman peaks do not depend on the system pressure. These findings indicate that the structural transition does not occur and the H_2 gradually occupies empty small cages of s-II THF hydrate depending on the system pressure under the present experimental condition.

Notation

Nomenclature

p: pressure [Pa]
T: temperature [K]
x: mole fraction of aqueous solution

Subscript

THF: THF solution

Literature Cited

[1] Dyadin, Y. A.; Larionov, E. G.; Aladko, E. Y.; Manakov, A. Y.; Zhurko, F. V.; Mikina, T. V.; Komarov, V. Y.; Grachev, E. V. "Clathrate Formation in Water-Noble Gas (Hydrogen) Systems at High Pressures.", *Journal of Structral Chemistry*, **40**, 790-795 (1999).

[2] Mao, W. L.; Mao, H.; Goncharov, A. F.; Struzhkin, V. V.; Guo, Q.; Hu, J.; Shu, J.; Hemley, R. J.; Somayazulu M.; Zhao, Y. "Hydrogen Clusters in Clathrate Hydrate.", *Science*, **297**, 2247-2249 (2002).

[3] Mao, W. L.; Mao, H. "Hydrogen Storage in Molecular Compounds.", *Proceedings of the National Academy of Sciences of the USA*, **101**, 708-710 (2004).

[4] Hawkins , R. E.; Davidson, D. W. "Dielectric Relaxation in the Clathrate Hydrates of Some Cyclic Ethers.", *Journal of Physical Chemistry*, **70**, 1889-1894 (1966).

[5] Gough, S. R.; Davidson, D. W. "Composition of Tetrahydrofuran Hydrate and the Effect of Pressure on the Decomposition.", *Canadian Journal of Chemistry*, **49**, 2691-2699 (1971).

[6] Kang, S. -P.; Lee, H.; Lee, C. -S.; Sung, W. -M. "Hydrate Phase Equilibria of the Guest Mixtures Containing CO_2, N_2 and Tetrahydrofuran.", *Fluid Phase Equilibria*, **185**, 101-109 (2001).

[7] Seo, Y. -T.; Kang, S. -P.; Lee, H. "Experimental Determination and Thermodynamic Modeling of Methane and Nitrogen Hydrates in the Presence of THF, Propylene Oxide, 1, 4-Dioxane and Acetone.", *Fluid Phase Equilibria*, **189**, 99-110 (2001).

[8] Florusse, L. J.; Peters, C. J.; Schoonman, J.; Hester, K. C.; Koh, C. A.; Dec, S. F.; Marsh K. N.; Sloan, E. D. "Stable Low-Pressure Hydrogen Clusters Stored in a Binary Clathrate Hydrate.", *Science*, **306**, 469-471 (2004).

[9] Lee, H.; Lee, J. -W.; Kim, D. Y.; Park, J.; Seo, Y. -T.; Zeng, H.; Moudrakovski, I. L.; Ratcliffe, C. I.; Ripmeester, J. A. "Tuning Clathrate Hydrates for Hydrogen Storage.", *Nature*, **434**, 743-746 (2005).

[10] Makino, T.; Sugahara, T.; Ohgaki, K. "Stability Boundaries of Tetrahydrofuran + Water System.", *Journal of Chemical Engineering Data*, **50**, 2058-2060 (2005).

[11] Strobel, T. A.; Taylor, C. J.; Hester, K. C.; Dec, S. F.; Koh, C. A.; Miller, K. T.; Sloan, E. D., Jr. "Molecular Hydrogen Storage in Binary THF-H_2 Clathrate Hydrates.", *Journal of Physical Chemistry B*, **110**, 17121-17125 (2006).

[12] Ohgaki, K.; Makihara, Y.; Takano, K. "Formation of CO_2 Hydrate in Pure and Sea Waters.", *Journal of Chemical Engineering of Japan*, **26**, 558-564 (1993).

[13] Manakov, A. Y.; Goryainov, S. V.; Kurnosov, A. V.; Likhacheva, A. Y.; Dyadin, Y. A.; Larionov, E. G. "Clathrate Nature of the High-Pressure Tetrahydrofuran Hydrate Phase and Some New Data on the Phase Diagram of the Tetrahydrofuran - Water System at Pressures up to 3 GPa.", *Journal of Physical Chemistry B*, **107**, 7861-7866 (2003).

[14] Tulk, C. A.; Klug, D. D.; Ripmeester, J. A. "Raman Spectroscopic Studies of THF Clathrate Hydrate.", *Journal of Physical Chemistry A*, **102**, 8734-8739 (1998).

[15] Prasad, P. S. R.; Prasad, K. S.; Thakur, N. K. "Laser Raman Spectroscopy of THF Clathrate Hydrate in the Temperature Range 90 - 300 K.", *Soectrochimica Acta Part A*, **68**, 1096-1100 (2007).

[16] Fink, U.; Wiggins, T. A.; Rank, D. H. "Frequency and Intensity Measurements on the Quadrupole Spectrum of Molecular Hydrogen.", *Journal of Molecular Spectroscopy*, **18**, 384-395 (1965).

[17] Sugahara, K.; Sugahara, T.; Ohgaki, K. "Thermodynamic and Raman Spectroscopic Studies of Xe and Kr Hydrates.", *Journal of Chemical & Engineering Data*, **50**, 274-277 (2005).

[18] Sugahara, K.; Yoshida, M.; Sugahara, T.; Ohgaki, K. "Thermodynamic and Raman Spectroscopic Studies on Pressure-Induced Structural Transition of SF_6 Hydrate.", *Journal of Chemical & Engineering Data*, **51**, 301-304 (2006).

[19] Dyadin, Yu. A.; Kuznetsov, P. N.; Yakovlev, I. I.; Pyrinova, A. V. "The System Water - Tetrahydrofuran in the Crystallization Region at Pressures up to 9 kbar.", *Doklady Chemistry*, **208**, 9-12 (1973).

Chapter VII

Stability Boundary and Cage Occupancy on Hydrogen + Tetra-*n*-butyl Ammonium Bromide Mixed Gas Hydrate

Abstract

Phase equilibrium curves of tetra-*n*-butyl ammonium bromide mixed gas hydrates were measured in a pressure range from 0.1 MPa to 13.6 MPa for the stoichiometric and non-stoichiometric aqueous solutions. The equilibrium curve of hydrogen + tetra-*n*-butyl ammonium bromide mixed gas hydrate shifts to the high-temperature side from that of hydrogen + tetrahydrofuran mixed gas hydrate. The difference of equilibrium temperature is about 8 K for the hydrogen + tetra-*n*-butyl ammonium bromide mixed gas hydrate. Three-phase equilibrium curves for the non-stoichiometric aqueous solutions are shifted to the low-temperature or high-pressure side from that of the stoichiometric ones. Each three-phase equilibrium curve converges at the vicinity of equilibrium point of the pure tetra-*n*-butyl ammonium bromide hydrate for the mother aqueous solution of same mole fraction. Raman spectra show that hydrogen is enclathrated in only the small cage, while tetra-*n*-butyl ammonium bromide occupies the large cages of mixed gas hydrate. The selectivity of hydrate-cage occupancy by hydrogen does not change with the variation of mole fraction in the aqueous solution and the difference of hydrate unit-cell structure for the hydrogen + tetra-*n*-butyl ammonium bromide mixed gas hydrate.

Keywords: gas hydrate; phase equilibria; cage occupancy; hydrogen; solution; gas storage

VII-1 Introduction

Recently, the mixed gas hydrate containing H_2 has become the object of an attention as a potential medium that enables to storage and transport H_2 at relatively mild conditions [1-5]. It is required for the assistant component to construct the clathrate hydrate by itself at moderate conditions. The generated hydrate has some empty cages, where can be occupied with H_2 molecules. Tetrahydrofuran (hereafter, THF) is familiar as the assistant additive, which forms the s-II hydrate containing sixteen empty S-cages per unit lattice. In the literatures [1, 3, 5], it has been reported that H_2 + THF mixed gas hydrate can generate at much lower pressure than the pure H_2 hydrate. In the Chapter VI, I have also investigated the H_2 + THF mixed gas hydrate system by thermodynamic and Raman spectroscopic methods. It is necessary to search the suitable additives or innovative methods which enable the safe and bulk storage of H_2 using gas hydrates under low-pressure and high-temperature conditions.

Shimada *et al*. [6] and Oyama *et al*. [7] have reported that isobaric phase equilibrium (T - x) relations for the tetra-*n*-butyl ammonium bromide (hereafter, TBAB) hydrate have the maximum temperature point (285.15 K) at atmospheric pressure with 40.5 mass% (3.7 mol%) water solution. As shown in **Fig. VII-1**, TBAB hydrate is a semi-clathrate hydrate where TBAB is incorporated with the water molecules to construct the hydrate cage. TBAB hydrate also has some empty S-cages in common with THF hydrate. The higher stability of TBAB hydrate than THF hydrate indicates that H_2 storage in TBAB hydrate has prospects of large advantage. There are various reports about the crystal structure and the role of bromine for the TBAB hydrates [8-10], however, the structure of TBAB hydrate is considered to be less certain. The hydration numbers of these structures are 26 and 38, which are described as Type A and Type B, respectively [6, 7]. The concentration of aqueous TBAB solutions results in differences of the crystal structure and thermodynamic stability of TBAB hydrate. It is necessary to determine both the phase behavior and H_2 occupancy in the H_2 + TBAB + water mixed system.

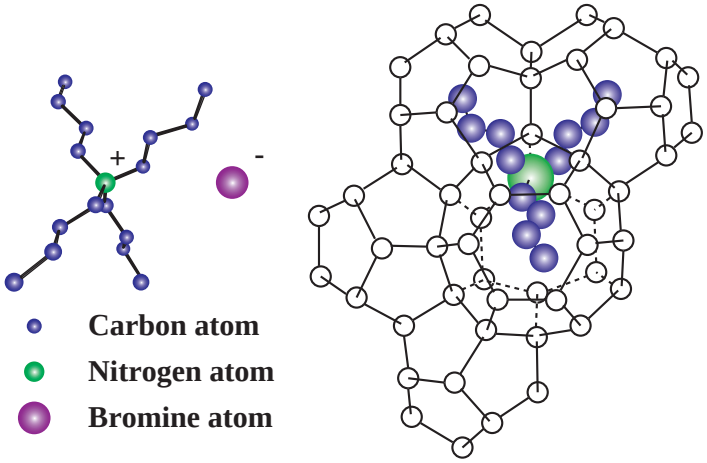

Figure VII-1 Schematic illustration of TBAB molecule and Type A TBAB hydrate.

In the Chapter VII, thermodynamic stabilities of H_2 + TBAB mixed gas hydrate were measured. In addition, Raman spectra for the single crystals of H_2 + TBAB mixed gas hydrates were measured under the three-phase (gas, aqueous solution, and hydrate phases) coexisting conditions. In addition, the dependence of thermodynamic stability and H_2 occupancy on mole

fraction of aqueous solution were also investigated for the three mixed gas hydrate systems.

VII-2 Experimental Section

VII-2.1 Apparatus

The experimental apparatus for the phase equilibrium measurements and Raman spectroscopic analyses were the same as the ones in the Chapter VI. A detail description was given in the previous chapter.

The system temperature was measured within an uncertainty of 0.02 K using a thermistor probe (Takara D-632), which was inserted into a hole in the cell wall. The probe was calibrated with a Pt resistance thermometer defined by ITS-90. The system pressure was measured by a pressure gage (Valcom VPRT) calibrated by RUSKA quartz Bourdon tube gage (Direct Reading Pressure Gage, series 6000) with an estimated maximum uncertainty of 0.01 MPa.

VII-2.2 Procedures

In the Chapter VII, the phase equilibrium (temperature - composition) relation was measured for the pure TBAB hydrate system. The TBAB aqueous solution prepared at a desired mole fraction was introduced into the glass tube. We have also adopted the method similar to the "*T*-cycle method [11]" for this equilibrium measurement. At first, the system temperature was decreased and kept constant at the point of pressure depression which is caused by the H_2 + each additive mixed gas hydrate formation. We cannot directly measure the equilibrium composition of aqueous phase under the coexistence of gas hydrate phase. Therefore, the content was heated very gradually and step by step (0.1 K each) until there was a negligibly small amount of gas hydrate left in order to minimize change of concentration in the aqueous solution. The interval time was taken adequately (at least one day) for establishing equilibrium state at each temperature step. When the last particle of hydrates disappeared on gradually heating, we adopted this point as the equilibrium point. In order to eliminate a hysteresis effect, we have used the annealing method (0.05 K one cycle per day) in addition to the "*T*-cycle method [11]". We never fail to repeat several times the *T*-cycle and annealing methods. In addition, we also repeated the same equilibrium measurements using the fresh solution at the same mole fraction.

For the three-phase equilibrium measurements and Raman spectroscopic analyses, the procedures were similar to those of the Chapter VI. A detail description was given in the previous chapter.

VII-2.3 Materials

Research grade H_2 (mole fraction purity 0.999999) was obtained from the Neriki Gas Co., Ltd. The maximum impurity was 0.2 ppm of nitrogen. Research grade TBAB (mole fraction purity 0.980) and the distilled water were obtained from the Wako Pure Chemical Industries, Ltd. All of them were used without further purifications.

VII-3 Results & Discussion

VII-3.1 Phase Equilibria

Stability boundaries of pure TBAB hydrates

In the Chapter VII, the phase equilibrium (temperature - composition) relations for the pure TBAB hydrate system was also measured under the atmospheric conditions. The result is shown

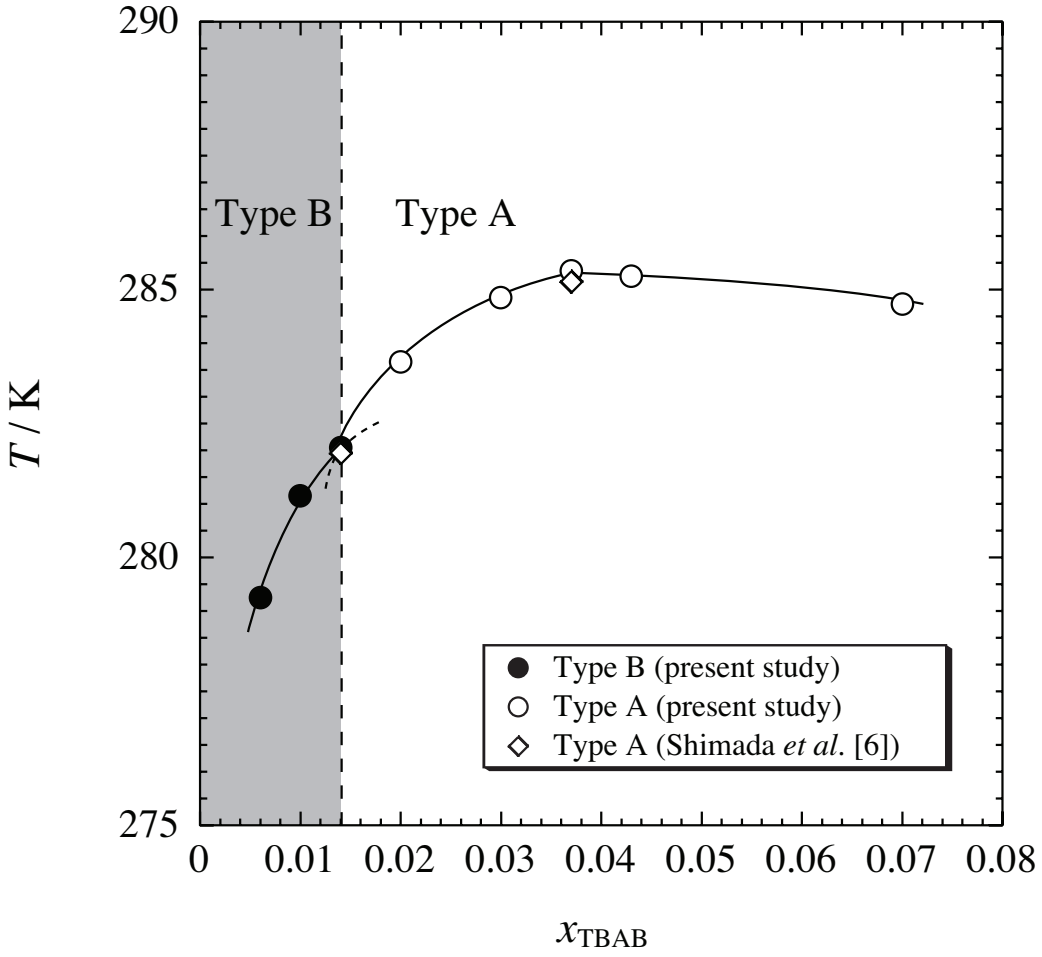

Figure VII-2 Phase equilibrium (T - x) relation for the pure TBAB hydrate system under the atmospheric conditions.

in **Fig. VII-2**. Interestingly, it has been reported that a structural phase transition occurs, depending on the mole fraction of aqueous solution, for the pure TBAB hydrate [6-9, 12]. In the mole fraction region of $x_{TBAB} < 0.014$, the Type B TBAB hydrate generates preferentially. On the other hand, the Type A TBAB hydrate is more stable than the Type B in the mole fraction region of $x_{TBAB} > 0.014$. As shown in **Fig. VII-2**, Type A TBAB hydrate is most stable at $x_{TBAB} = 0.037$ (40.5 mass%) which is the stoichiometric concentration of the Type A TBAB hydrate [6, 7], where the equilibrium temperature is 285.35 K. This maximum equilibrium temperature of Type A TBAB hydrate agrees well with the previous one [6, 7, 12]. The structural-transition point of TBAB hydrates between Type A and Type B would be located at $x_{TBAB} = 0.014$ and 282.15 K in the present study. The phase behavior for the pure TBAB hydrate system obtained in the present study agrees with that of previous reports [6, 7, 12]. For convenience, the description of Types A and B is adopted hereafter following Shimada's expression.

H_2 + TBAB mixed gas hydrate ~Stoichiometric (Type A) aqueous solution~

Phase equilibria for the H_2 + TBAB mixed gas hydrate system are summarized in **Table VII-1** and shown in **Fig. VII-3** accompanied with that of H_2 + THF mixed gas hydrate system. As shown in **Fig. VII-3**, the mole fraction of TBAB aqueous solutions x_{TBAB} is 0.037, which is the stoichiometric concentration of the Type A pure TBAB hydrates. The three-phase equilibrium curve of H_2 + TBAB mixed gas hydrate converges at the atmospheric temperature

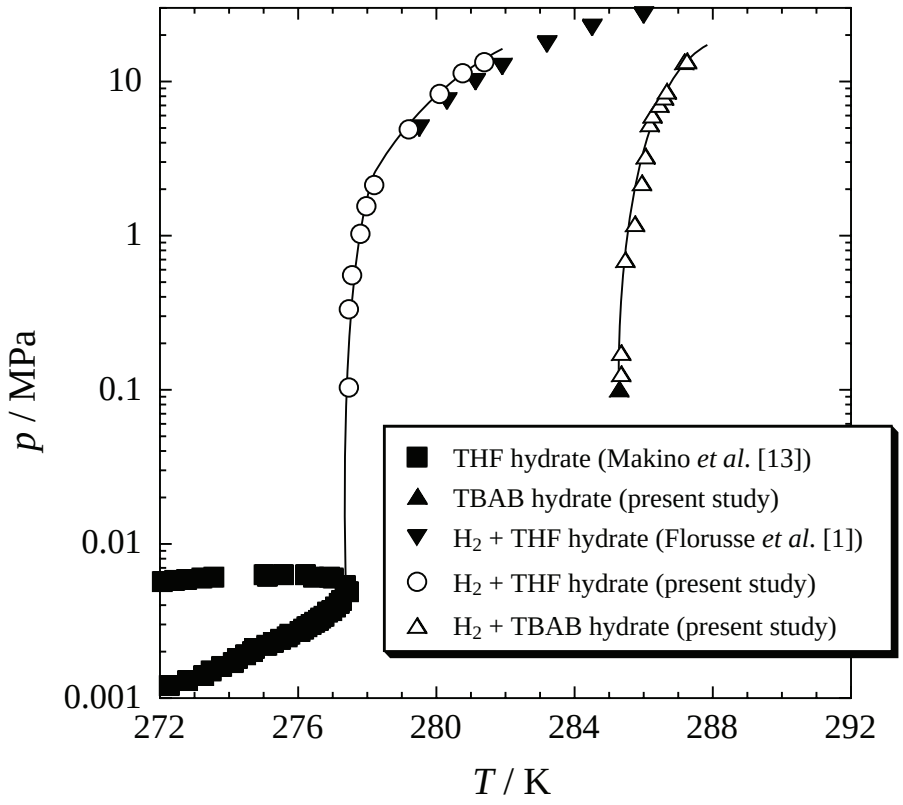

Figure VII-3 Three-phase equilibrium curves of H_2 + THF and H_2 + TBAB mixed gas hydrate systems. The solid lines are fitting lines for experimental data.

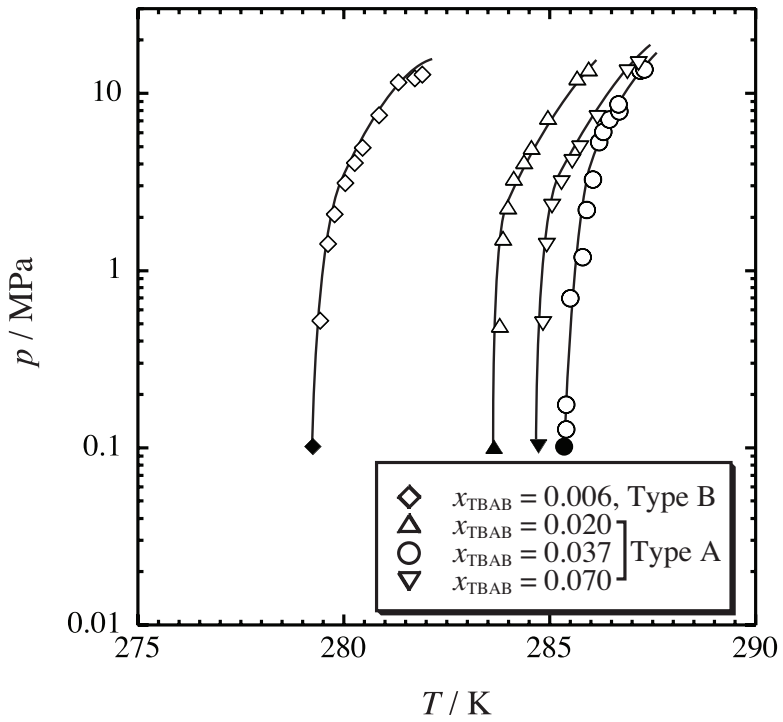

Figure VII-4 Three-phase equilibrium curves of the H_2 + TBAB mixed gas hydrate system at various mole fractions. Closed keys represent the three-phase equilibrium points of pure TBAB hydrates at atmospheric pressure. The solid lines are fitting lines for the experimental data.

point of stoichiometric pure TBAB hydrate (Type A). The equilibrium temperature for the pure TBAB hydrate of stoichiometric composition at atmospheric pressure is 285.35 K. The equilibrium curve vertically rises up in the pressure range up to 2 MPa. The phase behavior of H_2 + TBAB hydrate is similar to that of H_2 + THF hydrate, while the three-phase equilibrium curve of H_2 + TBAB hydrate shifts to the higher temperature of about 8 K than that of H_2 + THF hydrate.

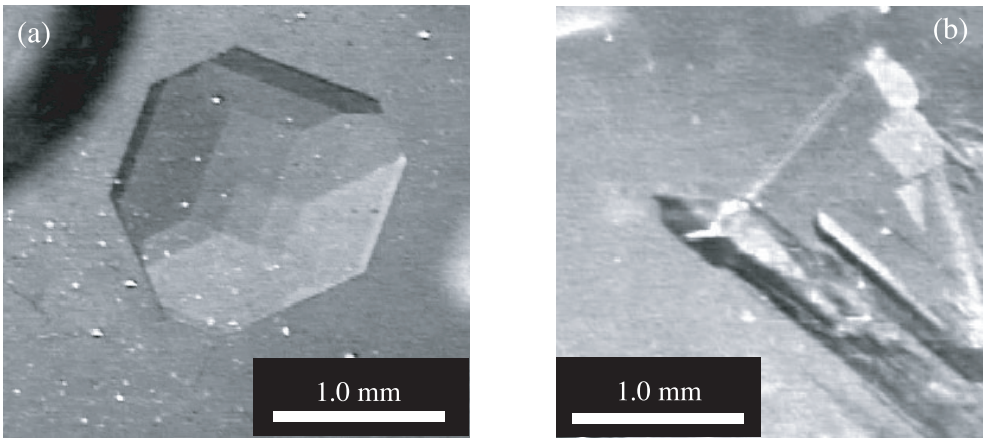

Figure VII-5 Photos of a hydrate crystal for the H_2 + TBAB mixed gas hydrate at x_{TBAB} = 0.070 (Type A) (a) and x_{TBAB} = 0.006 (Type B).

Table VII-1 Phase equilibrium data fot the H_2 + TBAB mixed gas hydrate system at various TBAB mole fractions.

	T / K	p / MPa		T / K	p / MPa
x_{TBAB} = 0.006	279.43	0.52		285.46	0.70
Type B	279.62	1.41		285.75	1.19
	279.78	2.07		285.94	2.19
	280.04	3.11		286.05	3.27
	280.27	4.03		286.17	5.30
	280.46	4.92		286.26	6.05
	280.86	7.50		286.45	7.10
	281.33	11.5		286.59	7.93
	281.73	12.1		286.67	8.66
	281.91	12.7		287.19	13.4
x_{TBAB} = 0.020	283.79	0.49		287.30	13.6
Type A	283.87	1.52	x_{TBAB} = 0.070	284.84	0.50
	283.99	2.28	Type A	284.93	1.39
	284.13	3.32		285.06	2.30
	284.38	4.09		285.29	3.12
	284.56	4.95		285.55	4.12
	284.96	7.30		285.74	4.91
	285.67	12.2		286.16	7.30
	285.95	13.7		286.89	13.2
x_{TBAB} = 0.037	285.35	0.13		287.16	14.7
Type A	285.35	0.18			

H_2 + TBAB mixed gas hydrate ~Non-stoichiometric aqueous solution~

Phase equilibrium (pressure - temperature) relations for the H_2 + TBAB mixed gas hydrate systems at various TBAB concentrations are also summarized in **Table VII-1** and shown in **Fig. VII-4**. The three-phase equilibrium curves of H_2 + Type A TBAB mixed gas hydrate, which were obtained from the TBAB aqueous solution of x_{TBAB} = 0.020 and 0.070, converge at the vicinity of each atmospheric equilibrium temperature (283.65 K and 284.73 K) of pure

TBAB hydrate prepared from the same mole fraction solution, respectively. In the case of x_{TBAB} = 0.006, the three-phase equilibrium curve of H_2 + TBAB mixed gas hydrate converges at the vicinity of temperature of 279.25 K, which agrees with the equilibrium temperature of Type B pure TBAB hydrate under the atmospheric conditions [6, 7]. That is, the H_2 + TBAB mixed gas hydrate of x_{TBAB} = 0.006 has the crystal structure originated from the Type B TBAB hydrate. **Fig. VII-5** shows a crystal of two types of H_2 + TBAB mixed gas hydrates; (a) Type A at x_{TBAB} = 0.070, (b) Type B at x_{TBAB} = 0.006. There seems to be morphologic differences between H_2 + Type A and Type B TBAB mixed gas hydrates, which the appearance of Type A and Type B hydrate would be table-like crystal and columnar or spicular, respectively. All three-phase equilibrium curves obtained in the present study shift to the side of lower-temperature than that of stoichiometric concentration. Each equilibrium curve vertically rises up in the pressure up to about 3 MPa, which may be attributed to the hydrogen content in the hydrate. Each three-phase equilibrium pressure increases continuously with the temperature increasing.

VII-3.2 Raman Spectroscopic Analysis

The Raman spectra for the H_2 + TBAB mixed gas hydrates under the three-phase

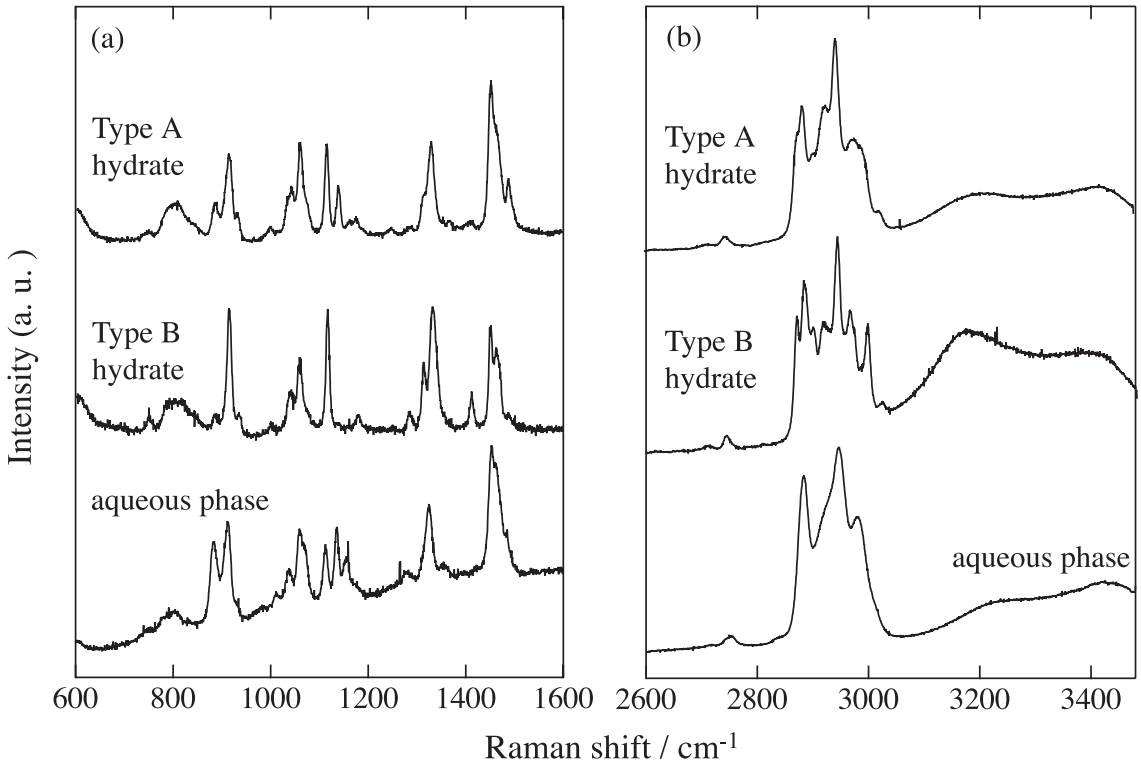

Figure VII-6 Raman spectra originated in TBAB in the aqueous and hydrate phases at various TBAB mole fractions in the low (a) and high (b) wavenumber ranges. In the hydrate phase, Type B: x_{TBAB} = 0.006, 281.73 K, 12.1 MPa; Type A: x_{TBAB} = 0.037, 287.20 K, 13.4 MPa.

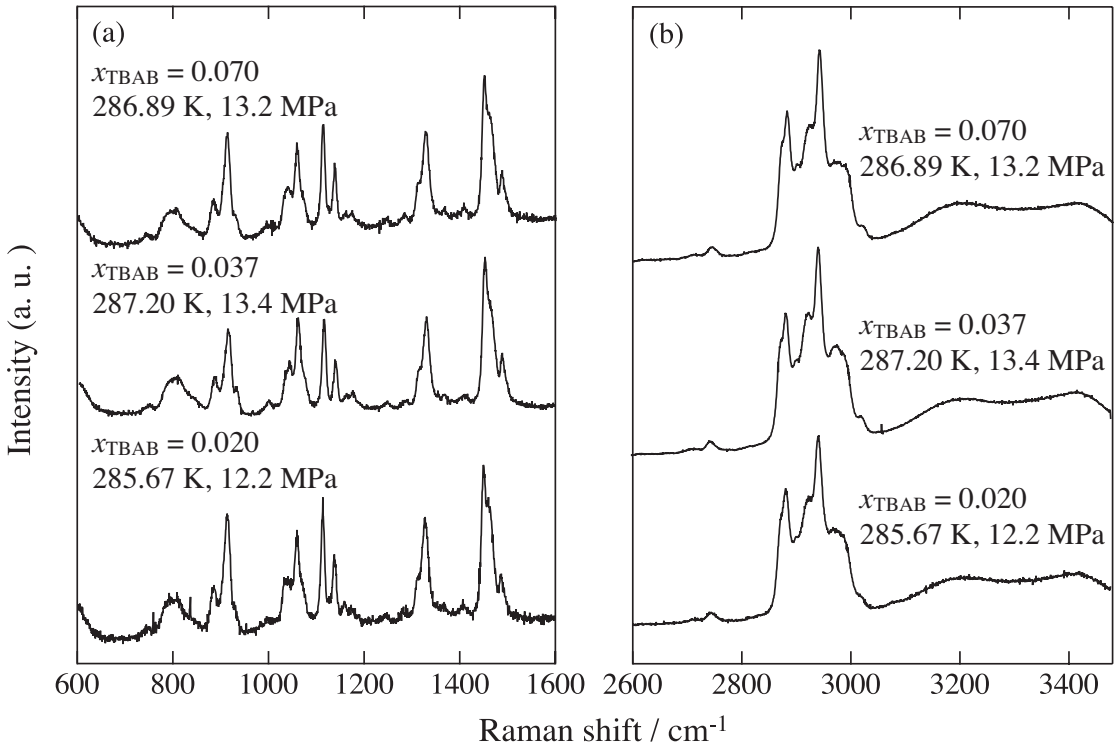

Figure VII-7 Raman spectra originated in TBAB in the Type A-hydrate phases at various TBAB mole fractions in the low (a) and high (b) wavenumber ranges.

equilibrium state obtained at x_{TBAB} = 0.006, 0.020, 0.037, and 0.070 are shown in **Figs. VII-6**, **-7**, and **-8**. The characteristic Raman peaks derived from TBAB molecule are detected around 700-1500 cm^{-1} and 2800-3000 cm^{-1} in the aqueous and hydrate phases. **Figs. VII-6** and **-7** show the Raman spectra of TBAB molecule for the H_2 + TBAB mixed gas hydrates. As shown in **Fig. VII-6**, the spectra are different between hydrate and aqueous solution phases. Moreover, the crystal structures (Type A and Type B) affect the Raman spectra, especially the peaks around 1100 cm^{-1}, 1400 cm^{-1}, and 2900 cm^{-1} of TBAB and the broad peak at 3200-3400 cm^{-1} corresponding intramolecular O-H vibration of host water lattice. That is, it is possible to distinguish the crystal type of H_2 + TBAB mixed gas hydrate by the Raman spectroscopy. On the other hand, there is no remarkable change of Raman spectra with the various TBAB concentrations for the H_2 + Type A TBAB mixed gas hydrate as shown in **Fig. VII-7**.

Fig. VII-8 shows that four peaks corresponding to the H-H stretching vibration mode are observed at (4130, 4147, 4159, and 4166 cm^{-1}) in the gas phase. In the aqueous and hydrate phases, a broad single peak is detected at 4140 and 4132 cm^{-1}, respectively. The position and shape of all peaks derived from H_2 in the hydrate phase agree well with one another. In addition, these peaks corresponding to the vibration of H_2 are consistent with that of H_2 + THF mixed gas hydrate system. There is no remarkable change of Raman spectra of H_2 vibration with the various crystal structure and TBAB concentrations. Therefore, the cage occupancy of H_2 for the H_2 + TBAB mixed gas hydrate is independent of TBAB concentrations in the aqueous solutions under the present experimental condition. That is, as shown in **Fig. VII-9**, the H_2 selectively

occupies the empty small cages of semi-clathrate hydrate, while the butyl-group of TBAB molecule occupies the other cages completely. The results obtained in this study are consistent with our previous data on the point that H_2 molecule occupies the only small cage for the H_2 + THF mixed gas hydrate. On the other hand, H_2 peaks in the H_2 + TBAB hydrate seem to be bit weaker than those of H_2 + THF hydrate. Type A TBAB hydrate is composed of ten S-cages,

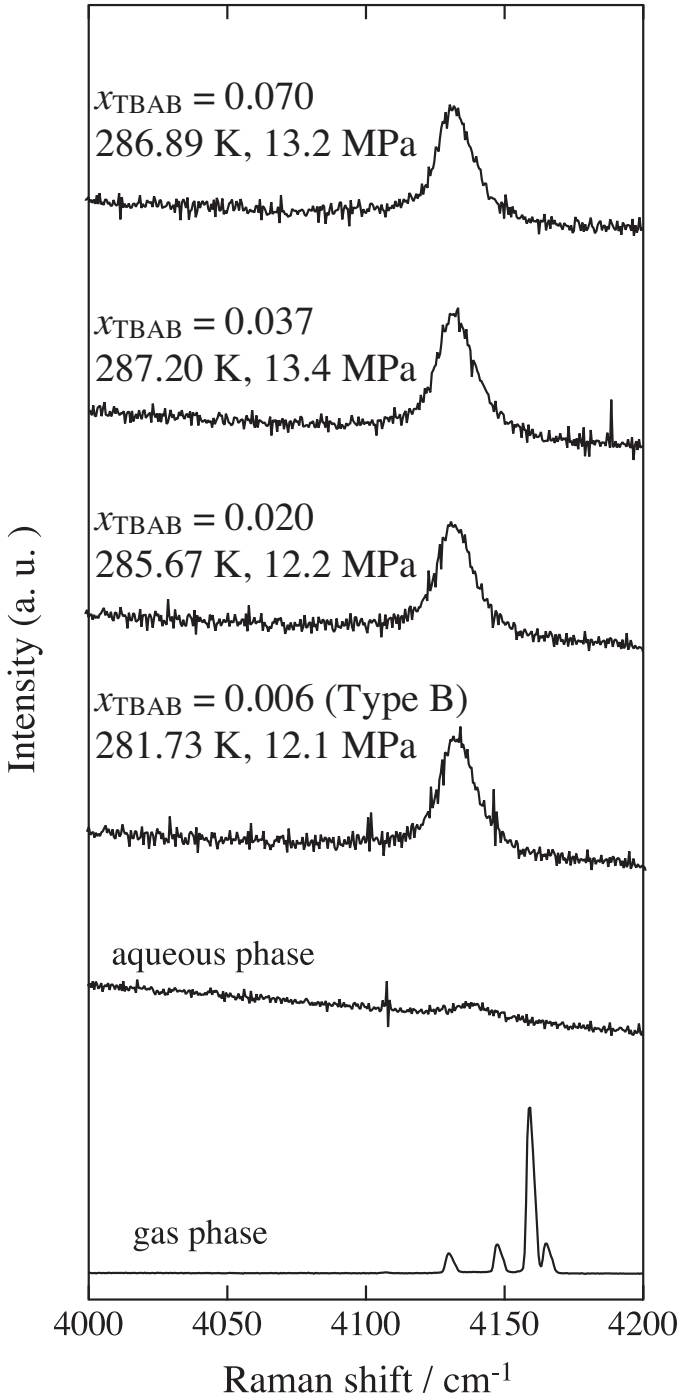

Figure VII-8 Raman spectra corresponding to the intramolecular vibration for H_2 in the gas, aqueous, and hydrate phases at various TBAB mole fractions. Panel contains typical spectra obtained in the gas and aqueous solution phases under the coexistence with Type A hydrate (x_{TBAB} = 0.037).

sixteen M-cages, and four pentakaidecahedrons (L'-cage) [6], and Type B hydrate consists of six S-cages, four M-cages, and four L'-cages [8]. In the TBAB hydrate, bromine makes a role of cage frame with the water molecules and tetra-*n*-butyl ammonium is enclathrated in the hollow center of four large cages. Therefore, the ratio of empty S-cages to all cages in TBAB hydrate is smaller than that of THF hydrate. This may be one of the reasons why H_2 peaks in the H_2 + TBAB hydrate seem to be bit weaker than those of H_2 + THF hydrate. That is, the storage capacity of H_2 in the TBAB hydrate seems to be smaller than that of the THF hydrate under the present experimental condition.

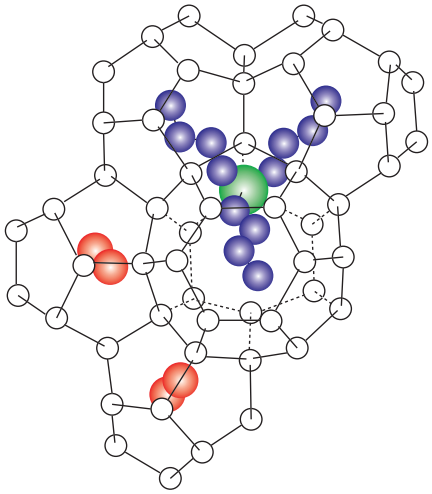

Figure VII-9 Schematic illustration of H_2 + TBAB mixed gas hydrate (Type A).

VII-4 Summary

Phase equilibria for the ternary system of H_2 + TBAB + water were measured at the various mole fractions of aqueous solution. The three-phase (hydrate + aqueous solution + fluid) equilibrium curves of H_2 + TBAB mixed gas hydrate converge at the equilibrium point of pure TBAB hydrate prepared from the same aqueous solution. The H_2 + TBAB mixed gas hydrate can exist at much higher (~8 K) temperature than that of H_2 + THF mixed gas hydrate. From Raman spectroscopy for the single crystal of H_2 + TBAB mixed gas hydrates, neither the difference of concentration in the aqueous TBAB solution nor crystal structure between Type A and Type B TBAB hydrates affects the cage-occupying selectivity of H_2. It is concluded that only the empty small cages of TBAB hydrate are occupied by one H_2 molecule in the TBAB mole fraction range from 0.006 to 0.070.

Notation

Nomenclature

p: pressure [Pa]

T: temperature [K]

x: mole fraction of aqueous solution

Subscript

TBAB: TBAB solution

Literature Cited

[1] Florusse, L. J.; Peters, C. J.; Schoonman, J.; Hester, K. C.; Koh, C. A.; Dec, S. F.; Marsh K. N.; Sloan, E. D. "Stable Low-Pressure Hydrogen Clusters Stored in a Binary Clathrate Hydrate.", *Science*, **306**, 469-471 (2004).

[2] Lee, H.; Lee, J. -W.; Kim, D. Y.; Park, J.; Seo, Y. -T.; Zeng, H.; Moudrakovski, I. L.; Ratcliffe, C. I.; Ripmeester, J. A. "Tuning Clathrate Hydrates for Hydrogen Storage.", *Nature*, **434**, 743-746 (2005).

[3] Strobel, T. A.; Taylor, C. J.; Hester, K. C.; Dec, S. F.; Koh, C. A.; Miller, K. T.; Sloan, E. D., Jr. "Molecular Hydrogen Storage in Binary THF-H_2 Clathrate Hydrates.", *Journal of Physical Chemistry B*, **110**, 17121-17125 (2006).

[4] Chapoy, A.; Anderson, R.; Tohidi, B. Low-Pressure Molecular Hydrogen Storage in Semi-clathrate Hydrates of Quaternary Ammonium Compounds. *Journal of American Chemical Society*, **129**, 746-747 (2007).

[5] Strobel, T. A.; Koh, C. A.; Sloan, E. D. "Hydrogen Storage Properties of Clathrate Hydrate Materials.", *Fluid Phase Equilibria*, **261**, 382-389 (2007).

[6] Shimada, W.; Ebinuma, T.; Oyama, H.; Kamata, Y.; Takeya, S.; Uchida, T.; Nagao, J; Narita, H. "Separation of Gas Molecules Using Tetra-*n*-butyl Ammonium Bromide Semi-Clathrate Hydrate Crystals.", *Japanese Journal of Applied Physics*, **42**, 129-131 (2003).

[7] Oyama, H.; Shimada, W.; Ebinuma, T.; Kamata, Y.; Takeya, S.; Uchida, T.; Nagao, J; Narita, H. "Phase Diagram, Latent Heat, and Specific Heat of TBAB Semiclathrate Hydrate Crystals.", *Fluid Phase Equilibria*, **234**, 131-135 (2005).

[8] Shimada, W.; Shiro, M.; Kondo, H.; Takeya, S.; Oyama, H.; Ebinuma, T.; Narita, H. "Tetra-*n*-butylammonium Bromide-Water (1 / 38).", *Acta Crystallographica Section C*, **C61**, o65-o66 (2005).

[9] Aladko, L. S.; Dyadin, Y. A.; Rodionova, T. V.; Terekhova, I. S. "Clathrate Hydrates of Tetrabutylammonium and Tetraisoamylammonium halides.", *Journal of Structural Chemistry*, **43**, 990-994 (2002).

[10] Gaponenko, L. A.; Solodovnikov, S. F.; Dyadin, Yu. A.; Aladko, L. S.; Polyanskaya, T. M. "Crystallographic Study of Tetra-*n*-butylammonium Bromide Polyhydrates.", *Zhurnal Structurnoi Khimii*, **25**, 175-177 (1984).

[11] Ohgaki, K.; Makihara, Y.; Takano, K. "Formation of CO_2 Hydrate in Pure and Sea Waters.", *Journal of Chemical Engineering of Japan*, **26**, 558-564 (1993).

[12] Fukushima, S.; Takao, S.; Ogoshi, H.; Ida, H.; Matsumoto, S.; Akiyama, T.; Otsuka, T. "Development of High-density Cold Latent Heat with Clathrate Hydrate.", *NKK Technical Report*, **166**, 65-70 (1999).

[13] Makino, T.; Sugahara, T.; Ohgaki, K. "Stability Boundaries of Tetrahydrofuran + Water System.", *Journal of Chemical Engineering Data*, **50**, 2058-2060 (2005).

Chapter VIII

General Conclusion

The gas hydrate systems generated from various mixtures containing from the smallest (H_2) to the largest guest (DMCH stereo isomers) were studied in this thesis. The gas storage and transportation, particularly H_2 storage technology, are the essential techniques for developing new society sustained by H_2 energies. I considered that gas hydrates have a huge potential as a medium for these applied techniques. There are a lot of important topics such as hydrate structure, phase equilibrium, cage occupancy, storage capacity for various mixed gas hydrate systems. These systems were investigated by mainly use of thermodynamic and Raman spectroscopic methods. The fundamental findings obtained in the present study are very important to develop the future technologies for utilization of natural gas or H_2 energies as well as to understand the characters of mixed gas hydrate. The author hopes that the present findings can contribute to develop the new society sustained by H_2 energies. In the Chapter I, earlier chapters (Chapters II-VII) have already divided into two categories according to the basic concept. The findings are summarized as follows:

Part A: Thermodynamic Properties of Mixed Gas Hydrates (Chapters II-V)

The four ternary systems containing H_2 + (CO_2 or hydrocarbons (C_2H_6, *c*-C_3H_6, or C_3H_8)) + water were studied. The s-H hydrate systems which are composed of DMCH stereo-isomers helped by Xe or CH_4 were studied. In addition, THF and TBAB were adopted as additives which depress the equilibrium pressure and the H_2 + CO_2 + (THF or TBAB) + water quaternary system (THF: at 280.1 K and 281.9 K, TBAB: 285.9 K) was studied. The isothermal phase equilibria were measured by means of TCD-GC. The single crystals were analyzed under the three-phase (gas, aqueous, and hydrate phases) equilibrium condition by use of Raman micro-spectrometer.

A-1 Phase Behavior

Three-phase (gas + aqueous + hydrate phases) equilibrium pressure increases monotonically with the H_2 composition of gas phase for all ternary systems of H_2 + (CO_2 or hydrocarbons (C_2H_6, *c*-C_3H_6, or C_3H_8)) + water. According to the thermodynamic analysis using numerical calculation in order to give the equilibrium fugacity of pure or hydrocarbon hydrate, the isothermal phase equilibrium relation for the ternary system of H_2 + C_3H_8 + water exhibits the different behavior from those of H_2 + (CO_2, C_2H_6 or *c*-C_3H_6) + water. In the only case of H_2 + C_3H_8 + water system, the experimental pressure shifts to the lower side than the estimated ones.

The equilibrium pressure of each s-H system helped by CH_4 is lower than that of pure CH_4 s-I hydrate. By adding a small amount of 1,1-DMCH, the equilibrium pressure can be reduced. The 1,1-DMCH is a suitable additive which makes a mild-pressure handling of natural-gas hydrate possible. The *cis*-1,4-DMCH, which generates the s-H hydrate in the presence of CH_4, can not generate the s-H hydrate in the presence of Xe. It is firstly suggested that the U-cage occupancy limit of large guest species depends on the function of help gas.

The equilibrium pressure of H_2 + CO_2 + water mixed system considerably is reduced with a small amount of THF or TBAB. In the H_2 + CO_2 + THF + water mixed system, the largest pressure depression is obtained when the THF concentration is the stoichiometric composition for the pure THF hydrate formation. The pressure depression for the H_2 + CO_2 + TBAB + water mixed system is greater than that of H_2 + CO_2 + THF + water mixed system. All three-phase equilibrium curves exhibit a stepwise increase around 0.2 in the H_2 mole fraction of gas phase. It is suggested that the H_2 molecule starts to occupy the hydrate cages at *ca*. 0.2 in the H_2 mole fraction of gas phase.

A-2 Cage Occupancy

In the H_2 + (CO_2 or hydrocarbons (C_2H_6, *c*-C_3H_6, or C_3H_8)) + water ternary systems, the Raman spectra reveals that the H_2 can occupy the S-cage of s-II C_3H_8 hydrate. The H_2 + C_3H_8 + water mixture can generate the mixed H_2 hydrate. On the other hand, the small cage in the CO_2, C_2H_6, and *c*-C_3H_6 hydrates cannot trap the H_2 even though all the S-cages are vacant in these two gas hydrates. The hydrate generated from the H_2 + (CO_2, C_2H_6 or *c*-C_3H_6) + water mixture is s-I hydrate originated in pure CO_2, C_2H_6 or *c*-C_3H_6 and the H_2 behaves only like a diluent gas toward the formation of these hydrates under the experimental conditions of this thesis. These results are good consistent with the isothermal phase equilibrium data including the numerical calculation.

The Raman spectroscopy for the hydrate single crystal generated from the H_2 + CO_2 + THF + water mixtures reveal that the cage occupancy of H_2 molecule change depending on the composition of H_2 in the gas phase. In the region higher than *ca*. 0.2 in the H_2 mole fraction of gas phase, the H_2 and CO_2 molecules are competitively enclathrated in the S-cages of s-II hydrate while the THF molecules occupy L-cages selectively.

Part B: Thermodynamic Stability of Hydrogen-containing Mixed Gas Hydrates for Hydrogen Storage (Chapters VI and VII)

The three-phase equilibrium (pressure - temperature) relations for the H_2 + water-soluble additive (THF or TBAB) mixed gas hydrate systems were measured at various concentrations in the aqueous solutions up to 15 MPa. In all mixed systems, the single crystals were analyzed under the three-phase (gas, aqueous, and hydrate phases) equilibrium condition by use of Raman microspectrometer in order to confirm the existence of H_2 in the hydrates directly. In addition, in the case of THF which is most familiar as a additive, the phase equilibrium measurement and Raman spectroscopic analysis were performed up to 200 MPa in order to investigate the pressure dependence on thermodynamic stability and cage occupancy. Finally, the storage capacity of H_2 in the THF hydrate was estimated by Raman spectroscopy under the three-phase (gas, hydrate, and aqueous phases) and isothermal (two-phase coexisting of gas and hydrate) conditions.

B-1 Phase Behavior

The three-phase equilibrium curves of H_2 + water-soluble additive (THF or TBAB) mixed

gas hydrate systems converge at the vicinity of the equilibrium point of the pure hydrate for the mother aqueous solution of same mole fraction. The equilibrium curve of H_2 + TBAB mixed gas hydrate shifts to the high-temperature side from that of H_2 + THF mixed gas hydrate. The difference of equilibrium temperature is *ca*. 8 K in the case of the H_2 + TBAB mixed gas hydrate. For each mixed system, three-phase equilibrium curves for the non-stoichiometric aqueous solutions are shifted to the low-temperature or high-pressure side from that of the stoichiometric ones.

Three-phase equilibrium curves of H_2 + THF mixed gas hydrate changes smoothly and successively from low-pressure to high-pressure region up to 200 MPa. That is, the structural transition does not occur for the H_2 + THF mixed gas hydrate system depending on the system pressure under the present experimental condition.

B-2 Cage Occupancy

It is directly confirmed from Raman spectroscopy that H_2 is enclathrated in the hydrate cages by adding a small amount of THF or TBAB. In these mixed gas hydrates, H_2 is enclathrated in only the small cage while THF or TBAB occupy the large cages of each mixed gas hydrate. These cage occupancies does not depend on the mole fraction in the aqueous solution for each mixed system.

Table VIII-1 shows the dependence of H_2 occupancy on all additive species adopted in this

Table VIII-1 Dependence of H_2 occupancy on various additive species.

Additives	Structure	H_2 occupancy	Conditions
CO_2	I	×	-
CH_4 [1, 2]	I	×	-
C_2H_6	I	×	-
c-C_3H_6	I	×	-
C_3H_8	II	○	~276 K, 2 MPa
THF	II	○	~280 K, 10 MPa
TBAB	*1	○	~288 K, 10 MPa

*1. semi-clathrate, tetragonal or orthorhombic [3]

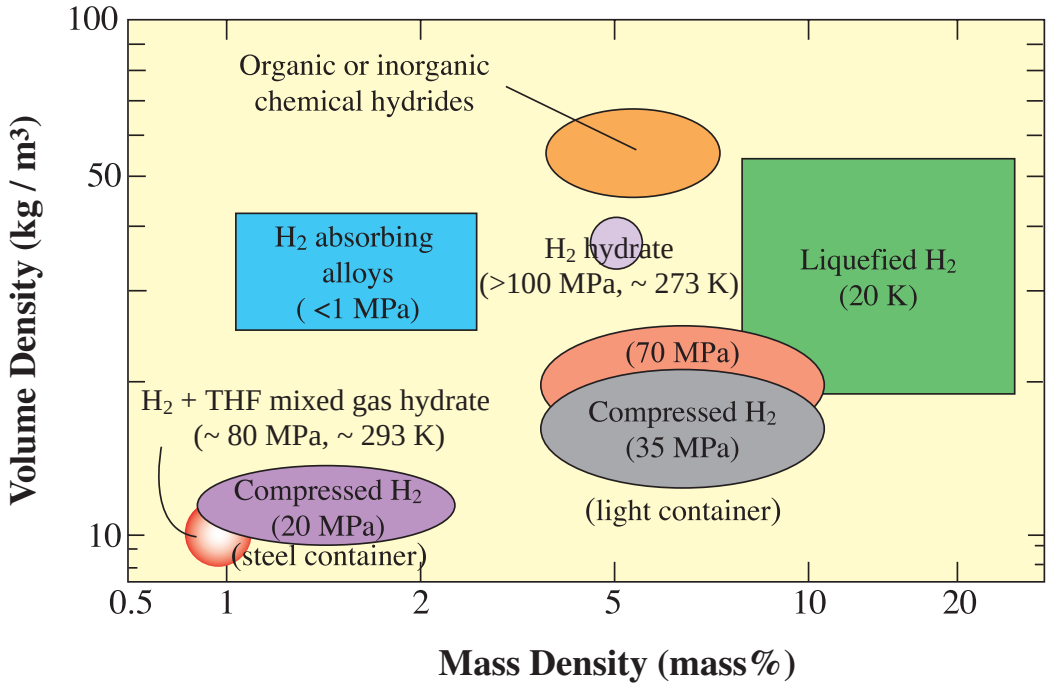

Figure VIII-1 Comparison of H_2 storage density for various storage technologies.

thesis. **Table VIII-1** indicates the characteristic property that the H_2 occupancy in the gas hydrates depends on the structure of unit-cell. That is, H_2 would be encaged with the small cages of s-II hydrate or semi-clathrate hydrate, while it cannot occupy those of s-I hydrate.

The Raman spectroscopy for the H_2 + THF mixed gas hydrate reveals that the amount of enclathrated H_2 molecules in the mixed gas hydrate increases as the system pressure rises and reaches about 1.0 mass% around *ca.* 80 MPa. On the other hand, the shift and shape of Raman peaks is independent of the system pressure. Therefore, the structural transition does not occur and the H_2 gradually occupies empty small cages of s-II THF hydrate depending on the system pressure under the present experimental condition.

Figure VIII-1 shows the storage density of H_2 for various storage media and methods. The storage amount of H_2 in the THF hydrate is *ca.* 1.05 mass% and 10.38 kg / m^3, which is calculated on the assumption that one H_2 molecule can occupy the S-cage of THF hydrate completely. THF hydrate includes the more empty S-cages in the unit cell than other additive hydrates. At present, this storage amount of H_2 in the THF hydrate seems to be the largest among other mixed gas hydrates. As shown in **Fig. VIII-1**, from only the point of view of storage capacity, mixed gas hydrates containing H_2 are unfortunately inferior to other storage methods. However, mixed gas hydrates containing H_2 have a number of advantages as the H_2 storage material. For example, the storage material is harmless water containing little bit additive. In addition, the H_2 storage in molecular form is possible at relatively mild conditions. Hence, it is suggested that H_2 mixed hydrate holds promise of future growth for the H_2 storage material.

Following the experimental data obtained in the Chapters VI and VII, it is suggested that the assistance of an additive enables us to perform the storage and transportation of H_2 using gas

hydrates as "molecular storehouse" at relatively mild conditions. However, there is several issues such as the limitation of the storage amount of H_2 in the H_2-containing mixed gas hydrates and the toxicity of additives. I eagerly realizes that further studies about the more innovative additives are required.

Suggestions for Future Studies

This thesis comes to an end with some suggestions of further and expanded studies for the mixed gas hydrates containing H_2 in the future.

Experiments in a wide range of pressure and temperature

In this thesis, the experiments were performed at *ca*. 276 - *ca*. 300 K up to 200 MPa. However, the region to investigate further remains. For example, it was previously reported that H_2 can be encaged with the cages of CO_2 hydrate at extremely low temperature conditions [4, 5]. Therefore, further experiments at higher pressure and lower temperature conditions than this thesis will be required.

Measurements by means of other devices and equipments

In this thesis, the findings were obtained from thermodynamic and Raman spectroscopic analyses. There is information required for the application of gas hydrates to H_2 energy utilization, for example, location and mobility of H_2 in hydrate cages. Needless to say, there are many experimental methods and tools such as Neutron Diffraction and Scattering, Nuclear Magnetic Resonance (NMR), Electron Spin Resonance (ESR), Molecular Dynamics (MD) Simulation, and so on. In particular, Neutron Scattering and NMR have a potential as the tool in order to determine the position, mobility, and enclathration mechanism of H_2 in the hydrate cages [6-8]. The enclathration mechanism of H_2 in the mixed gas hydrates under the assistance of suitable additives is still unclear. I speculate that there is difference of H_2 difusivity between pure H_2 and H_2 mixed hydrates. The size of H_2 is somewhat smaller than that of polygonal face of hydrate-cages, and consequently H_2 can diffuse inside the unit-cell structure through polygonal faces of hydrate-cages. According to the previous report [8], the diffusion rate of H_2 through the larger hexagonal faces of the L-cages is much larger than that through the smaller pentagonal faces of the S-cages. In the case that the L-cages are occupied with additive molecules, for example THF, it is reasonable to guess that H_2 cannot diffuse through the hexagonal faces of the L-cages because there are nuisances in the L-cages. Therefore, the diffusion rate of H_2 in the H_2 mixed hydrate is smaller than that of pure H_2 hydrate, and consequently H_2 may be entrapped in the H_2 mixed hydrate under much milder conditions than the pure H_2 hydrate. Anyway, I believe that H_2 enclathration mechanism can be the guidance for

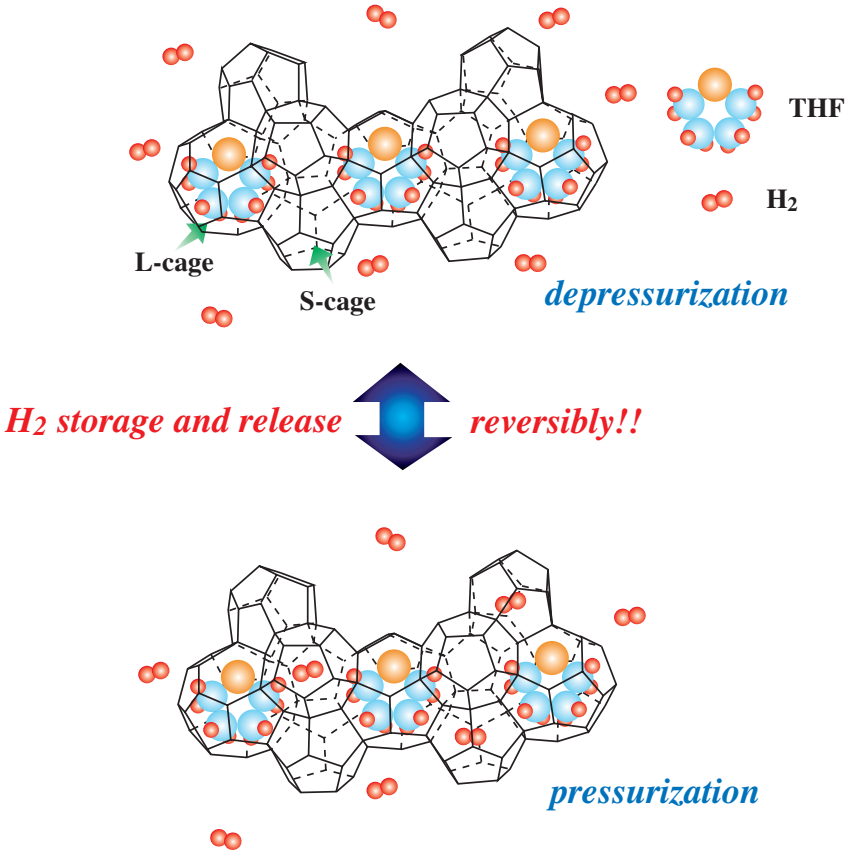

Figure VIII-2 Schematic illustration of "storage and release" process by pressurization or depressurization without the destruction of hydrate cages.

the search of effective additives. The author expects these tools to elucidate the property of H_2-containing mixed gas hydrate in more detail from the view of micro scale.

Search of effective additives for the H_2 storage using mixed gas hydrates

As mentioned above, it is necessary for the effective H_2 storage using mixed gas hydrates that we find more innovative additives. As the indispensable property for this additive, the author would like to enumerate three special feature as follows:

1. Formation of hydrates at a mild condition by itself
2. Possession of many empty cages in unit-cell structure
3. Successive and linear connection of empty cages in unit-cell structure

First of all, it is important to find the additive which can satisfy the feature 1. At present, tetra-*n*-butyl ammonium fluoride (hereafter, TBAF) is potential as an additive. TBAF can form the hydrate at ~301 K and atmospheric pressure, whose equilibrium temperature is much higher than that of THF or TBAB. Accurate analysis and investigation about the thermodynamic stability of H_2 + TBAF mixed gas hydrate are required.

For example, the THF molecule, which is considered as the most effective additive for the

H_2 storage using mixed gas hydrates at present, forms the s-II hydrate. THF can form the hydrate at atmospheric pressure and ~277 K. In addition, in the case of s-II type, S-cage is twice as much as L-cage and these S-cages connect linearly and successively with each other. Therefore, as shown in **Fig. VIII-2**, the H_2 molecule can diffuse through these S-cages in the THF hydrate [8, 9] and consequently the "storage and release" processes of H_2 can be performed reversibly by pressurizing or depressurizing without the destruction of hydrate cages. For this applied technology, it is required that the velocity and repetition of H_2 storage and release are investigated. The author expects scientists to find the additive which covers above three key-factors.

Literature Cited

[1] Chen, G. -J.; Sun, C. -Y.; Guo, T. -M. "A New Technique for Separating (Hydrogen + Methane) Gas Mixtures Using Hydrate Technology.", *Proceeding of the 4th International Conference on Gas Hydrates*, **2**, 1016-1020 (2002).

[2] Skiba, S. S.; Larionov, E. G.; Manakov, A. Y.; Kolesov, B. A.; Kosyakov, V. I. "Investigation of Hydrate Formation in the System H_2 - CH_4 - H_2O at a Pressure up to 250 MPa.", *Journal of Physical Chemistry B*, **111**, 11214-11220 (2007).

[3] Aladko, L. S.; Dyadin, Y. A.; Rodionova, T. V.; Terekhova, I. S. "Clathrate Hydrates of Tetrabutylammonium and Tetraisoamylammonium halides.", *Journal of Structural Chemistry*, **43**, 990-994 (2002).

[4] Kim, D. -Y.; Lee, H. "Spectroscopic Identification of the Mixed Hydrogen and Carbon Dioxide Clathrate Hydrate.", *Journal of American Chemical Society*, **127**, 9996-9997 (2005).

[5] Kumar, R.; Wu, H. -J.; Englezos, P. "Incipient Hydrate Phase Equilibrium for Gas Mixtures Containing Hydrogen, Carbon Dioxide and Propane", *Fluid Phase Equilibria*, **244**, 167-171 (2006).

[6] Lokshin, K. A.; Zhao, Y.; He, D.; Mao, W. L.; Mao, H. -K.; Hemley, R. J.; Lobanov, M. V.; Greenblatt, M. "Structure and Dynamics of Hydrogen Molecules in the Novel Clathrate Hydrate by High Pressure Neutron Diffraction.", *Physical Review Letters*, **93**, 125503-1-125503-4 (2004).

[7] Hester, K. C.; Strobel, T. A.; Sloan, E. D.; Koh, C. A.; Huq, A.; Schultz, A. J. "Molecular Hydrogen Occupancy in Binary THF-H_2 Clathrate Hydrates by High Resolution Neutron Diffraction", *Journal of Physical Chemistry B*, **110**, 14024-14027 (2006).

[8] Okuchi, T.; Takigawa, M.; Shu, J.; Mao, H.; Hemley, R. J.; Yagi, T. "Fast Molecular Transport in Hydrogen Hydrates by High-Pressure Diamond Anvil Cell NMR.", *Physical Review B*, **75**, 144104-1-144104-5 (2007).

[9] Alavi, S.; Ripmeester, J. A. "Hydrogen-Gas Migration through Clathrate Hydrate Cages.", *Angewandte Chemie International Edition*, **46**, 6102-6105 (2007).

List of Publications and Presentations

Publications (papers)

Main works for this thesis

{1} Takeshi Sugahara, Tsutomu Hara, Shunsuke Hashimoto, and Kazunari Ohgaki
"Icosahedron Cage Occupancy of Structure-H Hydrate Helped by Xe --1, 1-, *cis* -1, 2-, *trans* -1, 2-, and *cis* -1, 4-Dimethylcyclohexanes--."
Chemical Engineering Science, **60**, 1783-1786 (2005).

{2} Tsutomu Hara, Shunsuke Hashimoto, Takeshi Sugahara, and Kazunari Ohgaki
"Large Pressure Depression of Methane Hydrate by Adding 1, 1-Dimethylcyclohexane"
Chemical Engineering Science, **60**, 3117-3119 (2005).

{3} Takeshi Sugahara, Shu Murayama, Shunsuke Hashimoto, and Kazunari Ohgaki
"Phase Equilibria for H_2 + CO_2 + H_2O System Containing Gas Hydrates."
Fluid Phase Equilibria, **233**, 190-193 (2005).

{4} Shunsuke Hashimoto, Shu Murayama, Takeshi Sugahara, and Kazunari Ohgaki
"Phase Equilibria for H_2 + CO_2 + Tetrahydrofuran +Water Mixtures Containing Gas Hydrates."
Journal of Chemical & Engineering Data, **51**, 1884-1886 (2006).

{5} Shunsuke Hashimoto, Shu Murayama, Takeshi Sugahara, Hiroshi Sato, and Kazunari Ohgaki
"Thermodynamic and Raman Spectroscopic Studies on H_2 + Tetrahydrofuran + Water and H_2 + Tetra-*n*-butyl Ammonium Bromide + Water Mixtures Containing Gas Hydrates."
Chemical Engineering Science, **61**, 7884-7888 (2006).

{6} Shunsuke Hashimoto, Takeshi Sugahara, Hiroshi Sato, and Kazunari Ohgaki
"Thermodynamic Stability of H_2 + Tetrahydrofuran Mixed Gas Hydrate in Nonstoichiometric Aqueous Solutions."
Journal of Chemical & Engineering Data, **52**, 517-520 (2007).

{7} Shunsuke Hashimoto, Shu Murayama, Takeshi Sugahara, and Kazunari Ohgaki
"Fundamental Studies for A New H_2 Separation Method Using Gas Hydrates."

Physics and Chemistry of Ice, 209-216 (2007).

{8} Shunsuke Hashimoto, Takeshi Sugahara, Masato Moritoki, Hiroshi Sato, and Kazunari Ohgaki
"Thermodynamic Stability of H_2 + Tetra-*n*-butyl Ammonium Bromide Mixed Gas Hydrate in Nonstoichiometric Aqueous Solutions."
Chemical Engineering Science, **63**, 1092-1097 (2008).

{9} Shunsuke Hashimoto, Takeshi Sugahara, Masato Moritoki, Hiroshi Sato, and Kazunari Ohgaki
"Thermodynamic Stability on Mixed Gas Hydrates Containing Hydrogen."
Journal of Physics: Conference Series, **submitted**.

{10} Takeshi Sugahara, Hiroki Mori, Jun Sakamoto, Shunsuke Hashimoto, Kyohei Ogata, and Kazunari Ohgaki
"Cage Occupancy of Hydrogen in Carbon Dioxide, Ethane, Cyclopropane, and Propane Hydrates."
The Open Thermodynamics Journal, **2**, 1-6 (2008).

Other works

{11} Jun Sakamoto, Takaaki Tsuda, Shunsuke Hashimoto, Takeshi Sugahara, and Kazunari Ohgaki
"Thermodynamic and Raman Spectroscopic Studies on Hydrogen + Tetra-*n*-Butyl Ammonium Fluoride + Water Ternary System Containing Gas Hydrates.", **submitted**.

{12} Kyohei Ogata, Shunsuke Hashimoto, Takeshi Sugahara, Masato Moritoki, Hiroshi Sato, and Kazunari Ohgaki
"Pressure Dependence of Hydrogen Storage Capacity for Tetrahydrofuran Hydrate.", **submitted**.

{13} Shunsuke Hashimoto, Arata Sasatani, Takeshi Sugahara, and Kazunari Ohgaki
"Isothermal Phase Equilibria for Methane + Ethane + Water Ternary System Containing Gas Hydrates.", **submitted**.

Presentations (international conferences)

{1} Shunsuke Hashimoto, Shu Murayama, Takeshi Sugahara, and Kazunari Ohgaki
"Phase Equilibria for H_2 + CO_2 + Tetrahydrofuran + Water Mixed System Containing Gas Hydrates."
The 7th International 21st Century COE Symposium on Integrated EcoChemistry (*COEIEC VII*), P01, Hawaii Prince Hotel Waikiki, USA, *December* 20 (2005).

{2} Shunsuke Hashimoto, Shu Murayama, Takeshi Sugahara, and Kazunari Ohgaki
"Fundamental Studies for A New H_2 Separation Method Using Gas Hydrates.",
The 11th International Conference on the Physics and Chemistry of Ice 2006 (*PCI2006*), O31, Bremerhaven, Germany, *July* 23-28 (2006).

{3} Shunsuke Hashimoto, Shu Murayama, Takeshi Sugahara, Hiroshi Sato, and Kazunari Ohgaki
"Thermodynamic and Raman Spectroscopic Studies on Mixed Gas Hydrates Containing Hydrogen."
The 8th International 21st Century COE Symposium on Integrated EcoChemistry (*COEIEC VIII*), P35, Keihanna Interaction Plaza, Nara, Japan, *August* 28-29 (2006).

{4} Shunsuke Hashimoto, Takeshi Sugahara, Masato Moritoki, Hiroshi Sato, and Kazunari Ohgaki
"Thermodynamic Stability of H_2 + Tetrahydrofuran Mixed Gas Hydrate in Non-Stoichiometric Aqueous Solutions."
The 9th International 21st Century COE Symposium on Integrated EcoChemistry (*COEIEC IX*), PC04, Awaji Yumebutai International Conference Center, Hyogo, Japan, *January* 16-18 (2007).

{5} Shunsuke Hashimoto, Takeshi Sugahara, Masato Moritoki, Hiroshi Sato, and Kazunari Ohgaki
"Thermodynamic Stability of Mixed Gas Hydrates Containing Hydrogen."
The Joint 21st AIRAPT & 45th EHPRG International Conference on "High Pressure Science and Technology", P0164, The Department of Physics and Astronomy of the University of Catania, Catania, Sicily, Italy, *September* 17-21 (2007).

{6} Shunsuke Hashimoto, Shu Murayama, Takeshi Sugahara, Hiroshi Sato, and Kazunari Ohgaki
"Thermodynamic and Raman Spectroscopic Studies on Mixed Gas Hydrates Containing

Hydrogen."
The 1st SCEJ (Kansai-Branch) / SSCCI Joint International Conference on Chemical Engineering, P05, Osaka Science & Technology Center, Osaka, Japan, *December* 5-6 (2007).

{7} Shunsuke Hashimoto, Jun Sakamoto, Kyohei Ogata, Takeshi Sugahara, and Kazunari Ohgaki
"Search for Effective Additives for Hydrogen Storage Using Gas Hydrates."
The 1st International Global COE symposium on Global Education and Bio-Environmental Chemistry (GCOEBEC-1), P3-25, Hotel Hankyu Expo Park, Osaka, Japan, *January* 27-29 (2008).

Acknowledgments

First of all, the author would like to really appreciate Professor Kazunari Ohgaki (Division of Chemical Engineering, Department of Materials Engineering Science, Graduate School of Engineering Science, Osaka University) throughout the student life in Ohgaki laboratory as well as the present studies. The completion of the author' s studies and this thesis is largely owing to his helpful advice and precise guidance. The author expresses his gratitude to Professor Yoshiro Inoue (Division of Chemical Engineering, Department of Materials Engineering Science, Graduate School of Engineering Science, Osaka University), Professor Toshio Kasai (Division of Physical Chemistry, Department of Chemistry, Graduate School of Science, Osaka University), and Professor Masayoshi Nakano (Division of Chemical Engineering, Department of Materials Engineering Science, Graduate School of Engineering Science, Osaka University) for their helpful suggestions and comments.

The author expresses his thanks to Associate professor Hiroshi Sato (Division of Chemical Engineering, Department of Materials Engineering Science, Graduate School of Engineering Science, Osaka University) for his many comments on this study and to Dr. Masato Moritoki for his technical support of experimental apparatus. The author is thankful to Mr. Masao Kawashima for his kind assistance in the GHAS (Gas Hydrate Analyzing System) room. Thanks are made to Mr. Keisuke Sugahara, Assistant Professor Takashi Makino (Department of Applied Chemistry, Kobe City College of Technology), Dr. Kei Takeya, all the other colleagues of Ohgaki Laboratory, all classfellow in Division of Chemical Engineering, and all my friends for their collaboration. In particular, the author expresses his special thanks to the members of research group (hydrogen group), Mr. Shu Murayama, Mr. Hiroki Mori, Mr. Jun Sakamoto, Mr. Kyohei Ogata, and Mr. Takaaki Tsuda for their kind experimental supports.

The author would like to take this opportunity to express his thanks to Associate professor Shigeo Sasaki (Department of Materials Science and Technology, Graduate School of Engineering, Gifu University), Associate professor Tsutomu Uchida (Department of Applied Science and Engineering, Graduate School of Engineering, Hokkaido University), Associate professor Kenji Yasuoka (Department of Mechanical Engineering, Graduate School of Science and Technology, Keio University), Assistant Professor Takuo Okuchi (Department of Earth and Environmental Sciences, Graduate School of Environmental Studies, Nagoya University), and Assistant Professor Atsushi Tani (Department of Earth and Space Science, Graduate School of Science, Osaka University) for their valuable advice and support in a few international conferences.

The author expresses heartily his special thanks to Assistant Professor Takeshi Sugahara (Division of Chemical Engineering, Department of Materials Engineering Science, Graduate School of Engineering Science, Osaka University) for numerous advices, assistances,

suggestions, discussions, and encouragements, which were essential to spend the student life as well as to complete the present studies and this thesis.

Finally, the author wishes to be grateful to his parents, Katsumi Hashimoto and Mayumi Hashimoto, to his little sister, Kana Hashimoto, to his grandmothers, Tsuyuko Hashimoto and Aiko Isono for their hearty encouragements and continuous supports, to Ms. Junko Shimada for her affectionate encouragement.

This work was financially supported by New Energy Industrial Technology Development Organization (NEDO) from 2005 to 2006. The author shows his gratitude for the center of excellence (21th century COE) program "Creation of Integrated EcoChemistry" and the Global COE program "Global Education and Research Center for Bio-Environmental Chemistry" of Osaka University.

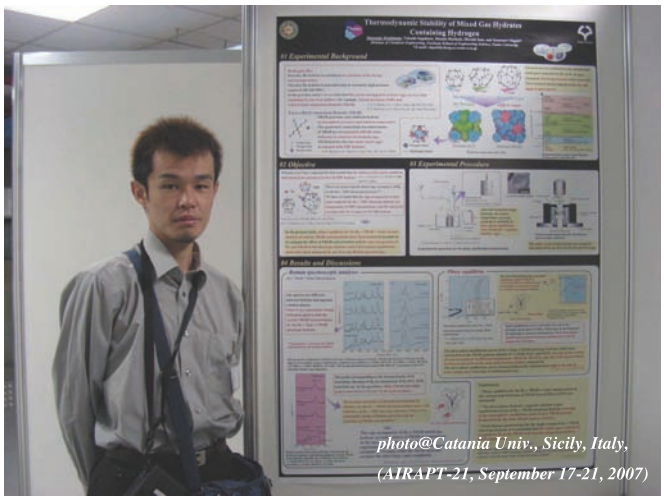

March 2008

Osaka University

Shunsuke HASHIMOTO

橋本　俊輔

Ohgaki Laboratory,
Division of Chemical Engineering,
Department of Materials Engineering Science,
Graduate School of Engineering Science,
Osaka University